Università degli Studi di Cagliari

DOTTORATO DI RICERCA

Scuola di dottorato in scienze e tecnologie chimiche e farmaceutiche

Indirizzo/ corso in scienze e tecnologie chimiche

Ciclo XXIII

TITOLO TESI

DNA based biosensors for environmental and medical applications

Settore scientifico disciplinari di afferenza

CHIM/02 CHIMICA FISICA

Presentata da: *Francesca Cugia*

Coordinatore Dottorato Prof. *Mariano Casu*

Tutor Prof.ssa *Maura Monduzzi*
Dott. *Andrea Salis*

Esame finale anno accademico 2009 - 2010

ABSTRACT

In the present thesis two electrochemical DNA based biosensors were developed using screen printed electrode as transducers.

Biosensors are defined as a self-containing integrated devices, capable of providing specific quantitative or semi-quantitative analytical information using a biological recognition element which is in contact with a transduction element.

The first DNA biosensor realized was applied to the rapid screening of toxic substances. The biosensor was constructed immobilizing a double helix DNA (Calf Thymus DNA) onto screen-printed electrodes. Subsequently, the biosensor was used for the determination of the toxicity of different kinds of common surfactants.

Surfactant interactions with double stranded DNA were evaluated measuring the height of the guanine oxidation peak. Indeed, the interactions with toxic substances raises structural and conformational modifications of DNA causing decrease of guanine peak. The intensity of the guanine oxidation peak, was measured through Square Wave Voltammetry (SWV).

Moreover, the toxicity of some selected surfactants was investigated both in sea water and tap water, and data were compared to those obtained in acetate buffer. The interaction between surfactants and Calf Thymus DNA in solution and adsorbed on the sensor surface was also investigated through FTIR and FTIR-ATR spectroscopy respectively.

The second kind of biosensor studied was a Genosensor, that is an analytical device where the biological recognition element is a single strand oligonucleotide sequence. These sequences referred as capture probe are capable to recognize selectively a complementary sequence (RNA or DNA), named target, by a hybridization reaction. Among the sequence probes, modified locked nucleic acid (LNA) and the peptide nucleic acid (PNA) were used. In this case the screen printed electrode

was used only as transducer while the hybridization assay was conducted onto paramagnetic micro beads.
The genosensor was used for the analytical detection of DNA and RNA sequences. In particular, the analytical properties of PNA and LNA capture probes with classical DNA sequences were compared. Hybridization with RNA target as well as with the corresponding DNA sequence was also performed. Differential pulse voltammetry (DPV) was used to perform the electrochemical measurements.

ACKNOWLEDGEMENTS

First of all I would like to express my sincere gratitude to my supervisor Prof. Maura Monduzzi for her encouragement and precious suggestions during this work and Dr. Andrea Salis for his invaluable help and guidance.

Thanks are due to Projects MIUR DM28142 of the Sardinian Biomedicine District, MIUR Prin 2008, grant number 2006030935, for financial support. Sardegna Ricerche Polaris is thanked for free access to the instruments belonging to the Nanobiotechnology laboratories. In addition thanks are due to CSGI and CNBS for general expertise support.

Thanks are due Sardinia Region, Project Master & Back. A particular acknowledgement is dedicated to Prof. Marco Mascini and to his group for the expert and friendly environment at the Department of Chemistry of Florence University. A special mention goes to Dr. Serena Laschi for her dedication in helping me and answering all of my numerous questions.

Thanks to all my colleagues (Amita, Brajesh, Daniela, Elisabetta, Luca, Marcella, Marco and Viviana) at the Biocatalysis laboratory with whom I spent many great moments and who have always encouraged and helped me.

I would also like to thank: Davide Espa, Maria Varotto, Elisa Sessini and Flavia Artizzu for their support, enthusiasm and friendship.

Lastly, I offer my regards to all of those who supported me during the completion of the project.

CONTENTS

LIST OF ABBREVIATIONS AND SYMBOLS

Abbreviation	*Meaning*
A	Adenine
AOT	Sodium dioctyl sulfosuccinate
ATR	Total reflection accessory
DDAB	Didodecylmethylammonium bromide
DNA	Deoxyribonucleic acid
DPV	Differential Pulse Voltammetry
dsDNA	Double strand DNA
C	Cytosine
CCP	Critical packing parameter
CMC	Critical micelle concentration
CPyCl	Cetylpyridunium chloride
CTAC	Hexadecyltrymethylammonium chloride
EC	Effective concentration
G	Guanine
HLB	Hydrophilic lipophilic balance
LC	Lethal concentration
LNA	Locked nucleic acid
miRNA	MicroRNA
NA	Nucleic Acid
PEGMO	Polietylenglycolmonooleate
PF 127	Pluronic 127
PNA	Peptide nucleic acid
RNA	Ribonucleic acid
RSD %	Relative standard deviation
SDS	Sodium dodecyl sulfate
ssDNA	Single strand DNA
SPE	Screen printed electrode
SWV	Square Wave Voltammetry
T	Thymine
TCA	Taurocholic acid
U	Uracil

Chapter I

General Introduction

1.1 BIOSENSOR: DEFINITION, FUNCTION AND APPLICATIONS

According to IUPAC, a ***biosensor*** is defined as a self-containing integrated device, capable of providing specific quantitative or semi-quantitative analytical information using a biological recognition element which is in contact with a transduction element (Figure1.1).[1]

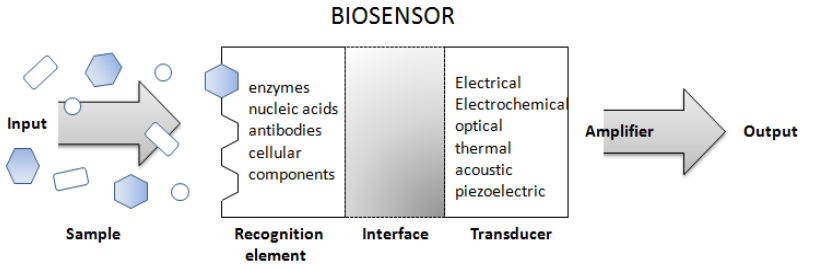

Figure 1.1: Biosensor detection principle.

Both the biological and the transduction elements are essential. The first works as a ***bioreceptors*** (biorecognition element), and has a powerful molecular recognition capability. The biological element can be an enzyme, a single or double DNA strand, an antibody or a cellular component of a living system. The ***transducer element*** translates the interaction of the biorecognition element into a detectable signal. If the signal intensity is proportional to the concentration of the analyte quantitative analysis can be carried out.[2] The biorecognition element enables the sensor to respond selectively to a particular analyte or group of analytes, thus avoiding interferences from other substances. This property, together with compact size, one-step reagentless analysis, and sensitivity make biosensors very attractive in comparison with conventional analysis techniques. Some interesting commercial biosensors are already available for the detection of glucose, lactate,

penicillin and urea, but their number is still limited in comparison with the research efforts for their development.

1.2 BRIEF HISTORY OF BIOSENSORS

The modern concept of biosensor is due to Leland C. Clark Jr. He invented the oxygen electrode, and its subsequent modification with enzymes. In 1962 at a New York Academy Sciences symposium he described "how to make electrochemical sensors (pH, polarographic, potentiometric or conductometric) more intelligent" by adding "enzyme transducers as membrane enclosed sandwiches". The first example was illustrated by entrapping the enzyme Glucose Oxidase in a dialysis membrane over an oxygen probe. The decrease of oxygen concentration was proportional to glucose concentration. The term enzyme electrode was coined by Clark and Lyons.[3] Clark's ideas became a commercial product in 1973 with the successful launch of the glucose analyser commercialized by Yellow Springs Instrument Company (Ohio). This was based on the amperometric detection of hydrogen peroxide and was the first biosensor-based laboratory analyser .

Guilbault and Montalvo were the first to develop a potentiometric enzyme electrodes. They realized a glass electrode coupled with urease to measure urea concentration in the blood.[4] Starting from 1970, several other authors started to couple an enzyme with an electrochemical sensor to develop a biosensor. In 1975 Divis suggested that bacteria could also be used as the biological element in microbial electrodes for the measurement of ethanol.[5] In 1975 Lubbers and Opitz[6] proposed the term "optode" to describe a fibre-optic sensor to measure carbon dioxide or oxygen. They developed an optical biosensor that was used for ethanol detection by immobilizing alcohol oxidase at the end of a fiber-optic oxygen sensor.[7]

In 1976, Clemens et al.[5] incorporated an electrochemical glucose biosensor in an artificial pancreas and this was later marketed with the commercial name the Biostator. In the same year, the pharmaceutical group La Roche (Switzerland) introduced the Lactate Analyser LA 640 for which the soluble mediator, hexacyanoferrate, was used to carry electrons from lactate dehydrogenase to the amperometric electrode. This was not a commercial success at that time, but subsequently it became an important forerunner of a new generation of mediated-biosensors for lactate analysis in sport and clinical fields.

In 1982, Shichiri et[8] al. described the first needle-type enzyme electrode for subcutaneous implantation. This result was a major advance in the in vivo application of glucose biosensors. Companies are still pursuing this possibility, but no device for general use is available yet.

The biosensors based on the use of enzymes involving catalytic action are referred as catalytic biosensor. Lately bioaffinity biosensors that make use of antibodies and receptor molecules having affinity towards analytes have been developed. In 1980s, the first bioaffinity biosensor was developed using radio-labelled receptors immobilized onto a transducer surface. Biosensor based on ELISA have also been developed using labeled antibody or labeled antigen coupled with a suitable transducer. The “cell biosensors” were also developed during 1980s, making use of whole microbiological cells or organelles to measure the level of various drugs or environmental toxicants. Biosensor research is currently investigating a wide variety of devices using biological element, such as enzymes, nucleic acids, cell receptors, antibodies and intact cells, in combination with various transduction mechanisms.[9] These biosensors can be applied to a wide range of analytical systems in health care, food and drink, process industries, environmental monitoring defence and security.[9]

1.3 BIOSENSOR CLASSIFICATION

Biosensors may be classified according to the biological element and the mode or signal transduction.

1.3.1 Receptor: biological recognition element

Biocatalytic recognition element: these biosensors are based on a reaction catalysed by bio-macromolecules. Continuous consumption of substrate (S) is obtained due to the action of biocatalyst incorporated into the sensor. The responses are monitored by the integrated detector. Three types of biocatalysts are commonly used.

- Enzymes (mono or multi-enzyme): these are the most common and well-developed recognition systems.
- Whole cells (micro-organisms, such as bacteria, fungi, eukaryotic cells or yeast) or cell organelles or particles (mitochondria, cell walls).
- Tissues (plant or animal tissue slice).

The biocatalyst based biosensors are the most studied and the most frequently applied to analysis of biological matrices since the pioneering work of Clark & Lyons.[3] One or more analytes, usually named substrates (S and S') react in the presence of enzyme (s), whole cells or tissue culture and yield one or several products (P and P') according to the general reaction scheme:

$$S + S' \xrightarrow{biocatalyst} P + P'$$

Biocomplexing or bioaffinity recognition element: the biosensor principle is based on the interaction of the analyte with macromolecules or organized molecular assemblies that have either been isolated from their

original biological environment or engineered. The equilibrium is usually reached and there is no further net consumption of the analyte by the immobilized biocomplexing agent. The equilibrium responses are monitored by an integrated dectector. In some cases, this biocomplexing reaction is itself monitored using a complementary biocatalytic reaction. Transient signals are then monitored by the integrated detector.

a. *Antibody-antigen interaction*.

The most developed biosensors that use biocomplexing receptors are based on immunochemical reactions, i.e. binding of the ***antigen*** (Ag) to a specific ***antibody*** (Ab). Formation of such Ab-Ag complexes has to be detected under conditions where non-specific interactions are minimized. Each Ag determination requires the production of a particular Ab, its isolation and, usually, its purification. In order to increase the sensitivity of immuno-sensors, enzyme labels are frequently coupled to Ab or Ag, thus requiring additional chemical synthesis steps.

b. Receptor/antagonist/agonist.

Protein receptor-based biosensors have recently been developed. The result of the binding of the analyte, here named agonist, to immobilized channel receptor proteins is monitored by changes in ion fluxes through the channels.[1]

A developing field in electrochemical biosensors is the use of chips and electrochemical methods to detect binding of oligonucleotides (gene probes). There are two approaches currently developed. The first one intercalates into the oligonucleotide duplex, during the formation of a double stranded DNA on the probe surface, a molecule that is electroactive. The second approach directly detects guanine oxidation.[1]

1.3.2 Detection or measurement mode: electrochemical transduction

An electrochemical biosensor is a self-contained integrated device, where the biological recognition element is in contact with an electrochemical transduction element.

Electrochemical biosensors are mainly used for the detection of hybridized DNA, DNA-binding drugs, glucose concentration, etc. The basic principle for this class of biosensors is that many chemical reactions produce, or consume, ions or electrons which, in turn, cause some change in the electrical properties of the solution which can be sensed out and used as measuring parameter. Electrochemical biosensors can be classified on the basis of the electrical parameters measured as: (1) conductimetric, (2) amperometric and (3) potentiometric:

1) Conductimetric biosensors

Many enzymatic reactions, such as that of urease, and many biological membrane receptors may be monitored by conductometric or impedimetric devices, using microelectrodes.[1] Since the sensitivity of the measurement is hindered by the parallel conductance of the sample solution, usually a differential measurement is performed in the presence and in the absence of an enzyme.

2) Amperometric biosensors

Amperometry is based on the measurement of the current resulting from the electrochemical oxidation or reduction of an electroactive specie. It is usually performed by maintaining a constant potential at a Pt, Au- or C based working electrode, or an array of electrodes with respect to a reference electrode, which may also serve as the auxiliary electrode, if currents are low (10^{-9} to 10^{-6} A).

3) Potentiometric biosensors

In this type of sensor the measured parameter is the potential difference between a working and a reference electrode or two reference electrodes separated by a perm selective membrane, when there is no significant current flowing between them. The transducer may be an ion-selective electrode (ISE), which is an electrochemical sensor based on thin films or selective membranes as recognition elements.[1]

1.3.2.1 Screen-printed electrodes (SPE) as electrochemical transducers

In recent years, with the aim of developing rapid, inexpensive and disposable biosensors, the use of screen-printing technology for the production of electrodes has obtained significant importance.[10] The most common disposable electrodes are produced by thick-film technology. A thick-film biosensor configuration is based on different sequentially deposited layers of inks or pastes onto an insulating support or substrate. The process allows the realization of a film with determined thickness and shape, by the use of different inks. This technique is more advantageous since it allows for the fast mass production of highly reproducible electrodes, at low cost for disposable use and high reproducibility and definition. In addition, these sensors avoid the contamination between samples, and show a reproducible sensitivity.

The possibility to use different inks to print electrodes permits to obtain sensors having different features. With regard to the supports, the inks can be printed on glass, ceramic and plastic sheets. The choice of material depends on the final use of the cell, and on the kind of ink used in the printing process. All supports have common characteristic such as chemical inertia and high properties of electric insulation. The most used inks are based on noble metals such as gold, platinum and silver. The most interesting materials for printed electrochemical sensors are the

graphite-based inks, because of their low polymerization temperature (from room temperature to 120°C) and the possibility to be printed on plastic sheets. Besides, this material permits to obtain easily modified sensors and biosensors since graphite can also be mixed with different compounds, for example metals.

1.3.2.2 Preparation of screen printed electrodes

The screen printing process consists in forcing inks of different characteristics through a screen into a surface of a polyester sheet with a squeegee. Typical thickness of the film is around 20 µm. The inks consist of finely divided particles of different materials in a mixture with thermoplastic resins. In order to obtain the silver pseudo-reference electrode the first layer printed is the silver based ink. The auxiliary and working electrodes are obtained through the second layer, and are made of graphite ink. After each step, the sheets are heated at 120° C for 10 min to achieve the polymerization of the printed films. In the last step an insulating ink is used to delineate the working electrode surface (Ø=3mm) and then heated at 70°C for the curing. Each electrode printed on the polyester flexible sheet can easily be cut by scissors and fits a standard electrical connector. In some cases to facilitate handling, the screen-printed electrochemical cells are stuck on a rigid polycarbonate-based support. Each electrode can be used only once. The scheme of these three printing steps of a screen-printed electrode sheet is reported in Figure 1.2 a. Figure 1.2 b shows the final appearance of SPE.
In chapter five screen-printed electrodes were used for transduction and as a support for the immobilization of DNA, and in the chapter six only for transduction.

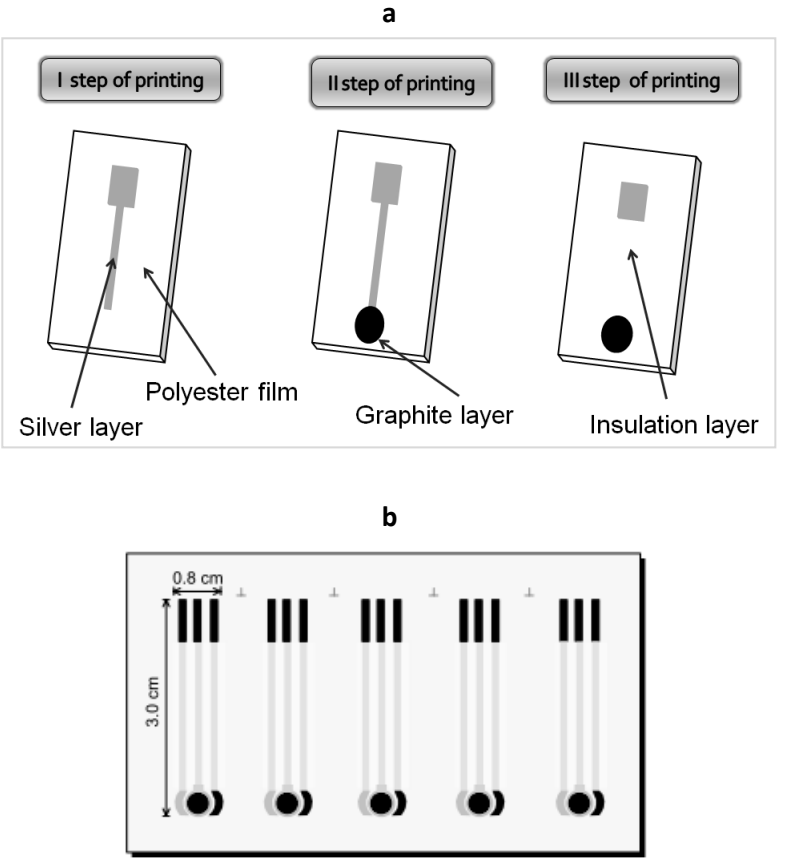

Figure 1.2. a) Scheme of printing steps of screen-printed electrodes produced using thick film technology; b) Screen-printed electrodes produced using thick film technology.

1.4 NUCLEIC ACID BASED BIOSENSOR: DEFINITION AND APPLICATIONS

A ***nucleic acid*** (NA) biosensor is an analytical device incorporating an oligonucleotide (original or modified) or a more complex structure of NA (like double stranded DNA) integrated with a signal transducer. NA biosensors can be used to detect DNA and RNA fragments or other biological and chemical species. Most NA biosensors are based on the highly specific hybridization of complementary strands of DNA or RNA molecules. ***Hybridization*** is the process of establishing sequence-specific interactions between two or more complementary strands of nucleic acids into a single hybrid. DNA or RNA will bind to their complement under normal conditions. The biosensors based on this principle are referred as ***genosensor***.[11] In other applications selected NAs play the role of highly specific receptor of biologic and/or chemical species, such as target proteins, pollutants or drugs. In addition, the interaction of chemical compounds with DNA molecules has been exploited for toxicity screening assays.

Nucleic acid biosensors can be of different types:

- those containing single strands of DNA or RNA which can hybridize with specific complementary sequences. Such biosensors can be used to detect nucleic acids, distinguish between DNA or RNA, and search for specific sequences;
- those containing double stranded DNA or RNA which can bind to specific compounds such as drugs or proteins;

1.4.1 Structure of Nucleic Acids

A nucleic acid is a polyelectrolyte that carry genetic information used in the development and functioning of all known living organisms, with the exception of some viruses.

The most common nucleic acids are deoxyribonucleic acid (DNA) and ribonucleic acid (RNA). Artificial nucleic acids include peptide nucleic acid (PNA) and locked nucleic acid (LNA), as well as glycol nucleic acid (GNA) and threose nucleic acid (TNA). Each of these differs from naturally-occurring DNA and RNA by changes in the backbone of the molecule.

1.4.1.1 Deoxyribonucleic acid (DNA)

DNA is a polyelectrolyte whose monomeric unit is called ***nucleotide***. Nucleotides are composed by different subunits: a nitrogenous base, a sugar (pentose), and a phosphate group (Figure 1.3).

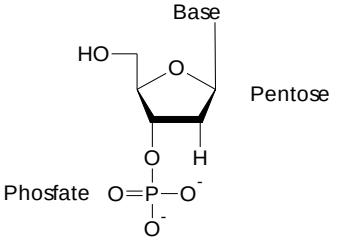

Figure. 1.3: Structure of a nucleotide

Nitrogenous bases are derivatives of two compounds, pyrimidine and purine. DNA contains two purine bases, ***adenine*** *(A)* and ***guanine*** *(G)*,and two pyrimidine bases, ***cytosine*** *(C)* and ***thymine*** *(T)* (Figure 1.4).

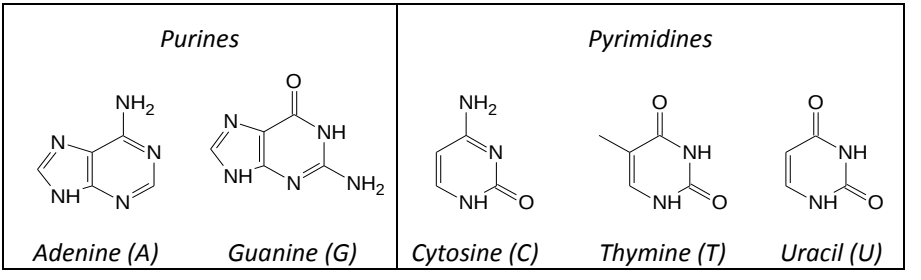

Figure.1.4: Major purine and pyrimidine bases of nucleic acids

In the case of RNA, the uracil replace the thymine (paragraph 1.4.1.2). The nucleotides are covalently bonded through phosphate groups bridges by a phosphodiester linkage. Therefore the covalent bonds of nucleic acid consist of alternating phosphate and pentose residues, while the nitrogenous bases are side groups connected to the backbone at regular intervals. The backbone is hydrophilic, the phosphate groups have a very low pKa (≈1), and are completely ionized and hence negatively charged (one charge for nucleotide) at pH 7.[12] Figure 1.5 shows the structure for a strand backbone, that constitutes the primary structure of DNA.

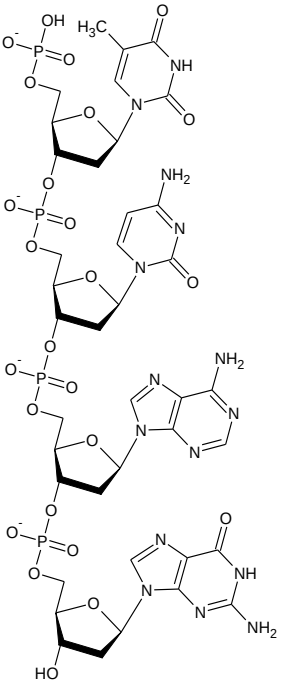

Figure 1.5: Covalent backbone structure of DNA

Free pyrimidines and purines are weakly basic compounds. Pyrimidines are planar molecules and purines are quasi planar. This geometry, and the

fact that bases are hydrophobic and low soluble in water (at quasi neutral pH), makes them packed in a base-stacking configuration, in which two o more bases are positioned with the plane of the rings parallel. The hydrophobic stacking interaction involves van der Waals and dipole-dipole interaction between the bases. The stacking minimizes the contact with the water and is one of the two important modes of interaction between bases in nucleic acids. The other is the hydrogen bond formed between the bases that allows for the complementary association of the strands of DNA.

Two strands of DNA form a "***double helix***" structure, which was firstly discovered by James D. Watson and Francis Crick in 1953. Watson and Crick proposed the base pairing rule: A pairs only with T, and G pairs only with C. These two types of base pairs are responsible of the formation of double-stranded DNA.

Different configurations of ds-DNA do exist (***A,B and Z-form***).

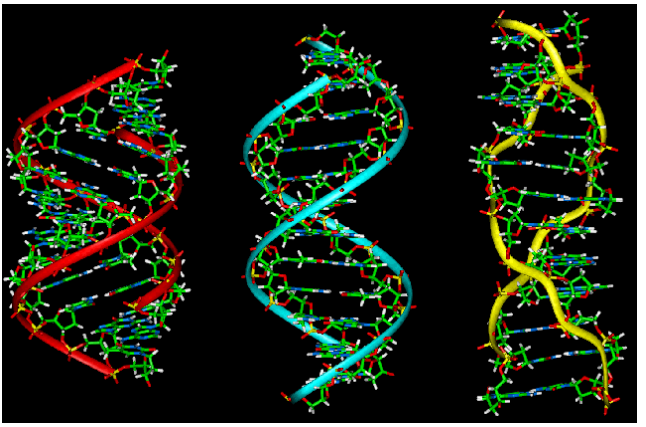

Figure 1.6. The structures of DNA: A, B and Z

In native form (B) DNA strands are organized through a double helical conformation with a diameter of about 20 Å and two periodicities along their long axis. The primary periodicity is 3.4 Å, and corresponds to the

separation of the adjacent bases. The bases undergo a rotation of 36°. Hence the helical structure is repeated after 10.5 base pairs on each chain, that is, for an interval of 36 Å, the secondary periodicity.

The spaces between the turns of the phosphate groups in the external part of the helix structure are termed ***grooves***. Due to of the asymmetry in the base pairs in the B-form, the grooves have unequal width, the narrower referred as minor groove and the wider referred as the major groove. The major groove is easily accessible to proteins.[13]

The B-form described above is the most stable structure under physiological conditions. However, two other structures have been well characterized in crystallographic studies. They are believed to occur in nature, named the A-form and the Z-form.

DNA adopts the A-form upon dehydration. It has also been suggested that it forms when DNA is complexed with oppositely charged species, that is, when the electrostatic repulsions between the phosphate groups decrease.

Table 1.: Structural characteristics of the A,B and Z Forms of DNA[14]

Helical sense	A-Form Right-Handed	B-Form Right-Handed	Z-Form Left-Handed
Diameter	≈ 26 Å	≈ 20 Å	≈ 18 Å
Bp per helical turn	11.6	10.5	11.6
Helix rise per bp	2.6 Å	3.4 Å	3.7 Å
Charge density	0.77 e^-/Å	0.59 e^-/Å	0.54 e^-/Å

The Z form of DNA structure differs from the other two forms since it has a left-handed helical sense. This form has one more base turn and rise of 0.38 nm per base pair. Whereas all the nucleotides along the B-DNA have the same conformation, the nucleotides along the left-handed DNA alternate the syn and the anti conformations of the bases.

The different configurations of ds-DNA due to the asymmetry in shape and linkage of nucleotides, and each backbone has an observable direction ability. The two strands in a DNA are oriented in different directions, that is an antiparallel orientation. This means that one of the extremities of the DNA chain terminates at the hydroxyl(-OH) group of the third carbon in the sugar ring (3'end), and the complementary chain at the chemical group attached to the fifth carbon of the sugar molecule (5'end). The direction ability has consequences on the biological function of DNA (for example in the replication).

1.4.1.2 Ribonucleic acid (RNA)

The primary structure of ***ribonucleic acids (RNA***) is very similar to that of DNA, but differs in two important structural details: RNA nucleotides contain ribose instead of deoxyribose and the base uracil instead of thymine.

RNA has a single-stranded structure in most of its biological roles and has a much shorter chain of nucleotides than DNA. However, RNA molecules can form double helix structure in the presence of complementary sequences.

It is possible to find several classes of RNA in the cell, each one with a distinct biological function. There are three major types of RNA that are mainly involved in protein synthesis. Messenger RNA (mRNA) carries the genetic information from one, or more genes to the ribosomes where the corresponding protein is synthesized. Ribosomal RNA (rRNA) is a component of the ribosomes where proteins are synthesized. Transfer RNA (tRNA) are small nucleotides molecules (74-93 nucleotides) that translate the information of mRNA into a specific sequence of amino acids. In addition, there are many other types of RNAs playing other roles in the cell.

1.4.1.3 Analogous of Nucleic Acid: PNA and LNA

Peptide Nucleics Acids (PNA) are the most known of the neutral analogues of nucleic acids. These are synthetic molecules where the sugar phosphate backbone of natural nucleic acids has been replaced by a synthetic peptide usually formed by N-(2-amino-ethyl)-glycine units (Figure 1.7), resulting in an achiral and uncharged mimic.

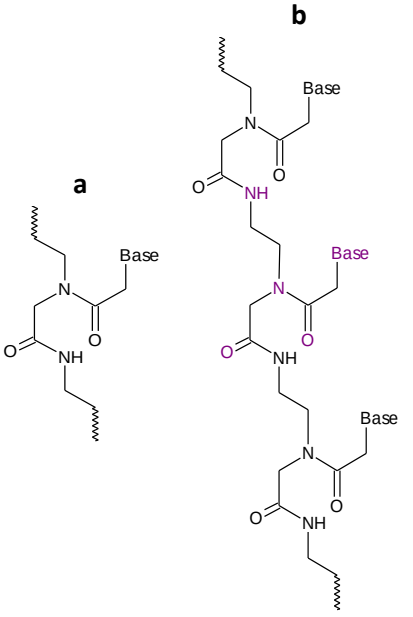

Figure 1.7: (a) Structure of PNA nucleotide; (b) structure of PNA oligonucleotide

PNAs show considerable hybridization properties and have many interesting applications. They are chemically stable and resistant to hydrolytic (enzymatic) cleavage, and thus not expected to be degraded inside a living cell. PNAs are able to recognize sequence specific of DNA and RNA according to Watson-Crick rules. PNA oligomers also show great specificity in binding to complementary DNA strands. Since the backbone

of PNA does not contain charged phosphate groups, the binding between PNA and DNA strands is stronger than between DNA and DNA strands, due to the lack of electrostatic repulsion. In addition the hybrid complexes exhibit high thermal stability .

Since their discovery, PNAs have attracted the attention of chemists and biologists because of their interesting chemical, physical, and biological properties, and their potential to act as active components for diagnostic as well as pharmaceutical applications.

However, PNAs applications are limited since they have low water solubility; they are not recognized as substrates for DNA enzymes; they cannot easily go across cellular membrane.[15]

Synthetic peptide nucleic acid oligomers have recently been used in molecular biology and diagnostic assays. Due to their high binding strength there is not need to design long PNA oligomers. Usually oligonucleotide probes constituted by 20–25 bases are required.

LNA oligonucleotides are defined as DNA or RNA nucleotides containing one or more ***Locked Nucleic Acid (LNA)*** nucleotides. LNA nucleotides are a class of nucleic acid analogues where the ribose ring is "locked" by a methylene bridge connecting the 2'-O atom and the 4'-C atom (Figure 1.8).

LNA nucleotides contain the same bases that form DNA and RNA and are able to form base pairs according to standard Watson-Crick rules. The locked ribose conformation enhances base stacking and backbone organization. This decreases the flexibility of the ring and blocks the ribofuranose structure in a rigid frame bicycle. This structure is very stable and has a high hybridization capability.[16] LNA oligonucleotides have a high affinity and specificity towards complementary nucleotide strands of DNA and RNA.[17] Indeed, double helices containing LNA oligonucleotides have greater thermodynamic stability than a double helix of DNA and RNA. The "bridge" blocks the ribose in 3'- endo conformation, as in the case of DNA and RNA in the A-form. The change of helical conformation and the

higher stability open new perspectives concerning the studies of affinity with DNA. LNA nucleotides are used to enhance the sensitivity and the specificity in Microarray based DNA, real-time PCR and in other molecular biology techniques that need highly specific oligonucleotide probes.

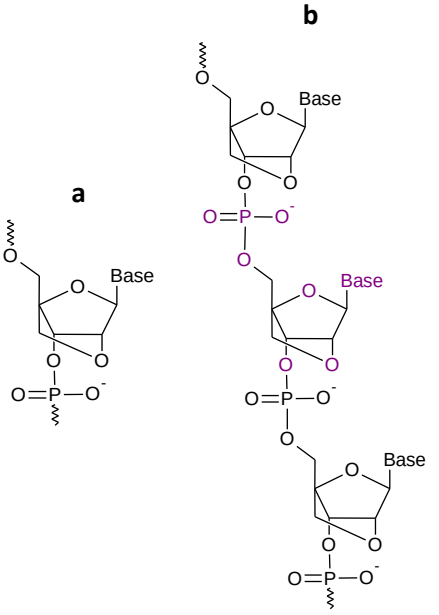

Figure 1.8: (a) Structure of LNA nucleoside; (b) structure of LNA oligonucleotide

1.4.2 DNA-based biosensors for environmental application

More recently there has been a great interest for the use of nucleic acid based biosensors for environmental applications. These sensors have rapidly found applications in areas such as screening of impurities in pharmaceutical products, the search for the release of genetically

engineered microbes in the environment, or to investigate mutations in gene sequences.
In this thesis, two different kinds of biosensors-based on screen printed electrode transducers-were used. Firstly, an electrochemical DNA-based biosensor was used for the determination of surfactants toxicity. Then, in order to develop a new kind of NA biosensor, we investigated the properties of PNA and LNA as capture probes. For the realization of an electrochemical hybridization assay a screen printed electrode was used as the transducer.

1.4.2.1 DNA Biosensor Principle

The guanine oxidation peak obtained through square wave voltammetry was used as the transduction signal to detect DNA toxic agents. The result of the interaction between double stranded calf thymus DNA and a toxic substance is the decrease of guanine oxidation peak (Figure1.9).

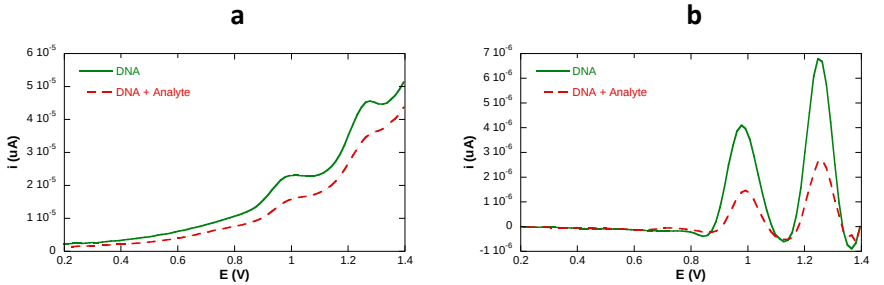

Figure 1.9. Redox behavior of guanine (+1.0V) and adenine (+1.25V) bases after a square wave voltammetric scan carried out with graphite screen printed working electrode. a) the oxidation peaks before and after the interaction with a toxic agent. b) the same peaks after baseline correction.

This decrease is due to the interaction of genotoxic substances with the DNA helix that causes structural and conformational modifications (Figure 1.10).

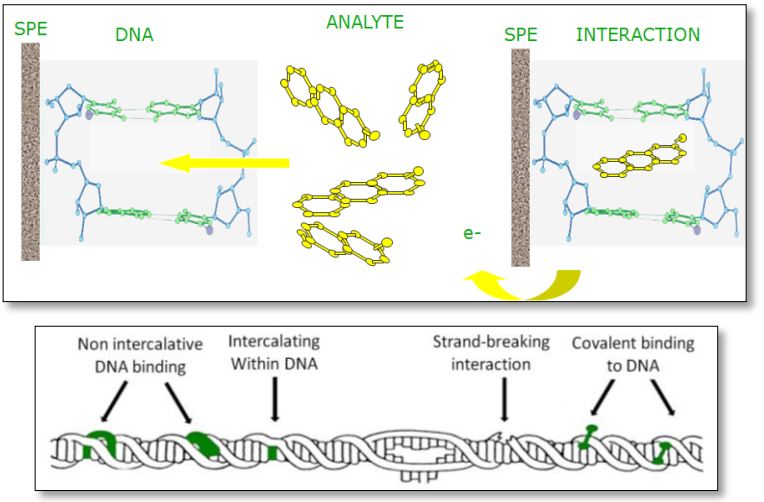

Figure 1.10 : possible kind of interactions between chemical compounds and DNA

As reported in chapter five, DNA modifications are estimated as the percentage of guanine oxidation peaks decrease (G%). Also the adenine oxidation peak could be used but the guanine peak is preferred since it gives more reproducible results.

1.4.3 Genosensors

In the last two decades, the field of molecular diagnostics has grown rapidly due to the discovery of new genes involved in different diseases. The development of novel therapeutics based on the regulation of gene expression provides revolutionary opportunities in the area of pharmaceutical new science. To improve patient care, the analysis of gene sequences and the study of gene regulation play fundamental roles in the rapid development of molecular diagnostics and in drug discovery.
Some methods more commonly used in the diagnostic laboratory are based on the analysis of specific gene sequences. In particular, the analysis of specific gene sequences exploits DNA hybridization reaction

for the its simplicity. In DNA hybridization, the target gene sequence is identified by a DNA probe that forms a double-stranded hybrid with its complementary nucleic acid (Figure 1.11). The reaction is highly efficient and extremely specificity also in the presence of a mixture of many different, non-complementary, nucleic acids. DNA probes are single-stranded oligonucleotides, labelled with either radioactive or non-radioactive material, to provide detectable signals for DNA hybridization.

In order to make DNA testing more convenient, more economically feasible, and ultimately more widely used, DNA biosensors (*genosensor*) have been developed. A genosensor is a biosensor that employs an immobilized oligonucleotide as the biorecognition element. Typically, the design of an electrochemical genosensor involves immobilization of the DNA probe, the hybridization with the target sequence, the labelling and the electrochemical investigation. However, deviations from this general scheme have to be considered when using modified magnetic beads for electrochemical genosensing.

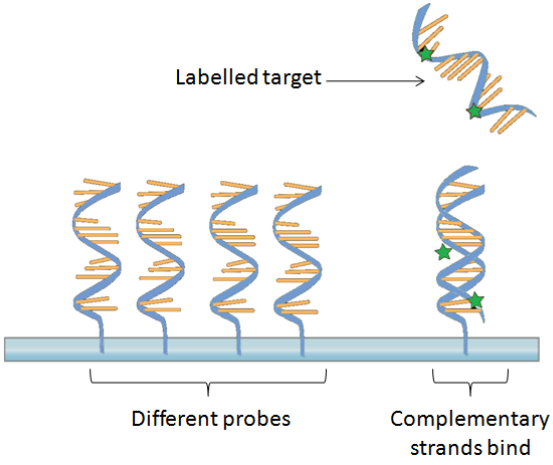

Figure 1.11: Sequence- specific recognition

We have used this kind of DNA biosensor for the analytical detection of DNA as well as RNA sequences (chapter six). In particular, we have studied RNA sequences related to microRNA (miRNAs). MicroRNAs regulate target gene expression through translation repression or mRNA degradation. These non-coding RNAs are emerging as important modulators in cellular pathway, and they appear to play a key role in tumors genesis.

To this aim is important to identify miRNAs and their targets that are essential to promote cancer development and metastasis. Hence, these microRNAs may provide new therapeutic opportunities.[18]

REFERENCES

1. Thévenot, D. R.; Toth, K.; Durst, R. A.; Wilson, G. S., Electrochemical biosensors: recommended definitions and classification. *Biosensors and Bioelectronics* **2001,** 16, (1-2), 121-131.
2. Mairal, T.; Cengiz Özalp, V.; Lozano Sánchez, P.; Mir, M.; Katakis, I.; O'Sullivan, C., Aptamers: molecular tools for analytical applications. *Analytical and Bioanalytical Chemistry* **2008,** 390, (4), 989-1007.
3. Clark, L. C.; Lyons, C., Electrode systems for continuous monitoring cardiovascular surgery
Ann. N. Y. Acad. Sci. **1962,** 102, (1), 29-45.
4. Guilbault, G. G.; Montalvo, J. A., Urea Specific Enzyme Electrode. *J. Am. Chem . Soc* **1969,** 91, 2164–2169.
5. Joshi, R., *Biosensors* Gyan Books ed.; Delhi, 2006.
6. Arnau Vives, A., *Piezoelectric transducers and applications* Springer ed.; 2004.
7. Völkl, K. P.; Opitz, N.; Lübbers, D. W., Continuous measurement of concentrations of alcohol using a fluorescence-photometric enzymatic method. *Fresenius' Journal of Analytical Chemistry* **1980,** 301, (2), 162-163.
8. Shichiri, M.; Yamasaki, Y.; Kawamori, R.; Hakui, N.; Abe, H., Wearable artificial endocrine pancreas with needle-type glucose sensor. *The Lancet* **1982,** 320, (8308), 1129-1131.
9. Collings, A. F.; Caruso, F., Biosensors: recent advances. *Rep. Prog. Phys* **1997,** 60, (11), 1397–1445.
10. Bergveld, P.; Turner, A. P. F., *Fabrication and mass production. In: Advances in Biosensors Suppl. 1: Chemical Sensors for In Vivo Monitoring.* London, 1993.
11. Palchetti, I.; Mascini, M., Biosensor Technology: A Brief History. In *Sensors and Microsystems*, Springer, Ed. 2010; pp 15-23.
12. Cantor, C. R.; Schimmel, P. R., *Biophysical Chemistry: Part I: The Conformation of Biological Macromolecules* San Francisco, 1980.
13. Nekludova, L.; Pabo, C. O., Distinctive DNA conformation with enlarged major groove is found in Zn-finger-DNA and other protein-DNA complexes. *Proc Natl Acad Sci U S A* **1994,** 91 (15), 6948-6952.

14. Dias, R.; Lindman, B., *DNA interaction with Polymers and Surfactants*. 2008.
15. Bonham, M. A.; Brown, S.; Boyd, A. L.; Brown, P. H.; Bruckenstein, D. A.; Hanvey, J. C.; Thomson, S. A.; Pipe, A.; Hassman, F.; Bisi, J. E.; Froehler, B. C.; Matteucci, M. D.; Wagner, R. W.; Noble, S. A.; Babiss, L. E., An assessment of the antisense properties of RNase H-competent and steric-blocking oligomers *Nucl. Acids Res.* **1995,** 23, (7).
16. Dominick, P. K.; Keppler, B. R.; Legassie, J. D.; Moon, I. K.; Jarstfer, M. B., Nucleic acid-binding ligands identify new mechanisms to inhibit telomerase. *Bioorganic & Medicinal Chemistry Letters* **2004,** 14, (13), 3467-3471.
17. Vester, B.; Wengel, J., LNA (Locked Nucleic Acid): High-Affinity Targeting of Complementary RNA and DNA. *Biochemistry* **2004,** 43, (42), 13233-13241.
18. Cho, W. C. S., MicroRNAs in cancer- from research to therapy. *Biochimica et Biophysica Acta (BBA) - Reviews on Cancer* 1805, (2), 209-217.

Chapter II

Analytes

2.1 SURFACTANTS

Surfactants are amphiphilic molecules which consist of two parts, a water soluble ***hydrophilic head*** and a water insoluble ***hydrophobic tail***. The word surfactant derives by the contraction of surface-active-agent and indicates a substance which exhibits surface or interfacial activity.
Hydrophobic groups tend to minimize the contacts with water and the chains in water self-assembly to reduce the free energy of the system. In addition, these substances tend to be adsorbed at interfaces. When surfactant molecules are at the liquid-gas or liquid-liquid interface, the hydrophobic tails extend out of the bulk water phase, while the water soluble heads remain in the water phase. This alignment of surfactant molecules alter the surface properties of water at the water/air or water/oil interface. The driving force of the phenomena is the lowering of the interfacial free energy. When the boundary between water and air is covered by surfactant molecules the surface tension is reduced.
In water surfactants tend to form aggregates referred as ***micelles***. Micelle formation, or ***micellization,*** can be viewed as an alternative mechanism to adsorption at interfaces. Micelles are formed at very low surfactant concentrations in water. The concentration at which micellas start to form is definite as the ***critical micelle concentration (CMC)***. This important feature depends mostly on the chemical structure of the surfactant but also on co-solutes, for instance, salts in the case of ionic surfactants or temperature, particularly for nonionic surfactants.
CMC can be determined by measuring the variation of different physicochemical parameters (surface tension, equivalent conductivity, self-diffusion, osmotic pressure, turbidity and solubilization) of an aqueous solution, as a function of the surfactant concentration.[1]
Surfactant self-assembly leads to different structures, some of which are shown in Figure 2.1.

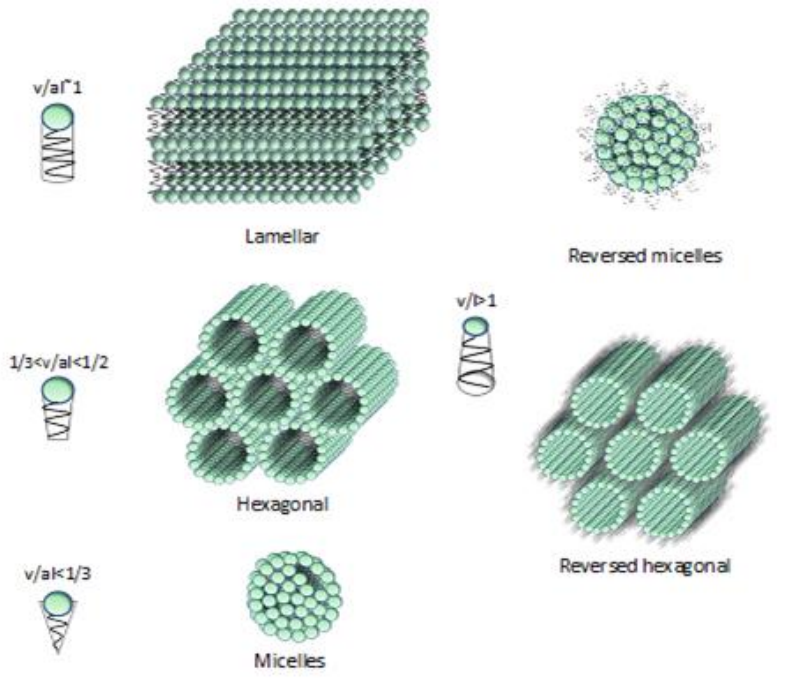

Fig. 2.1: Some example of molecular structure resulting from surfactant self-assembly. Critical packing parameters (CPPs) of surfactant molecules and preferred aggregate structures for geometrical packing.

The aggregate structure forms as a result of the balance between the polar and non polar parts of surfactants molecule, generally described as the ***hydrophilic lipophilic balance (HLB***). However, different approaches are based on the concepts of surfactant packing and the spontaneous curvature of the surfactant film. The ***critical packing parameter (CCP)*** is estimated by the following equation:

$$CPP = \frac{v}{(l_{max} \cdot a)} \qquad \text{Equation 2.1}$$

Where a is the headgroup area, l is take as 80% of the extended length, and v is the volume of the hydrophobic part of a surfactant molecule.
As Figure 2.1 shows, simple geometrical consideration can give an indication of the structure formed by a given amphiphile, depending on the relative value of CCP, from normal structure to reversed structures.

2.1.1 Classification of surfactants

Surfactants are classified according to the nature of their hydrophilic head in four classes: cationic, anionic, non ionic and zwitterionic surfactants.

Cationic surfactants are dissociated in water into an amphiphilic cation and an anion. Usually the polar head of cationic surfactants is an ammonium groups bound to different alkyl chains, according to the general formula:

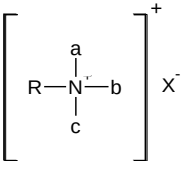

where *R* is a long hydrocarbon chain (C_{10}-C_{18}), *X* is a halide, sulfate, or methosulphate ion; and *a*, *b* and *c* may be H, small alkyl groups.
Also double-chained ammonium surfactants, where two R groups are present, are commonly used. The primary use of cationic surfactants is related to their tendency to adsorb at negatively charged surfaces. Hence they can be used as anticorrosive agents for steel, dispersants for inorganic pigments, for fertilizers and bactericides.

Anionic surfactants are historically the earliest and the most common surfactants. They are dissociated in water as an amphiphilic anion, and a cation. The most commonly used hydrophilic groups are carboxylates,

sulphates, sulphonates and phosphates. General formulas of anionic surfactants are as follows:

- Carboxylates: $C_nH_{2n+1}COO^-X$
- Sulphates: $C_nH_{2n+1}OSO_3^-X$
- Sulphonates: $C_nH_{2n+1}SO_3^-X$
- Phosphates: $C_nH_{2n+1}OPO(OH)O^-X$

where n≥8 atoms and the counter ion X is usually Na^+, K^+ or NH_4^+.

Non ionic surfactants contain polar groups unable to dissociate, but possessing a significant affinity to water and other polar substances. Usually these groups incorporate atoms of oxygen, nitrogen, phophorpous or sulphur (alcohols, amines, ethers, etc.). Among the non ionic surfactants, the most common are oxyethylated alkyl phenols, fatty alcohols, fatty acids, amines and block-copolymer surfactants (oxyethylene non ionic surfactants), where the polar parts of the molecules consist of repeated oxyethylene group – CH_2-O-CH_2- and closing –OH, -COOH or –NH_2 group.
They are compatible with charged molecules and easily used in mixtures with other ionic surfactants, which often result in beneficial associations.

Zwitterionic or ***amphoteric*** surfactants present both acid and basic functional groups. This is the case of synthetic products like betaines or sulfobetaines, and also natural substances such as aminoacids and phospholipids. They are usually used in association with other surfactants (anionic or nonionic) for particular applications. Since the optimal surface activity of amphoteric surfactants takes place around neutral pH, they are particularly appreciated in personal care products (shower gels, foam baths, shampoos, etc.) for their mildness and skin compatibility.

2.1.2 Surfactants Toxicity

Surfactants harmful effects on the environment are well known. The acute toxicity of surfactants to organisms is highly variable, depending on the chemical structure of the surfactant and the organism. In general, aquatic organisms are more susceptible to surfactants than terrestrial organisms. Surfactants can be adsorbed at the biological membranes and disrupt biological functions. Moreover, surfactants can be remove inhibit the enzyme activities.[2]

Several types of toxicity tests indicate that chronic toxicity of anionic and non ionic surfactants occur at concentrations < 1ppm.[3] Generally, non ionic and anionic surfactants tented to be more toxic at lower concentration than cationic surfactants.[4]

Toxicity caused by surfactants is influenced by several factors including the molecular structure of the surfactants, water hardness, temperature and dissolved oxygen. The most important factors are the molecular structure of the surfactants. Their toxicity is probably due to damage that surfactants cause to cellular protein and cell membrane.[4]

Acquatic toxicity of surfactants is usually measured on fish, daphnia and algae. The toxic index is expressed as LC_{50} (for fish) or EC_{50} (for daphnia and algae), where LC and EC stand for lethal and effective concentration, respectively. Values below 1 mgL^{-1} after 96 h testing on fish and algae, and 48 h on Daphia are considered toxic. Environmentally benign surfactants should, preferably, be above 10 mgL^{-1}.[5]

Verge and Moreno[6] studied the effects of anionic surfactants on *Daphnia Magna*. In this study, the acute toxicity of various linear alkyl benzene sulphonates (LAS), alkyl sulphates and alkyl ethoxy sulphates was determined. The study was carried out to obtain a valid set of data of the above surfactants for environmental classification and labeling according to European legislation. The results indicate that commercial LAS should

be classified as dangerous for the environment with respect to their effects on *Daphnia Magna.*

R.J Rosen at al.[7, 8] studied the relationship between the interfacial properties of surfactants and their toxicity to aquatic organism. They found that the toxicity of surfactants depends on their tendency to be adsorbed by the organisms and on their ability to penetrate the cell membranes of the organisms. The interfacial activity is expressed by the physic-chemical parameter :

$$\Delta G_{ad}^{0} / A_{min} \qquad \text{Equation 2.2}$$

where ΔG^{0}_{ad} is the standard free energy of adsorption of the surfactant at the air-solution interface and A_{min} is the minimum cross-sectional area of e surfactant at the liquid/air interfaces.

The analogous parameter at the liquid/solid interface:

$$\Delta_S^l G_{ad}^{0} / {}_s^l A_{\ min} \qquad \text{Equation 2.3}$$

where: $\Delta_S^l G_{ad}^{0}$ is a standard free energy of adsorption at the liquid solid interface between the surfactant solution and an immobilized artificial membrane designed to mimic a cell membrane; ${}_s^l A_{\ min}$ is the minimum cross sectional area of the surfactant at the interface.

The solid is an immobilized artificial membrane that mimics a biological cell membrane. The results show that the toxicity increases with: an increase in the length of the hydrophobic chain and, in linear polyoxyethylene (POE) alcohols, with the decrease of the number of oxyethylene units in the molecules. Besides, for isomeric materials the toxicity decreases with branching or movement of the phenyl group to a more central position in the linear alkyl chain. This is due to the expected changes in the value of both ΔG^{0}_{ad} and A_{min}.[9]

The general nature of the relationships between interfacial activity of the surfactants and their biological effects in aqueous systems indicate that adsorption to a biological membrane is a critical parameter for predicting and understanding environmental effects.
Differences in toxicity potential between classes of surfactants exist. However, such classification does not allow an exact determination of such capacity of each surfactant. Even within the same class, each surfactants exhibits its own specific effects distinguishable from the others.[10]

2.2 MicroRNA

MicroRNAs (miRNAs) are a family of endogenous ≈22 nucleotides non-coding RNAs that regulate gene expression with a strong sequence specificity.[11] [12]
To date, over 8600 miRNAs have been identified and deposited in the online miRBase sequence database, including currently more than 690 miRNAs sequences for the human genome.[11]
Every cellular process is likely to be regulated by microRNAs, and an aberrant microRNAs expression signature is a hallmark of several diseases, including cancer. MicroRNAs expression profiling has indeed provided evidence of the association of these tiny molecules with tumor development and progression. An increasing number of studies have then demonstrated that microRNAs can function as potential oncogenes or oncosuppressor genes, depending on the cellular context and on the target genes they regulate.[13]

2.3.1 Implications of microRNAs in cancer

Defects in normal cell processes such as differentiation, proliferation, and apoptosis are all well-known to be involved in cancer pathogenesis. The

connection between miRNA and cancer was initially made since miRNAs were found to be involved in many cancer diseases. This connection promoted studies which further reinforced the correlation between miRNAs and cancer development. Researchers discovered that there is an aberrant miRNA expression when comparing various types of cancer with normal tissues. Although the association between miRNA and cancer has initially been suggested, the question still remain " whether the altered miRNA expression was a cause or a consequence of cancer".[14] In addition very few informations about the specific targets and functions of miRNAs are still available.

Some miRNAs are thought to have oncogenic activity while others have tumor suppressor activity (Table 2.1). It is important to note that these distinctions may not be so strict and that some miRNAs may express different activities depending on the situation and tissue type. Nevertheless, the majority of recent research provides results that point toward one category or the other. It is also possible to group miRNAs based on their various functions. Some play a single role while others contribute to cancer through multiple cellular functions.

Table2.1: Various Oncogenic and Tumor Suppressor miRNAs [15]

miRNA	Tumor suppressor Activity	Oncogenic Activity	Espression in cancer
Let-7 family	X		-
miR-9		X	+
miR-10a		X	+
miR-15a/16-1	X		-
miR-17-5p	X		-
miR-17-92 cluster		X	+
miR-21		X	+
miR-29b	X		-
miR-34 a	X		-
miR-106 a		X	+
miR-124 a	X		-
miR-127	X		-
miR-141		X	+
miR-142		X	+
miR-143	X		-
miR-145	X		-
miR-146 b		X	+
miR-155/bic		X	+
miR-181 b	X		-
miR-197		X	+
miR-200b		X	+
miR-221		X	+
miR-222		X	+
miR-346		X	+

REFERENCES

1. Dias, R.; Lindman, B., *DNA interaction with Polymers and Surfactants*. 2008.
2. Hrenovic, J.; Ivankovic, T., Toxicity of anionic and cationic surfactant to Acinetobacter junii in pure culture. *Central European Journal of Biology* **2007,** 2, (3), 405-414.
3. Board, N., *The Complete Technology Book on Detergents* National Institute of Industrial Research: 2003.
4. Gerardi, M. H., *Toxicity*. John Wiley & Sons, Inc.: 2006; p 173-209.
5. Tadros, T. F., *Applied Surfactants -Principles and Applications* wiley: 2005.
6. Verge, C.; Moreno, A., Effects of anionic surfactant on Daphnia magna. *Tenside Surfact. Det* **2000,** 37.
7. Rosen, M.; Fei, L.; Zhu, Y.-P.; Morrall, S., The relationship of the environmental effect of surfactants to their interfacial properties. *Journal of Surfactants and Detergents* **1999,** 2, (3), 343-347.
8. Rosen, M. J.; Li, F.; Morrall, S. W.; Versteeg, D. J., The Relationship between the Interfacial Properties of Surfactants and Their Toxicity to Aquatic Organisms. *Environmental Science & Technology* **2001,** 35, (5), 954-959.
9. Milton, D.; Rosen, J., Chapter I: Characteristic features of surfactants. In *Surfactant and interfacial phenomena*, Wiley-Interscience, Ed.
10. Effendy, I.; Maibach, H. I., Surfactants and experimental irritant contact dermatitis. *Contact Dermatitis* **1995,** 33, (4), 217-225.
11. Beier, V.; Hoheisel, J., MicroRNAs: small Molecules with big impact in cancer. *BIOforum europe* **2008**.
12. Pang, Y.; Young, C. Y. F.; Yuan, H., MicroRNAs and prostate cancer. *Acta Biochim Biophys Sin* **2010,** 42, 363–369.
13. Lorio, M. V.; Croce, C. M., MicroRNAs in Cancer: Small Molecules With a Huge Impact. *Journal of Clinical Oncology* **2009,** 27, (34), 5848-5856
14. Sassen, S.; Miska, E. A.; Caldas, C., MicroRNA—implications for cancer. *Virchows Arch* **2008,** 452, 1-10.

15. VandenBoom II, T. G.; Li, Y.; Philip, P. A.; Sarkar, F. H., MicroRNA and Cancer: Tiny Molecules with Major Implications. *Current Genomics* **2008,** 8, 97-109.

Chapter III

Instrumental techniques

3.1 INTRODUCTION

The following paragraphs describe the general principles of the analytical techniques used for this study. Square Wave Voltammetry (SWV) was used to study surfactants toxicity (chapter 4) and Differential Pulse Voltammetry (DPV) was used for the detection of specific DNA and microRNAs sequences (chapter 6). FTIR spectroscopy and zeta potential measurements were used to study the interactions between DNA and surfactants (chapters 4 and 5 respectively).

3.2 VOLTAMMETRY

Voltammetry is an analytical technique based on the measure of the current flowing through an electrode dipped in a solution containing electro-active compounds, while a potential scanning is imposed upon it. The resulting current-potential and current-time curves are analyzed to obtain information about solution composition. Voltammetric techniques can be used for the determination at trace level at trace level of many organic compounds and inorganic substances (mainly metal ions).The effects of the applied potential and the behavior of the redox current are reported by the laws described below.
A reversible electrochemical reaction involving the reduction of an analyte Ox to give a product Red can be writer as:

$$[Ox] + ne^- \leftrightarrows [Red] \qquad \text{Equation 3.1}$$

the application of a potential *E* modifies the respective concentration of Ox and Red species at the surface of the electrode in agreement with the Nernst equation:

$$E_{app} = E_A^0 - \frac{RT}{nF} ln \frac{[Red]}{[Ox]} \qquad \text{Equation 3.2}$$

where E_{app} is the potential difference between the working electrode and the reference electrode, E_A^0 is the standard electrode potential for the reaction, *R* is the ideal gas constant (8.3144 $Jmol^{-1}K^{-1}$), *T* is the absolute temperature (K), *n* is the number of exchanged electrons, *F* is *the* Faraday constant (96,485C/mol), $[Red]$ and $[Ox]$ are the molar concentrations of *Re*d and *Ox* species in a thin layer of solution close to the electrode surface.

For some voltammetric techniques it is useful to use the Butler-Volmer equation that gives the current as a function of concentration:

$$i = nFAK^0 \left\{ [Ox]K^0 exp\left[-\frac{\alpha nFE_{app}}{RT}\right] - [Red]K^0 exp\left[(1-\alpha)\frac{\alpha nFE_{app}}{RT}\right]\right\}$$

where:

- i: intensity current, A
- K^0: rate constant
- E_{app}: electrode potential, V
- *A*: electrode active surface area, m^2
- *T*: absolute temperature, K
- *n*: number of electrons involved in redox reaction
- *F*: Faraday constant, C/mol
- *R*: ideal gas constant, J/mol·K
- α: transfer coefficient, dimensionless

In most cases the current also depends directly on the flow of material to the electrode surface. When new species are produced at the surface, the increased concentration provides the driving force for its diffusion towards the bulk of the solution to the electrode surface. On the contrary, when species are destroyed, the decreased concentration promotes the diffusion of new material from the bulk solution. The

resulting concentration gradient and mass transport is described by Fick's law:

$$\Phi = -AD_O(\partial c_O/\partial x) \qquad \text{Equation 3.4}$$

where Φ (mol/m^3) is the flux of matter, D_O (m^2/s)is the diffusion coefficient of oxidized specie, *A is the* electrode active surface area (m^2) and x (m) is the distance from the electrode surface. An analogous equation can be written for the reduced species.

3.2.1 Excitation signals

In voltammetry the voltage of the working electrode is varied systematically while the current response is measured. Several different voltage-time functions, called ***excitation signals***, can be applied to the working electrode. The waveforms of four of the most common excitation signals used in voltammetry are shown in Scheme 3.1. The classical voltammetric excitation signal is a linear scan (Scheme 3.1a) in which the potential of the working electrode is changed linearly with time. The current flowing in the cell is then measured as a function of the applied voltage. Two pulse-type excitation signals are shown in Scheme 3.1 b and c: differential pulse voltammetry and square wave voltammetry. Currents are measured at various times during the lifetimes of these pulses, as discussed in paragraph 3.2.3 and 3.2.4. In the (Scheme 3.1 d) the potential is varied linearly between two values at a fixed rate (cyclic voltammetry). When the voltage reaches V_2 the scan is reversed and the voltage is swept back to V_1. This process may be repeated several times while the current is recorded as a function of potential.

	Type of pulse	*Waveform*	*Type of voltammetry*
a	Linear Scan	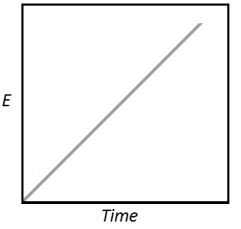	Linear voltammetry
b	Differential Pulse	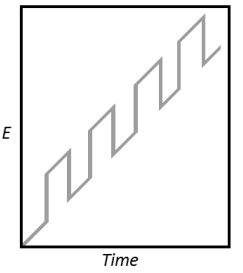	Differential pulse voltammetry
c	Square wave	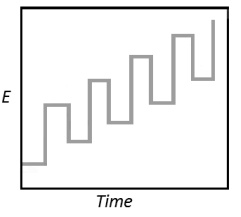	Square wave voltammetry
d	Triangular	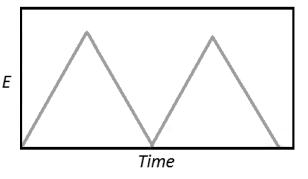	Cyclic voltammetry

Scheme 3.1: Potential versus time signals used in voltammetry

3.2.2 Voltammetric Instruments

Figure 3.1 shows as schematic representation of a voltammetric cell. The cell is made up of three electrodes immersed in a solution containing the analyte. The first is the ***working electrode***, that is the a transducer responding to the excitation signal and the concentration of the substance of interest in the investigated solution. Moreover, it permits the flow of large enough current to cause appreciable changes of the bulk composition. The most used working electrodes in voltammetry are made either of platinum or graphite.

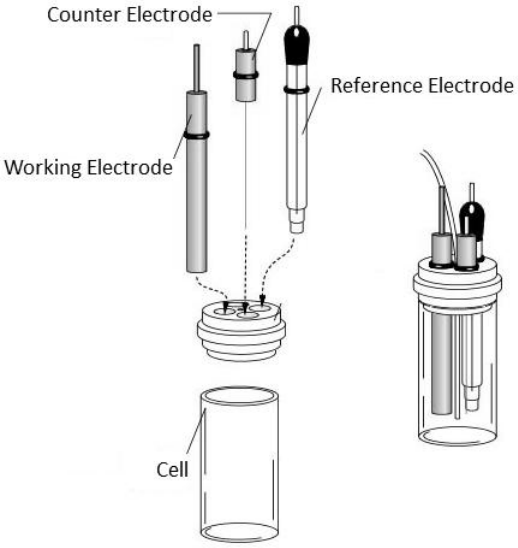

Figure 3.1: Schematic representation of a voltammetric cell.

The ***reference electrode*** maintains an invariant potential during the electrochemical measurement, allow for the observation, the measurement, or the control of the potential of working electrode. The most common reference electrode for aqueous solutions is the

silver/silver chloride electrode (Ag/AgCl). The third electrode is the ***counter electrode***, which function is to allow the flow through the cell. No processes of interest at its surface occur. Most often the counter electrode consists of a Pt wire or graphite.

A potentiostat controls the voltage between the working electrode and the counter electrode in order to maintain the potential difference between the working and the reference electrodes according to a preselected voltage-time program. During a measurement the potential of the working electrode versus the reference electrode is varied with time. The potential of the reference electrode remains constant throughout the experiment.

3.2.3 Voltammograms

Figure 3.2 shows a typical linear ***voltammogram*** for an electrochemical process involving the reduction of an analyte specie Ox to give a product Red (equation 3.1).

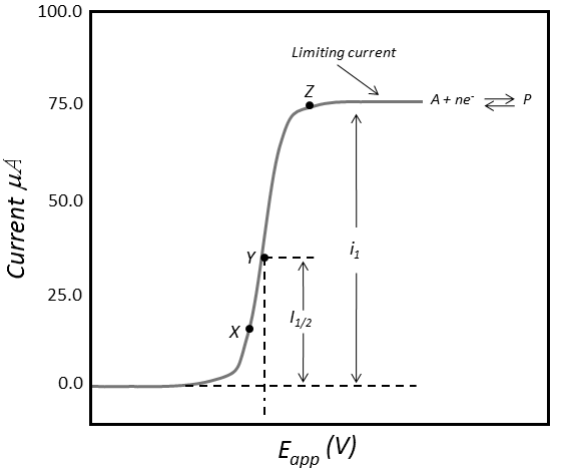

Figure 3.2 Linear voltammogram for the reduction of a hypothetical species A to give a product P.

Linear voltammograms generally have the shape of a sigmoidal curve referred as a voltammetric wave. The constant current beyond the steep rise (point Z in Figure 3.1) is named the ***limiting current*** (i_l). This is affected by the rate at which the reactant can be brought to the electrode surface by mass transport processes. Limiting currents are generally directly proportional to reactant the concentration, according to:

$$i_l = kc_A \qquad \text{Equation 3.5}$$

where c_A is the analyte concentration and k is a proportionality constant. Quantitative linear voltammetry is based on this relationship.

The potential at which the current is equal to one half of the limiting current is called the ***half-wave potential*** ($E_{1/2}$). The half-wave potential is closely related to the standard potential for the half-reaction but is usually not identical to that constant. Half-wave potentials are sometimes useful for the identification of the components of a solution. Linear voltammetry in which the solution is stirred or the electrode is rotated is called hydrodynamic voltammetry. Voltammetry with a dropping mercury electrode is called polarography.

3.2.4 Differential Pulse Voltammetry (DPV)

Figure 3.3a shows the most common excitation signals for differential pulse voltammetry (DPV). This waveform is obtained by superimposing a periodic pulse on a linear scan. Usually a small pulse, typically 50 mV, is applied. As shown in Figure 3.3a the current is measured alternately in two point of the signal: the first (S_1) before the application of the pulse, and the second (S_2) before the end of the pulse. The difference in current intensity per pulse Δi ($= i_{S_2} - i_{S_1}$) is recorded as a function of the linearly increasing voltage. A differential curve is obtained (Figure 3.3b) where the

height of the peak is directly proportional to the concentration of the analyte.

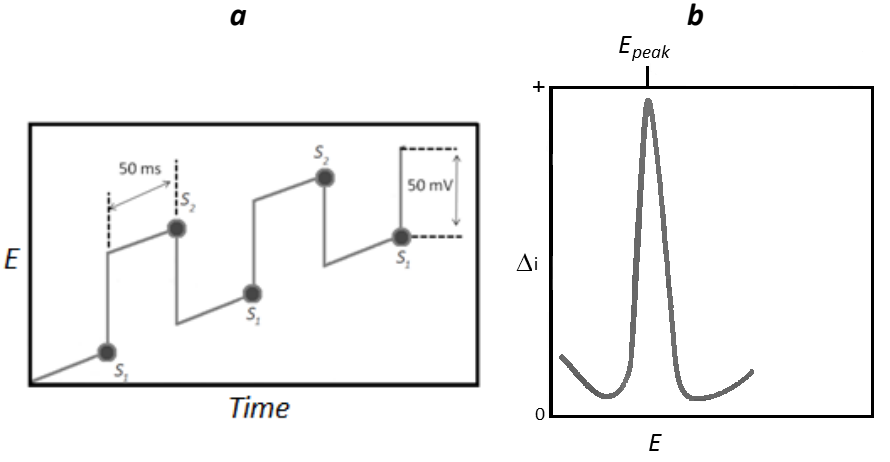

Figure 3.3: a) Exciting signal for differential pulse voltammetry; b) Voltammogram for a DPV experiment

For a reversible reaction, the peak of potential is approximately equal to the redox standard potential of the analyte.
One advantage of DPV respect to linear voltammetry is the possibility to identify substances half-wave potentials differing by 0.04 to 0.05 V in the position of peak maxima. Moreover, DPV has high sensitivity and significantly low detection limits.

3.2.5 Square-Wave Voltammetry (SWV)

Square-wave voltammetry (SWV) is a type of pulse voltammetry that offers the advantage of great speed and high sensitivity. Figure 3.4a shows a typical signal used . This is obtained by superimposing the pulse train. The length of each step of the staircase and the period of the pulses (τ) are identical, usually about 5 ms. The potential step of the staircase

(ΔE_s) is typically 10 mV. The magnitude of the pulse ($2E_{sw}$) is usually 50 mV.

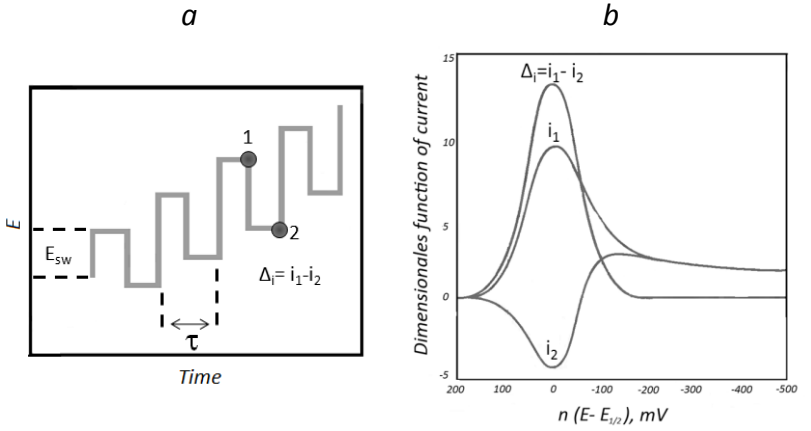

Figure 3.4: a) Generation of a square-wave voltammetry excitation signal; b) current response for a reversible reaction to excitation signal.

For a reversible redox reaction, the size of a pulse is enough large to cause the oxidation of the product during the reverse pulse. Thus, as shown in Figure 3.4b, the direct pulse produces a cathodic current i_1 whereas the reverse pulse gives an anodic current i_2. Usually, the difference in these currents Δi versus E is plotted to give a voltammogram as shown in Figure 3.3b. Moreover, Δi is directly proportional to the analyte concentration. Generally, quantitative applications are based on calibration curves in which either peak heights or areas are plotted versus analyte concentration. The maximum of potential peak corresponds to the polarographic half-wave potential. Detection limits for SWV are usually in the range 10^{-7} -10^{-8} M.

3.3 ZETA POTENTIAL

Most of colloidal substances acquire an electric surface charge when in contact with a polar solvent. This charge influences the distribution of ions in the polar medium. The ions with opposite charge are attracted to the surface and the ions with same charge are repelled from the surface.

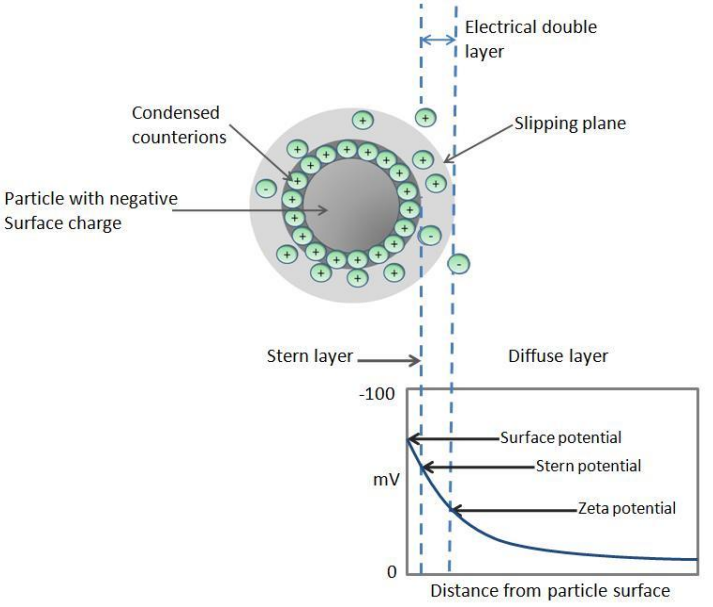

Fig. 3.5 : Scheme of the distribution of ions around a charged colloidal particle.

This phenomenon causes the formation of an electric double layer that can be divided in two parts; an internal region, called the ***Stern layer***, where the ions are strongly bound and an external, ***diffuse, region*** where they are only loosely bound. Within the diffuse layer there is an imaginary boundary inside which the ions and the particles form a stable entity. When a particle moves (e.g. due to gravity), ions within the boundary move with it, but any ion outside the boundary does not move with the

particle. This boundary is called the ***surface of hydrodynamic shear*** or *slipping plane*. The potential that exists at this boundary is referred as the ***Zeta potential***.

The Zeta potential value gives an indication of the potential stability of the colloidal system. When all the particles in the suspension have a large negative or positive Zeta potential, they tend to repel each other and there is no tendency to flocculate. However, if the particles have low Zeta potential values, the small repulsive force cannot prevent particles flocculation. Usually the boundary line between stable and unstable suspensions is taken at either +30mV or -30mV. Colloidal particles with more positive or more negative Zeta potentials are considered to be stable.

3.3.1 Zeta potential measurements

When an electric field is applied across an electrolyte, charged particles suspended in the electrolyte are attracted towards the electrode of opposite charge. Viscous forces acting on the particles tend to oppose to this movement. When the equilibrium between these two opposing forces is reached, the particles move with constant velocity. The velocity of the particle is dependent on the following factors:

- the strength of electric field or voltage gradient;
- the dielectric constant of the medium;
- the viscosity of the medium;
- the Zeta potential.

The velocity of a particle in an electric field is commonly referred to in term of Electrophoretic mobility.

The Zeta potential of the colloidal particle can be obtained by means of the Henry equation:

$$U_E = \frac{2\varepsilon z f(ka)}{3\eta} \qquad \text{Equation 3.6}$$

with :

$$f(ka) = [1 - e^{ka}\{5E_7\}(Ka) - 2E_5(ka)] \qquad \text{Equation 3.7}$$

where $f(ka)$ is the Henry's function; $E_n(ka)$ is the nth order exponential integral, z is the Zeta potential, U_E is electrophoretic mobility, ε is dielectric constant and η is the viscosity.

Figure 3.6 shows the cell used for the zeta potential measurements. It present electrodes at either end to which a potential is applied. Colloidal particles move towards the electrode of opposite charge, their velocity is measured and expressed in unit field strength as their mobility.

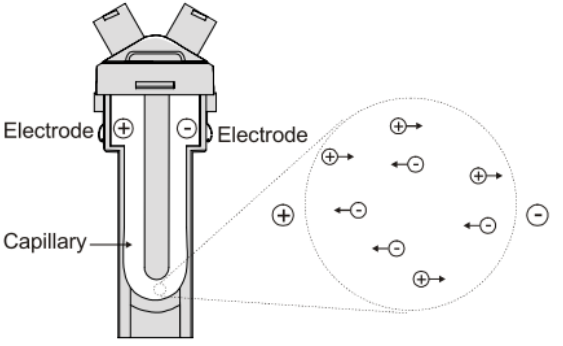

Figure 3.6: Cell for zeta potential measurements

Zeta potential measurement system comprises six main components (Figure 3.7). First of all a laser (1) is used to provide a light source to illuminate the particles within the sample. This light source is split to provide an incident and reference beam. The laser beam passes through the centre of the sample cell (2), and the scattering at an angle of 17° is

detected. When an electric field is applied to the cell, any particles moving through the measurement volume will cause a fluctuation of the light intensity detected. The fluctuation is proportional to the particle speed. A detector (3) sends this information to a digital signal processor (4) and then to a computer (5), where the software produces a frequency spectrum from which the electrophoretic mobility and hence the Zeta potential is calculated.

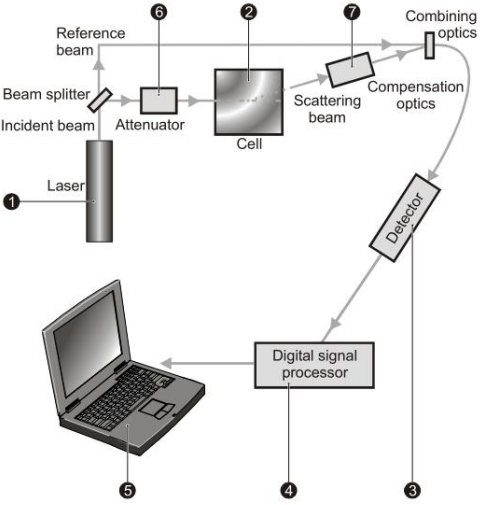

Figure 3.7: Schematic representation of system for Zeta potential measurements

The intensity of the scattered light within the cell must be within a specific range. If light intensity is too high then the detector will go in overloaded. To overcome this problem an “attenuator”(6) is used to reduce the intensity of the laser and hence reduce the intensity of the scattering.

To correct any differences due to the cell wall thickness and dispersant refraction, a compensation optics system(7) is installed within the scattering beam path.

3.4 INFRARED SPECTROSCOPY

Infrared (IR) spectroscopy gives information about the vibrational state of a molecule. Infrared radiation is the part of the electromagnetic spectrum between ≈ 13,000 to 10 cm^{-1}. Usually IR spectrum is divided in three spectral regions: the Near Infrared (NIR: 14000–4000 cm^{-1}), Mid Infrared (MIR: 4000–400 cm^{-1}) and Far Infrared (FIR: 400–10 cm^{-1}). The cm^{-1} is the unit of the wave number ($\bar{\nu}$), which is defined as:

$$\bar{\upsilon} = \frac{1}{\lambda} \qquad \text{Equation 3.8}$$

Where λ is the wave length of the IR radiation. Wave numbers are directly proportional to the frequency, and hence to the energy of the IR radiation.

The different vibrational modes of a molecule can be excited by irradiation with an IR radiation of a suitable energy. The different functional groups of a molecule absorb characteristic frequencies of IR radiation, so that each molecule has a characteristic IR spectrum. The spectral position and the intensity of IR bands permit the identification of the functional groups of a molecule, thus helping the elucidation of its structure. An IR spectrum is graph where transmittance (or absorbance) versus wave numbers are reported. An example of an IR spectrum of an organic molecule (acetone) is reported in Figure 3.8.

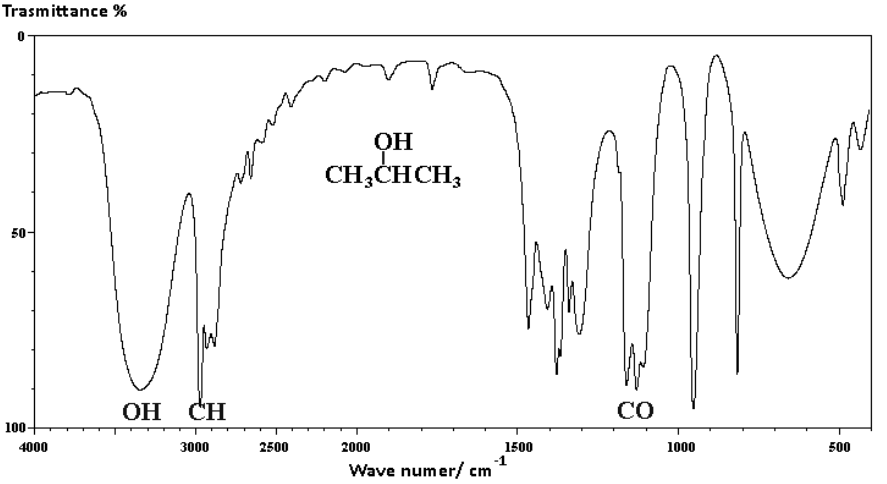

Figure3.8: The IR spectrum of acetone

Transmittance, T, is the ratio between radiant power transmitted by the sample (*I*) and the radiant power incident on the sample (I_0).

$$T = \frac{I}{I_0} \qquad \text{Equation 3.9}$$

Absorbance (A) is the logarithm (base 10) of the reciprocal of the transmittance (T).

$$A = log_{10}\left(\frac{1}{T}\right) = -log_{10}T \qquad \text{Equation 3.10}$$

3.4.1 Molecular Vibrations

At temperatures above the absolute zero, all the atoms of a molecule are in continuous vibration. When the frequency of a specific vibration is

equal to the frequency of the IR radiation incident on the molecule, the molecule absorbs the radiation. Each atom has three degrees of freedom, corresponding to motions along any of the three Cartesian coordinate axes. A polyatomic molecule of *n* atoms has 3*n* total degrees of freedom. However, 3 degrees of freedom are required to describe translation, the motion of the entire molecule through space.

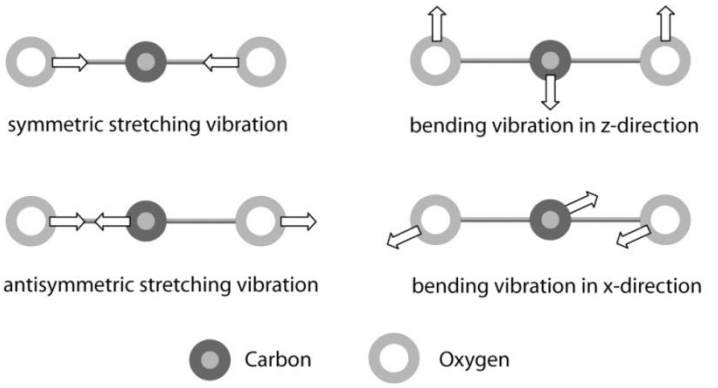

Figure 3.9: Normal vibrations of the CO_2 molecule

In addition, 3 degrees of freedom correspond to the rotation of the entire molecule. Therefore, a non-linear molecule has a number of 3*n* – 6 fundamental vibrations due to the remaining degrees of freedom. Linear molecules possess 3*n* – 5 fundamental vibrational modes since only 2 degrees of freedom are sufficient to describe the rotation. Among the 3*n* – 6 or 3*n* – 5 fundamental vibrations (also known as normal modes of vibration),only those that produce a net change in the dipole moment may result in an IR activity.

The main types of molecular vibrations are stretching and bending vibrations. Some of these vibrations are illustrated in Figure 3.9.

3.4.2 Fourier Transform Spectrometers

The spectrometer consists of a IR source, a beamsplitter, two mirrors, a laser and a detector. The beamsplitter and the mirrors are collectively called the interferometer. The instrumental parts of an IR spectrophotometer are schematized in Figure 3.10.

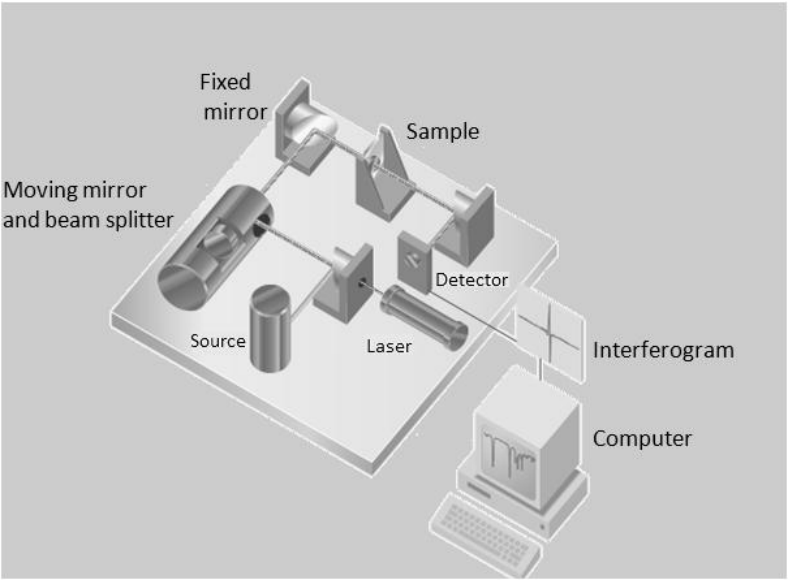

Fig. 3.10: Schematic representation of a spectrophotometer

The IR radiation from the source strikes the beamsplitter, which produces two beams of roughly the same intensity. One beam strikes a fixed mirror and returns, while the second strikes a moving mirror. A laser parallels the IR light, and also goes through the interferometer. The moving mirror oscillates at a constant velocity, timed using the laser frequency. The movement of the mirror generates an interference pattern during the motion. The IR beam then passes through the sample, where some energy is absorbed and some is transmitted. The transmitted portion

reaches the detector, which records the total intensity. The raw detector response yields an interferogram. The interference pattern contains the information about all wavelengths being transmitted at once, which is a function of the source, the beamsplitter, the mirrors and the sample.
This signal is digitized and processed through computer. The untangling of the frequencies into a spectrum is done by the Fourier transform algorithm, which gives the name to the whole spectrometer.

3.4.2.1 ATR-FTIR spectroscopy principles.

New generation of FTIR spectrophotometers allow to use differ sample holders as exchangeable accessories.

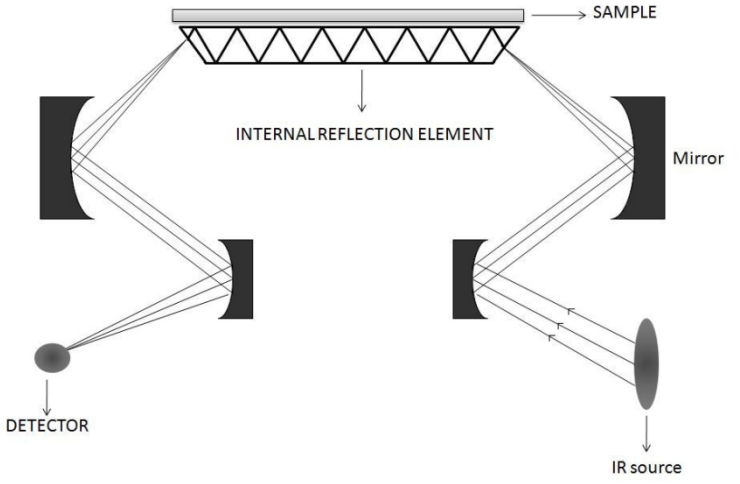

Figure 3.11: Schematic diagram of an attenuated total reflectance (ATR) accessory

An Attenuated Total Reflection (ATR) accessory operates by measuring the changes that occur in a totally internally reflected infrared beam when the beam comes into contact with a sample (Figure 3.11).

The crystal is made of a material with high refractive index (*n)* as diamond or germanium. Since the infrared data are collected from the reflected and not the transmitted radiation, also opaque samples can be investigated. Intensities can be enhanced by using multiple internal reflection in a trapezoidal crystal as a shown in Figure 3.5.

The principle of this technique can be summarized as follows (Figure 3.12). The interface between two different media as characterized by the refractive indexes n_1 and n_2. If $n_1 > n_2$ case is considered, a light beam goes from the dense medium 1 to the less dense medium 2. For this system the refraction law is:

$$n_1 sin\theta_i = n_2 sin\theta_r \qquad \text{Equation 3.11}$$

where θ_i and θ_r are the angle of incidence and the refraction angles, respectively, both definite with respect to normal surface. For a critical value of the incoming angle, $\theta_r = 90°$, $sin\theta_i = {}^{n_2}/_{n_1}$.For this angle of incidence and beyond, all light is reflected back into medium. This process is known as a ***total internal reflection***.

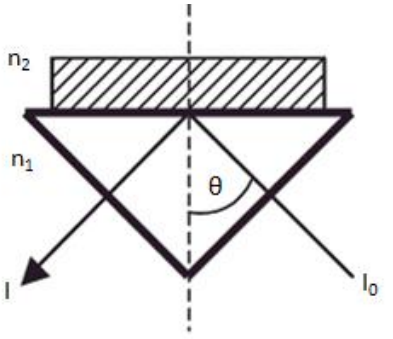

Figure 3.12: Experimentally geometry for ATR-IR spectroscopy.

Calculation of the propagation of a plane wave from a medium 1 into a medium 2 under condition of total reflection yields:

$$E = E_0 \cdot e^{-z/d_p}$$ Equation 3.12

where E_0 is the electrical field amplitude at the interface, which depends on the angle of incidence, the refractive indices, and the polarization of the field. The electric field components of the evanescent wave fall off exponentially with the distance z from the interface. According to Equation 3.12 d_p, the penetration depth of the evanescent wave is definite as the distance from the interface at which the electric field amplitude E has decayed to 1/e of its value at the interface, E_0.
The penetration depth is given by:

$$d_p = \frac{\lambda}{2\pi\sqrt{sin\theta_i - (n_2/n_1)^2}}$$ Equation 3.13

where λ is the wavelength. The penetration depth depends on the wavelength of the light and thus changes across the spectrum.
Quantitative analysis in ATR-IR spectra can be carried out by the application of the Lambert and Beer's law according to:

$$A = N\varepsilon c d_e$$ Equation 3.14

Where A is the absorbance resulting from N internal reflections, d_e and c are the thickness and the concentration of the sample respectively, ε is the molar extinction coefficient.

REFERENCES

1. Skoog, D. A.; West, D. M.; Holler, J. F.; Crouch, S. R., *Fundamentals of Analytical Chemistry*. Eighth ed.; Toronto, 2004.

2.Keller, R.; Mermet, J.-M.; Otto, O.; Widmer, H. M., *Analytical Chemistry*. Weinheim, 1998.

Chapter IV

Surfactants toxicity towards an electrochemical DNA biosensor

4.1 INTRODUCTION

The potential environmental toxicity of surfactants has been deeply studied. Different studies concerning the surfactants toxicity to small crustaceans as Daphnia magna[1, 2] and to aquatics organisms in general were reported.[3-5] According to those studies toxicity is strongly related to the chemical features of surfactants. For example, some works, in which different nonionic surfactants were compared, concluded that toxicity increases with the number of ethoxylate groups in the molecule.[1, 6] or when molecular weight increases.[1, 3] By contrast with toxicity, surfactants genotoxicity has not deeply been investigated. Genotoxic substances are able to cause modifications into nucleotide sequences or in the double helix structure of DNA. Depending on the method different results on surfactant genotoxicity have been found. For example Liwarska et al.[3] reported that sodium dodecyl sulphate (SDS) does not cause genotoxicity, whereas Sirisattha et al found that SDS is genotoxic, since induces oxidative stress effects on yeast cells, and the system responds producing genes to repair DNA.[7] Microcalorimetric measurements showed that SDS does not interact with DNA.[8] Didodecylmethylammonium bromide DDAB was studied by means of four different genotoxic tests (Salmonella/microsome assay; SCGE assay with primary rat hepatocytes; Micronuclears (MS) assay with peripheral human lymphocytes; MS assay with root tip cells of *Vicia faba*). The results showed that DDAB – and also other cationic surfactants - induce moderate, but significant, genotoxic effects in the eukaryotic cells at typical concentrations commonly found in wastewaters.[9]

The reasons for surfactants genotoxicity should be searched at molecular level studying the type of interactions among the different classes of surfactants with DNA helices. The first works concerning the study of DNA-surfactant interactions date back to 60 years ago. The aim of those studies was the purification of DNA through the use of cationic

surfactants.[10, 11] Successive studies, aimed to use DNA-surfactants complexes in gene therapy, allowed to investigate thoroughly the mechanisms of interactions between DNA and surfactants.[12, 13] In particular potentiometric and fluorescence microscopy studies showed that the interactions between cationic surfactants and DNA involve a two-step process.[11, 14, 15] First, the cationic surfactant binds to an isolated phosphate group on the DNA strand through electrostatic interactions, then, a highly cooperative binding event - that seems to involve hydrophobic interactions among the hydrocarbon chains of the surfactant - occurs. These further interactions strengthen the DNA-surfactants bonds because minimize the contact with water.[13, 16] In addition, it was found that DNA molecules undergo conformational changes (from the coil to globule states) due to the addition of very low concentrations (≈10^{-5} M) of cetyltrimethylammonium bromide (CTAB).[17, 18]

Most studies on DNA-surfactants interactions used cationic surfactants, whereas only few studies on the interaction between DNA and anionic surfactants have been reported.[8, 16, 19] Mel'nikov et al.[20] studied the effect of the nonionic surfactant Triton X-100 on the conformational behavior of DNA, through fluorescence microscopy. They found that DNA undergoes a coil to globule shape transition at high surfactant concentration. The formation of DNA globules was not detected at low Triton X-100 concentration.

In this chapter we used a DNA biosensor to study the potential toxicity of some common cationic, anionic, and non ionic surfactants. Surfactants are present in several products of general use such as shampoos, toothpastes, cosmetics, drugs, pharmaceutical formulations etc, therefore they represent a potential source of environmental pollution. The DNA biosensor performance was compared with that of the commercial toxicity test Toxalert®100 for sodium dioctyl sulfosuccinate (AOT) and Triton X 100 surfactants. Then, the DNA biosensor was used for the determination of the toxicity of nine commercial surfactants. The

major worth of this DNA biosensor is its rapidity compared to the most common biological tests for environmental risk assessment. Indeed, toxicity tests that use microorganism (i.e. *Vibrio fisherii*, *Daphnia magna*) [1, 2, 21] or sentinel organisms, like animals (i.e. *Lumbricus rubellus*, *Eisenia foetida*, *Ciprinus carpio*) [22-24] or plants (i.e. *Vicia faba*) [25], are slow (analysis generally needs 1–2 weeks), non specific, and expensive. On the contrary, biosensors are more specific and have low costs, thus can be used as early warning devices for the detection of environmental risk.

4.2. **MATERIALS AND METHODS**

4.2.1 Chemicals

Calf thymus double-stranded DNA type XV was purchased from Sigma (Milan, Italy). Sodium acetate (100%), sodium dioctyl sulfosuccinate (AOT) 98%, cetylpyridinium chloride monohydrate (CPyCl), taurocholic acid (TCA), poly(ethyleneglycol)-monooleate (PegMO), pluronic 127 (PF127)and Triton X 100 were from Sigma-Aldrich (Milan, Italy). Hexadecyl-trymethylammonium chloride (CTAC) ≥ 98%, and didodecylmethylammonium bromide (DDAB) ≥ 98% were purchased from Fluka. Sodium dodecyl sulfate (SDS) ≥ 90% was from Merk and Acetic acid ≥ 98% was from J.T. Backer. All samples were prepared by using purified water (conductivity ≤ 0.6 μS), prepared by means of a Millipore water purification system (Millipore, UK), as the solvent.
The luminometer Toxalert®100, bacteria *Vibrio Fisheri* and reagents were provided from Merck (Darmstadt, Germany).

4.2.2 Toxalert®100 procedure

In all the experiments the osmolality of all standard and sample solutions was adjusted to 2% NaCl for optimal reagent performance. To express the toxicity we have used the percentage of inhibition (I%), determined by

comparing the response given by a saline control solution to that corresponding to the sample as a function of incubation time. For all the experiments we used an incubation time of 5 min. Therefore the bioluminescence inhibition is determined by:

$$I\% = \left[\frac{\left(I_{oc} - I_f\right)}{I_{oc}}\right] x100 \qquad \text{Equation 4.1}$$

where I_{oc} is the corrected value of luminescence intensity of the control test suspension in relative luminescence unit (RLU) and I_f is the luminescence intensity of the test sample after the contact time of 5 min in RLU [26].

4.2.3 Electrochemical oxidation of guanine and adenine

The electrochemical mechanism of guanine and adenine oxidation was thoroughly investigated.[27, 28] The purine bases are involved in cellular energy transduction and signaling mediated by enzymatic oxidation reactions. Electrochemical processes involved in purine DNA base oxidation are similar to those involving enzymatic oxidation reactions and are of crucial importance to improve the interpretation of DNA drug/metal interactions that lead to oxidative damage of the biomolecule. [28-31]

The mechanism associated with the oxidation of guanine is schematically shown in Scheme 4.1a and is thought to be a - 4 e^-, - 4H^+ system, in which the guanine undergoes a first oxidation (-2e^-, - 2H^+) to 8-oxoguanine, then it undergoes a further reversible (-2e^-, -2H^+) oxidation.[32]

The oxidation of adenine at solid electrodes is expected to follow a three-step mechanism involving the total loss of six electrons and six protons [28, 33] (Scheme 4.1 b).

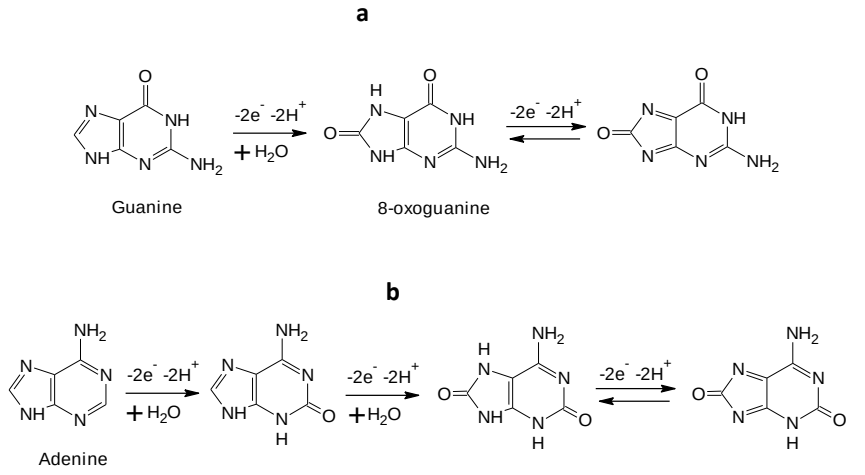

Scheme 4.1: Electrochemical oxidation mechanism of guanine (a) and adenine (b).

4.2.4. DNA-Biosensor functioning principle

Electrochemical measurements were performed through an Autolab PGSTAT-128 interfaced to an Acer TravelMate 5730 with Software GPES and screen-printed electrodes (paragraph 1.3.2.1). Square wave voltammetry (SWV) was the method used to detect the oxidation peak of guanine.

The measurement of samples with the DNA-modified screen-printed electrodes takes place in different steps. Firstly, the electrode surface - dipped in 2 mL of 0.25 M acetate buffer containing 10 mM KCl (pH = 4.75) - is pretreated by applying a potential of +1.6 V for 120 s and +1.8 V for 60 s. This step allows to oxidize the graphite impurities and to obtain a more hydrophilic surface to promote DNA immobilization. Then, screen-printed electrode (SPE) is dipped into 2 mL of DNA solution (50 ppm) in acetate buffer (0.25 M acetate buffer containing 10 mM KCl; pH 4.75), applying a potential of +0.5V (versus Ag-SPE) for 5 min, under stirring.

Figure 4.1 shows the guanine (~ +1.0 V *vs* Ag-SPE) and adenine (~ +1.25 V *vs* Ag-SPE) oxidation peaks before (Figure 4.1a) and after (Figure 4.1b) base line correction.

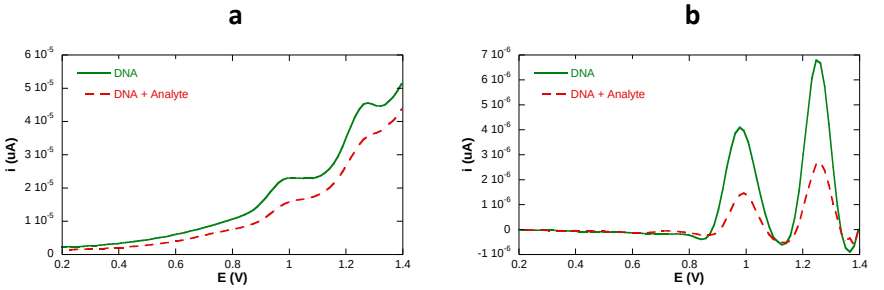

Figure 4.1. Redox behavior of guanine (+1.0V) and adenine (+1.25V) bases after a square wave voltammetric scan carried out with graphite screen printed working electrode. a) the oxidation peaks before and after the interaction with a toxic agent. b) the same peaks after baseline correction.

Analyte interactions with double stranded calf thymus DNA are evaluated measuring the height of the guanine oxidation peak since this is more reproducible than that of adenine. The result of this interaction is a decrease of guanine peak that was estimated by the parameter G%:

$$G\% = \frac{G_s}{G_b} x\ 100 \qquad \text{Equation 4.2}$$

where G_s is the height of the guanine oxidation peak in the presence of the analyte, and G_b the height of the guanine oxidation peak in the blank. Conventionally, if a sample has *G%* > 85% it is considered to be non toxic, if has a *G*% in the range 50- 85% it is considered to be moderately toxic, and if has *G* < 50% it is classified as toxic.[34]

A schematic block diagram of the experimental procedure is reported in Scheme 4.2.

The reproducibility of the guanine peak, calculated over three or more scans on different electrodes was estimated to be less than 10% of relative standard deviation (R.S.D.%).

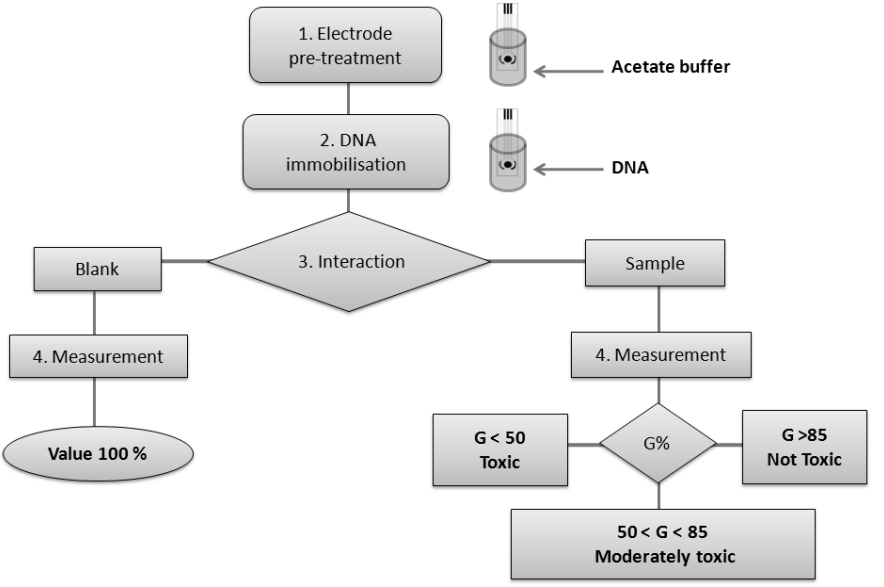

Scheme 4.2. Schematic drawing of the experimental procedure, which consisted in four steps: (1) electrode pre-treatment, (2) DNA immobilization on the electrode surface, (3) blank or sample interaction; (4) measurement.

4.2.5 Analysis of surfactant toxicity through DNA-biosensor

For blank and surfactant samples measurements, the incubation step was performed placing 10 µL of acetate buffer or sample solutions onto the working electrode surface for 2 min. After the interaction, the solution was removed and the screen-printed electrode was dipped into 2 mL of acetate buffer. Then a square wave voltammetric scan was used to evaluate the oxidation of guanine residues on the electrode surface. The height of the guanine peak (at +0.95 V *vs.* Ag screen-printed pseudo-

reference electrode) was measured. The scan was made using the following parameters: scan from +0.2 V to 1.35 V, E_{step} = 15 mV, $E_{amplitude}$ = 40 mV, Frequency = 200 Hz. The effect of the matrix on surfactant-DNA interaction was studied by dissolving the same amounts of surfactant (CTAC, AOT, Triton X 100) as in the case of acetate buffer both in tap water of Water Supply Company of Cagliari (pH 7.46; conductivity 0.30 mS/cm at 25°C) and sea water from 'Poetto' beach of Cagliari (pH 7.54; conductivity 45.2 mS/cm at 25°C).

4.2.6 Surface tension measurement

The critical micelle concentration (CMC) of surfactants was determined by surface tension measurements performed through a Tensiometer Sigma 703 according to duNouy Method. Surfactant solutions with different concentrations were prepared in acetate buffer (0.25 M acetate buffer containing 10 mM KCl; pH 4.75).

4.2.7 DNA-Screen Printed Electrodes storage

DNA was immobilized on SPE according to what reported in paragraph 4.2.4, then the DNA biosensors were lyophilized and stored into Petri dishes at room temperature for one month. The functioning of stored DNA-SPE was checked weekly by measuring the guanine oxidation peak both of the blank and a CTAC 5 mM solutions in acetate buffer.

4.3. RESULTS

4.3.1 Comparison between Toxalert®100 of AOT and Triton X 100 toxicity toward and DNA-biosensor.

As the first step of this work two surfactants (AOT and Triton X 100) were used for the comparison between the electrochemical DNA biosensor

and the commercial toxicity test Toxalert®100. This last is based on the bioluminescence inhibition of the bacterium *Vibrio fischeri* and thus directly related to the vitality (the metabolic status) of the bacterial cell. A toxic substance can cause changes of the cellular state to the cell wall, the cell membrane, the electron transport chain, the enzymes, and the cytoplasmatic constituents. These changes give rise to a decrease in the bioluminescence signal that is measured through a photomultiplier in a luminometer.

The results of the comparison between the two toxicity tests are reported in Figure 4.2 Toxicity is expressed in terms of 'inhibition (%)' for Toxalert®100 and in terms of -G% (= 100 - G%) for the DNA biosensor.

Although the two systems are based on very different methods, the curves show a comparable trend.

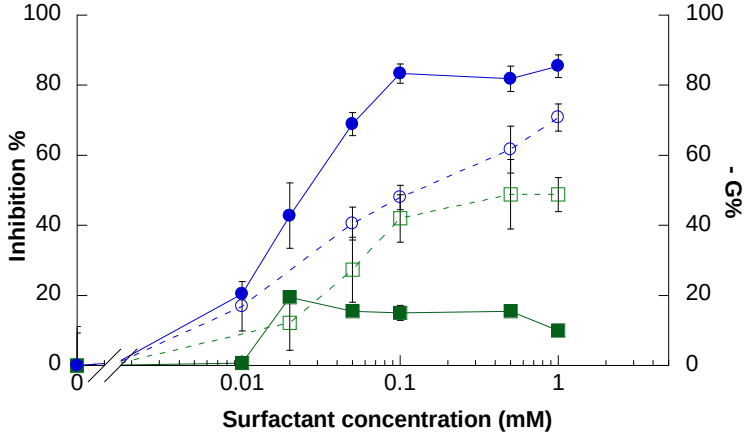

Figure 4.2. Toxalert® 100 and DNA biosensor response for AOT and Triton X 100 samples. (—•—) Inhibition % values for triton X 100 using Toxalert®100; (--o--) – G% values for Triton X 100 using DNA biosensor; (—■—) Inhibition % values for AOT using Toxalert®100; (--□--) - G% values for AOT using DNA biosensor.

In particular, at concentrations higher than 0.01M, the toxicity level of Triton X 100, detected by the Toxalert®100, is higher than that detected

by the DNA-biosensor. Differently, AOT resulted to be more toxic when analyzed through the DNA-biosensor with respect to the Toxalert®100. Moreover, toxicity reached a plateau value (at 0.1 mM for Triton X and 0.02 mM for AOT) for both surfactants when Toxalert®100 was used. Toxicity measurements carried out with ToxAlert®100 are very expensive due to the high cost of bacteria. On the contrary, the DNA biosensor uses a very small amount of DNA for every single measurement. Moreover, the DNA biosensor measurements are faster than those performed with Toxalert®100. DNA biosensors have already been tested for some classes of toxic compounds and also some surfactants [19, 35, 36], therefore it seemed interesting to explore their potentiality towards the toxicity of common types of cationic, anionic, and non ionic surfactants. Nine different surfactants, listed in Table 4.1, were chosen among those that are used in detergents, shampoos, toothpastes, cosmetics, drug carriers etc.

Table 4.1. Surfactants tested with the DNA Biosensor.

Surfactant	Molecular weight ($gmol^{-1}$)	Use
Hexadecyltrymethylammonium chloride (CTAC) 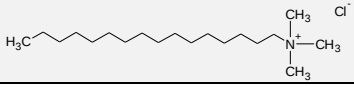	320.01	Antiseptic agent
Didodecylmethylammonium bromide (DDAB) 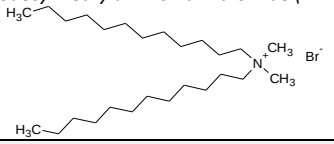	462.65	Cleanliness and disinfection of injured skin.
Cetylpyridunium chloride (CPyCl) 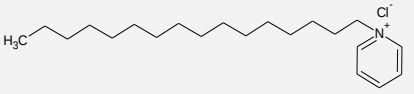	358.01	Mouthwashes, toothpastes, lozenges, throat sprays etc
Sodium dodecyl sulfate (SDS) 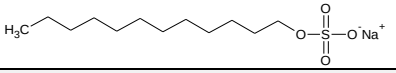	288.38	Soaps, shampoos, toothpaste and cleaning and hygiene products
Sodium dioctyl sulfosuccinate (AOT) 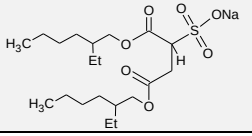	444.60	Wetting agent in agriculture
Taurocholic acid (TCA) 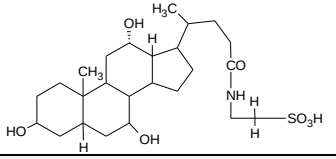	537.70	Biological detergent. Used in vaccines as a vehicle and drug delivery.
Polietylenglycolmonooleate (PEGMO) 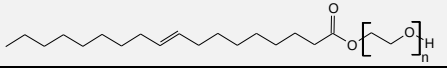	≈ 860	Pharmaceutical formulations
Pluronic 127 (PF127) $HO(CH_2CH_2O)_{106}-(CH_2CH_2(CH_3)O)_{70}-(CH_2CH_2O)_{106}H$	≈12700	Pharmaceutical formulations
Triton X 100 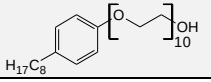	≈ 652.90	Detergent and pharmaceutical formulations

4.3.2 Toxicity of surfactants

Surfactants give self-association phenomena that are dependent on ionic strength of the water medium. Therefore, in order to critically evaluate the results, the critical micellar concentrations (CMC) of all surfactants were determined in the acetate buffer medium used for the measurements with DNA biosensors. The CMC in water (literature data) and in acetate buffer, here measured through surface tension measurements at 25 °C, are reported in Table 4.2. reports also the G% minimum value measured for each surfactant and the corresponding concentration.

The toxicity of the different surfactants (Table 4.1) was measured at room temperature (23±3°C). Figures 4.3, 4.4 ad 4.5 show the trend of toxicity – quantified in terms of G% - as a function of the concentration of the different surfactants.

The toxicity of cationic surfactants (Figure 4.3) Hexadecyltrymethylammonium chloride (CTAC), Cetylpyridunium chloride (CPyCl), and Didodecyldimethylammonium bromide (DDAB) increases with increasing surfactant concentration, and G% decreases reaching a minimum value. At higher concentrations G% increases up to a plateau value. The surfactant concentration at which a minimum value of G% is reached was 0.5 mM for CTAC, 1.0 mM for DDAB, and 0.125 mM for CPyCl. On the basis of the classification of toxicity, all surfactants are moderately toxic in correspondence of their minimum value of G% since it is equal to 55% for CTAC and DDAB, and 58% for CyCl. Taking into consideration CMC data reported in Table 4.2, it should be noticed that the cationic surfactants display a moderate toxicity for concentrations that are much higher than the CMC in the same medium, particularly in the case of CTAC.

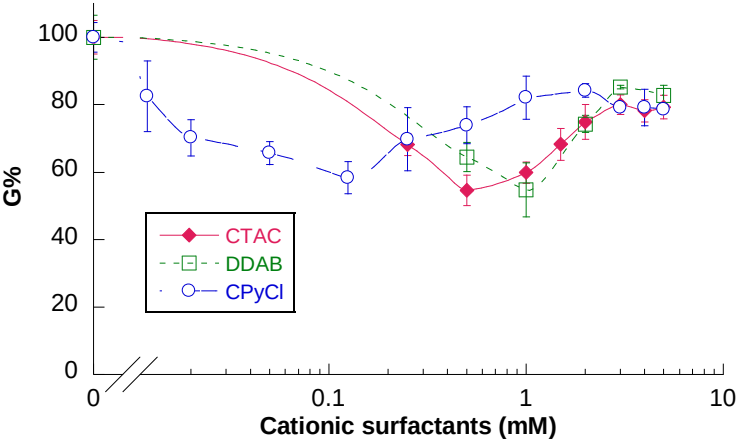

Figure 4.3: Guanine oxidation signal (G%) as a function of cationic surfactant concentration obtained by a DNA-biosensor.

Figure 4.4 shows the trend of toxicity of Sodium dodecyl sulfate (SDS), Dioctyl sulfosuccinate (AOT), and Taurocholic acid (TCA).

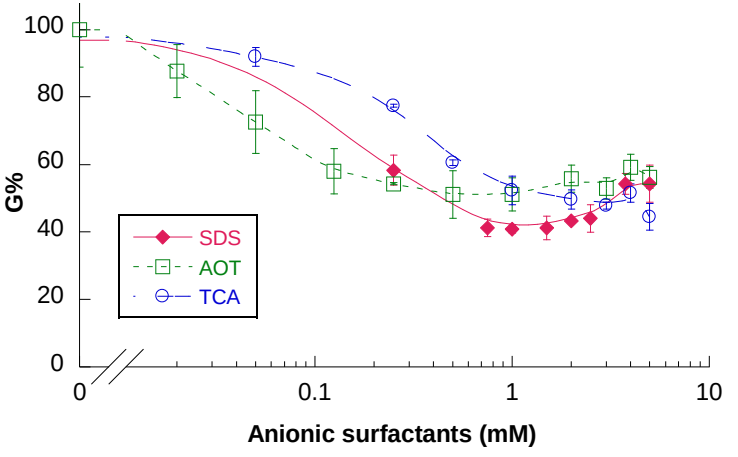

Figure 4.4: Guanine oxidation signal (G%) as a function of anionic surfactant concentration obtained by a DNA-biosensor

SDS shows a minimum value of G % (40%) that occurs in the range of concentration between 0.75-1.50 mM. This indicates that a concentration of SDS exceeding two-four times the cmc measured in buffer (see Table 4.2) can be associated to the highest degree of toxicity. As observed for cationic surfactants, higher concentrations slightly increase G% up to a plateau value. AOT shows a weakly significant minimum (G % = 50) for a concentration around 0.5 mM, whereas TCA reaches an asymptotic minimum (G % = 51) value for a concentration around 1 mM. These findings suggest that also AOT and TCA can be classified as toxic substances, particularly for concentrations greater than 0.5 and 1 mM, respectively. The toxicity data obtained for the nonionic surfactants (Pluronic 127, PEGMO, and Triton X 100) are shown in Figure 4.5.

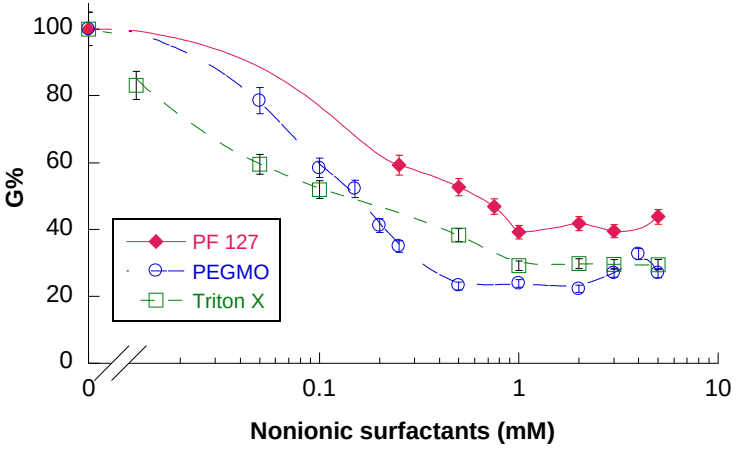

Figure 4.5: Guanine oxidation signal (G%) as a function of non ionic surfactant concentration obtained by a DNA-biosensor.

Also in this case, after an initial decrease, G% values reach a plateau. The lowest value of G% is equal to 23% for PEGMO, 39% for PF 127, and 29% for Triton X 100. These are values associated to a high degree of toxicity. It is worth noting that, as well as found for cationic surfactants, toxicity of

both anionic and non ionic surfactants is exerted when the concentration largely exceeds the CMC in all cases.

Table 4.2. Results obtained with the DNA biosensor and CMC values for each surfactant

	Surfactant	Minimum Value of G%	Surfactant concentration of the minimum (mM)	CMC (mM) in water	CMC (mM) in acetate buffer
Cationic	CTAC	55	≈ 0.5	1.00	0.01
	DDAB	55	≈ 1	0.15	0.02
	CPyCl	58	≈ 0.125	0.90	0.01
Anionic	SDS	41	≈ 1	8.00	0.37
	AOT	51	≈ 0.5	0.64	0.06
	TCA	50	≈ 1	8-12	0.40
Non Ionic	PEGMO	23	≈ 0.5	0.50	0.03
	PF 127	39	≈ 1	0.59	0.03
	TRITON X 100	29	≈ 1	0.20	0.07

4.3.3 Effect of the aqueous matrix on the toxicity

The effect of the aqueous matrix on the surfactant-DNA interactions was also investigated. To this purpose, different solutions of surfactants into two real water samples - tap water and sea water - were prepared. The aim of this study was to check whether the surfactants behavior changes in matrices more complex than acetate buffer. For these measurements the cationic surfactant CTAC, the anionic surfactant AOT, and the nonionic surfactant Triton-X 100 were chosen.

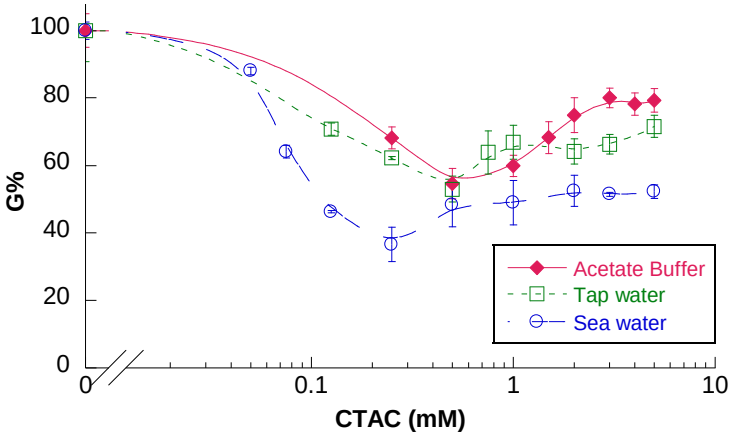

Figure 4.6: Guanine oxidation signal (G%) as a function of CTAC concentration obtained by a DNA-biosensor.

Figure 4.6 reports the trend of toxicity of CTAC in the different matrices. The three curves showed a similar trend with a minimum of the G% value at a surfactant concentration of 0.5 mM for acetate buffer and tap water and 0.25 mM for sea water. In sea water toxicity is always higher than that measured in tap water or in acetate buffer. The different matrix also affects the trends at concentrations higher than 2 mM where G% was lower in tap water than in acetate buffer.

Figure 4.7 reports the AOT behavior in the acetate buffer, tap and sea water. The G% values in sea water reach a high level of toxicity (G%<40) at very low surfactant concentrations (0.02 - 0.5 mM). At concentrations higher than 1 mM the different curves obtained in the three aqueous matrices follow a similar trend and give similar values of toxicity (G% >40).

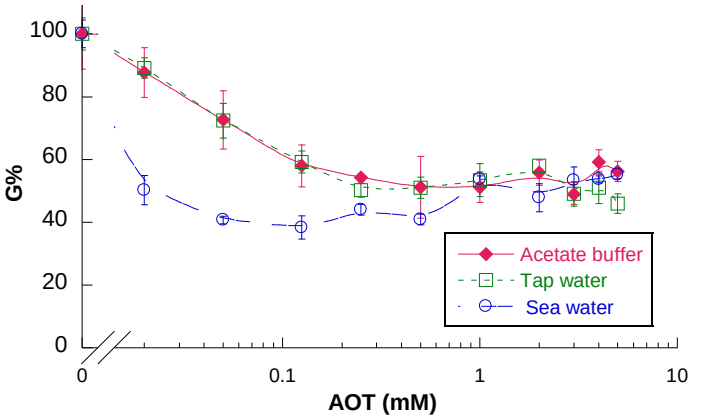

Figure 4.7: Guanine oxidation signal (G%) as a function of AOT concentration obtained by a DNA-biosensor.

Figure 4.8 shows the behavior of Triton X 100 in the different matrices; in the concentration range 0-0.1 mM the G% values almost overlap, whereas show a different behavior at concentrations higher than 0.1 mM. In particular at concentration 1 mM G% decreases in the order: tap water (G% >40) > sea water (G% ≈40) > acetate buffer (G% <40).

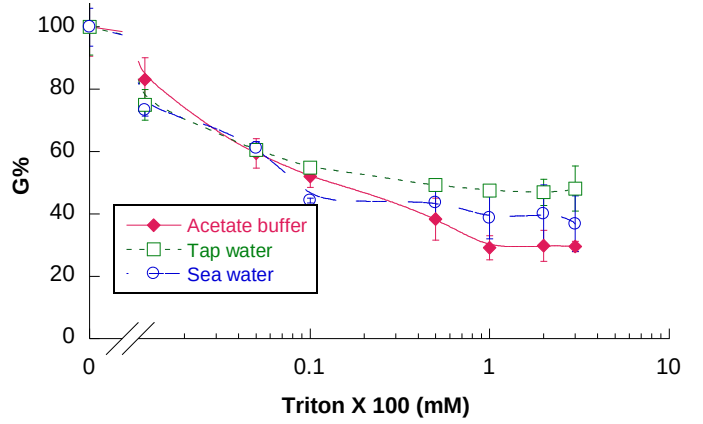

Figure 4.8: Guanine oxidation signal (G%) as a function of Triton X concentration obtained by a DNA-biosensor.

4.3.4 Stability towards storage of the immobilized DNA on screen-printed electrode

DNA immobilized on screen-printed electrodes were checked for storage stability also. The guanine oxidation peak of immobilized DNA samples, stored at room temperature in a Petri dish, was measured weekly using a solution of CTAC 5 mM in acetate buffer as sample. Figure 4.9 shows the current values (μA) obtained at different storage times. Blank and sample values increase but it is important to point out that G% - i.e. the ratio between blank and CTAC oxidation current - remains almost constant (≈ 77-83%).

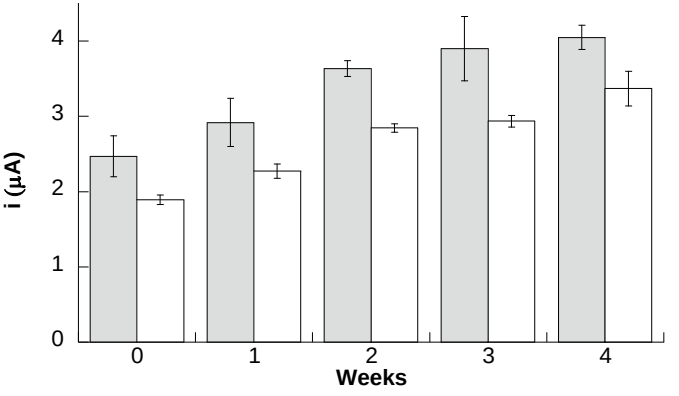

Figure 4.9: guanine oxidation signal G% as a function of storage time for blank (grey) and CTAC 5 mM (white)

4.4. DISCUSSION

The data reported in Table 4.2 demonstrate that all surfactants, with the exception of CPyCl, reach a minimum value of G% in the concentration range 0.5-1 mM.

In addition, the concentrations of surfactant corresponding to the lowest value of G% are significantly higher than the CMC in acetate buffer for all

surfactants. This indicates that the strongest surfactant-DNA interaction is obtained after the surfactant molecules have self assembled. It may be suggested that the self-assembled surfactant molecules are preferentially adsorbed at the solid (graphite-DNA) interface, and closely interact with DNA strands. This induces a reduction of the guanine oxidation peak, as quantified by SWV measurements. However, the occurrence of a plateau in most cases suggests that an equilibrium between the sites of interaction with DNA and the free micellar state is established as a result of both sterical hindrance and saturation of DNA sites.

Results reported in Table 4.2 also show that the order of toxicity of surfactants increases in the series: cationic < anionic < non-ionic. This fact agrees with what found in previous studies.[1, 3, 6] The European Community Environment Legislation classifies the toxicity of chemicals on the basis of Lethal Concentration 50 (LC50). LC50 is the concentration of a chemical which kills 50% of a sample population. According to this classification, all anionic surfactants studied are harmful (LC50 between 10 and 100mgL^{-1}), whereas nonionic surfactants are toxic (LC50 between 1 and 10 mgL^{-1}) [3]. Morral et al. [1] studied the toxicity of several surfactants through the test *Cladoceran Daphnia Magna* and found a model to relate the chain length of the surfactants to the toxic effect. These models predict that toxicity is higher for highly hydrophobic substances. Nonionic surfactants used in this work have higher molecular weights (Table 4.1) than cationic and anionic surfactants, and they are highly toxic. According to these results, several surfactants tested on aquatic organism resulted to be more toxic as their molecular weight increases.[1, 3] Moreover, from the previous order of increasing toxicity we may assert that, although DNA is an anionic polyelectrolyte, electrostatic interactions are not the driving force of the surfactant-DNA interaction. The higher toxicity values obtained with anionic and mainly with non ionic surfactants allows us to conclude that van der Walls forces play a significant role in promoting the interactions with DNA.

The effect of the matrix is not important if the toxicity of CTAC and AOT in acetate buffer and tap water is compared (Figure 4.7 and 4.8). Instead, the higher ionic strength of sea water that should screen the electrostatic interaction brings about an increase of the toxicity effects. This further reinforces the hypothesis that the DNA-surfactant interactions are strongly addressed also by van der Waals forces.

4.5. CONCLUSIONS

In the present chapter a fast and sensitive method to measure the level of toxicity of surfactants has been presented. This method uses an electrochemical DNA-based biosensor that, in comparison to traditional methods based on biological assays, is significantly faster. All surfactants studied, belonging to cationic, anionic, and non ionic categories, interact with DNA as determined by the decrease of the guanine oxidation peak. Cationic surfactants and SDS showed similar trends, i.e. the curve G% versus concentration presents a minimum (CTAC ≈ 0.5mM, DDAB ≈1 mM and CPyCl ≈ 0.125 mM). Differently, anionic and nonionic surfactants showed a linear decrease of G% with increasing concentration followed by an asymptotic value (SDS ≈1 mM, Triton X 100 ≤ 1mM, AOT < 0.5 mM, TCA <0.5 mM, PegMO < 0.5 mM, PF 127 < 0.3 mM) at the highest investigated concentrations. On the basis of the classification of G% values, cationic and anionic surfactants are moderately toxic whereas nonionic surfactants are clearly toxic. The matrix in which the surfactant is dissolved is able to modulate the interaction with DNA. In particular sea water seems to promote the interaction between surfactants and DNA as demonstrated by the low values of G%.
Finally, although surfactants interact with DNA giving a modification of its structure, genotoxicity could operate only when they are in effective contact. Fortunately, DNA of most living organisms is quite well protected by several biological barriers.

REFERENCES

1. Morrall, D. D.; Belanger, S. E.; Dunphy, J. C., Acute and chronic aquatic toxicity structure-activity relationships for alcohol ethoxylates. *Ecotoxicology and Environmental Safety* **2003,** 56, (3), 381-389.

2. Maki, A. W.; Bishop, W. E., Acute toxicity studies of surfactants to Daphnia magna and Daphnia pulex *Archives of Environmental Contamination and Toxicology* **1979**, 599-612.

3. Liwarska-Bizukojc, E.; Miksch, K.; Malachowska-Jutsz, A.; Kalka, J., Acute toxicity and genotoxicity of five selected anionic and nonionic surfactants. *Chemosphere* **2005,** 58, (9), 1249-1253.

4. Edwards, K. R.; Lepo, J. E.; Lewis, M. A., Toxicity comparison of biosurfactants and synthetic surfactants used in oil spill remediation to two estuarine species. *Marine Pollution Bulletin* **2003,** 46, (10), 1309-1316.

5. Rosen, M. J.; Li, F.; Morrall, S. W.; Versteeg, D. J., The Relationship between the Interfacial Properties of Surfactants and Their Toxicity to Aquatic Organisms. *Environmental Science & Technology* **2001,** 35, (5), 954-959.

6. Warne, M. S. J.; Schifko, A. D., Toxicity of Laundry Detergent Components to a Freshwater Cladoceran and Their Contribution to Detergent Toxicity. *Ecotoxicology and Environmental Safety* **1999,** 44, (2), 196-206.

7. Sirisattha, S.; Momose, Y.; Kitagawa, E.; Iwahashi, H., Toxicity of anionic detergents determined by Saccharomyces cerevisiae microarray analysis. *Water Research* **2004,** 38, (1), 61-70.

8. Chatterjee, A.; Moulik, S. P.; Majhi, P. R.; Sanyal, S. K., Studies on surfactant–biopolymer interaction. I. Microcalorimetric investigation on the interaction of cetyltrimethylammonium bromide (CTAB) and sodium dodecylsulfate (SDS) with gelatin (Gn), lysozyme (Lz) and deoxyribonucleic acid (DNA). *Biophysical Chemistry* **2002,** 98, 313-327.

9. Ferk, F.; Misik, M.; Hoelzl, C.; Uhl, M.; Fuerhacker, M.; Grillitsch, B.; Parzefall, W.; Nersesyan, A.; Micieta, K.; Grummt, T.; Ehrlich, V.; Knasmuller, S., Benzalkonium chloride (BAC) and dimethyldioctadecyl-ammonium bromide (DDAB), two common quaternary ammonium compounds, cause genotoxic effects in mammalian and plant cells at

environmentally relevant concentrations. *Mutagenesis* **2007,** 22, (6), 363-370.

10. Hamagucahndi, K.; Eiduscek, E., The Effect of Electrolytes on the Stability of the Deoxyribonucleate Helix. *Journal of the American Chemical Society* **1962,** 84, 1328-1338.

11. Osica, V. D.; Pyatigorskaya, T. L.; Polyvtsev, O. F.; Dembo, A. T.; Kliya, M. O.; Vasilchenko, V. N.; Verkin, B. l.; Sukharevsky, B. Y., Preliminary morphological and X-ray diffraction studies of the crystals of the DNA cetyltrimethylammonium salt. *Nucleic Acids Research* **1977,** 4, 1083-1096.

12. Kuhn, P. S.; Yan, L.; Barbosa, M. C., Charge inversion in DNA-amphiphile complexes: possible application to gene therapy. *Physica A* **1999,** 274, 8-18.

13. Smith, P.; Lynden-Bell, R. M.; Smith, W., Surfactant structure around DNA in aqueous solution. *Phys. Chem. Chem. Phys.* **2000,** 2, 1305-1310.

14. Hayakawa, K.; Santerre, P.; Kwak, J. C. T., The binding of cationic-surfactants by DNA. *Biophysical Chemistry* **1983,** 17, 175-181.

15. Shirahama, K.; Takashima, K.; Takisawa, N., Interaction between Dodecyltrimethylammonium Chloride and DNA. *The Chemical Society of Japan* **1987,** 60, 43-47.

16. Bhattacharya, S.; Mandal, S. S., Interaction of surfactants with DNA. Role of hydrophobicity and surface charge on intercalation and DNA melting. *Biochimica et Biophysica Acta* **1997,** 1323, 29-44.

17. Mel'nikov, S. M.; Sergeyev, V. G.; Yoshikawa, K., Discrete Coil-Globule Transition of Large DNA Induced by Cationic Surfactant. *Journal of the American Chemical Society* **1995,** 117, 2401-2408.

18. Mel'nikov, S. M.; Sergeyev, V. G.; Yoshikawa, K., Transition of Double-Stranded DNA Chains between Random Coil and Compact Globule States Induced by Cooperative Binding of Cationic Surfactant. *Journal of the American Chemical Society* **1995,** 117, 9951-9956.

19. Lucarelli, F.; Palchetti, I.; Marrazza, G.; Mascini, M., Electrochemical DNA biosensor as a screening tool for the detection of toxicants in water and wastewater samples. *Talanta* **2002,** 56, (5), 949-957.

20. Mel'nikov, S. M.; Yoshikawa, K., First-Order Phase Transition in Large Single Duplex DNA Induced by a Nonionic Surfactant. *Biochemical and Biophysical research communicarions* **1997,** 230, 514-517.
21. Tencaliec, A. M.; Laschi, S.; Magearu, V.; Mascini, M., A comparison study between a disposable electrochemical DNA biosensor and a Vibrio fischeri-based luminescent sensor for the detection of toxicants in water samples. *Talanta* **2006,** 69, (2), 365-369.
22. Malecki, M. R.; Neuhauser, E. F.; Loehr, R. C., The effect of metals on the growth and reproduction of Eisenia foetida (Oligochaeta, Lumbricidae). *Pedobiologia* **1982. ,** 24, (3), 129-137.
23. Langdon, C. J.; Piearce, T. G.; Black, S.; Semple, K. T., Resistance to arsenic-toxicity in a population of the earthworm Lumbricus rubellus. *Soil Biology and Biochemistry* **1999,** 31, (14), 1963-1967.
24. Rishi, K. K.; Jain, M., Effect of Toxicity of Cadmium on Scale Morphology in Cyprinus carpio (Cyprinidae) *Bulletin of Environmental Contamination and Toxicology* **1998,** 60, (2), 323-328.
25. Grant, W. F.; Lee, H. G.; Logan, D. M.; Salamone, M. F., The use of Tradescantia and Vicia faba bioassays for the in situ detection of mutagens in an aquatic environment. *Mutation Research/Fundamental and Molecular Mechanisms of Mutagenesis* **1992,** 270, (1), 53-64.
26. Merck, Toxalert®100 Operating Manual. **2000**.
27. Palecek, E., Adsorptive transfer stripping voltammetry: Determination of nanogram quantities of DNA immobilized at the electrode surface. *Analytical Biochemistry* **1988,** 170, (2), 421-431.
28. Glenn, D.; Philip, J. E., Electrochemical Oxidation of Adenine: Reaction Products and Mechanisms. *Journal of The Electrochemical Society* **1968,** 115, (10), 1014-1020.
29. Goyal, R. N.; Dryhurst, G., Redox chemistry of guanine and 8-oxyguanine and a comparison of the peroxidase-catalyzed and electrochemical oxidation of 8-oxyguanine. *Journal of Electroanalytical Chemistry* **1982,** 135, (1), 75-91.
30. Oliveira-Brett, A. M.; Diculescu, V.; Piedade, J. A. P., Electrochemical oxidation mechanism of guanine and adenine using a glassy carbon microelectrode. *Bioelectrochemistry* **2002,** 55, (1-2), 61-62.

31. Subramanian, P.; Dryhurst, G., Electrochemical oxidation of guanosine formation of some novel guanine oligonucleosides. *Journal of Electroanalytical Chemistry* **1987,** 224, (1-2), 137-162.
32. Li, Q.; Batchelor-McAuley, C.; Compton, R. G., Electrochemical Oxidation of Guanine: Electrode Reaction Mechanism and Tailoring Carbon Electrode Surfaces To Switch between Adsorptive and Diffusional Responses. *J. Phys. Chem. B* **2010,** 114, (21), 7423-7428.
33. Wang, Z.; Liu, D.; Dong, S., In situ infrared spectroelectrochemical studies on adsorption and oxidation of nucleic acids at glassy carbon electrode. *Bioelectrochemistry* **2001,** 53, (2), 175-181.
34. Bagni, G.; Osella, D.; Sturchio, E.; Mascini, M., Deoxyribonucleic acid (DNA) biosensors for environmental risk assessment and drug studies. *Analytica Chimica Acta 573–574* **2006**, 81-89.
35. Chiti, G.; Marrazza, G.; Mascini, M., Electrochemical DNA biosensor for environmental monitoring. *Analytica Chimica Acta* **2001,** 427, (2), 155-164.
36. Bagni, G.; Hernandez, S.; Mascini, M.; Sturchio, E.; Boccia, P.; Marconi, S., DNA Biosensor for Rapid Detection of Genotoxic Compounds in Soil Samples. *Sensors* **2005,** 5, (6), 394-410.

Chapter V

FTIR studies on interactions between surfactants and Calf Thymus DNA in solution and adsorbed on screen printed electrodes.

5.1 INTRODUCTION

The interactions between DNA and surfactants have been deeply studied, due to the great interest of biomedical sciences. The strong associative behavior between DNA and cationic surfactants has been used for many applications, i.e. the development of methods for DNA extraction and purification[1-3], as well as vehicles for gene delivery and gene transfection. The driving force for this strong association is the electrostatic interaction between the, positively charged head of the surfactant and the negative charges of DNA backbone. Potentiometric and fluorescence microscopy studies [4-6] showed that the interactions between cationic surfactants and DNA involve a two-step process. First, the presence of positive charges on surfactant facilitate electrostatic binding of molecules to the anionic phosphates groups of DNA; the result is the charge neutralization at the DNA backbone. Then, the hydrophobic chains of the surfactants interact with the hydrophobic interior of DNA, due to the spontaneous tendency of hydrophobic groups to minimize water contacts. Therefore, a highly cooperative binding event, that seems to involve hydrophobic interactions among the hydrocarbon chains of the surfactant, occurs.[7, 8] In addition, by means of fluorescence microscopy, it was found that DNA molecules undergo conformational changes. The double-stranded DNA exists in an elongated coil state in the native conformation. By adding CTAC up to a the concentration $\approx 10^{-5}$ M, DNA molecules maintain their native conformation. A further increase of CTAC concentration induces the collapse of DNA molecules towards a compacted globule state.[9, 10]

Kuhn et al. proposed a theoretical model that, considering both electrostatic and hydrophobic forces in surfactant-DNA systems, predicts the structure of DNA to be dependent on the surfactant chain length, the size of the polar head the concentrations of both components, the ionic strength, the pH, etc.[11, 12]

Most studies on DNA-surfactants interactions used cationic surfactants, whereas only few studies on the interaction between DNA and anionic surfactants have been reported.[8, 13, 14] Mel'nikov et al[15] studied the effect of the nonionic surfactant Triton X-100 on the conformational behavior of DNA through fluorescence microscopy. They found that DNA undergoes the coil to globule shape transition only at high (72wt% in aqueous solution) Triton X-100 concentrations.
In the previous chapter we investigated the toxicity of surfactants through a DNA biosensor.[16] DNA biosensors - based on Square Wave Voltammetry (SWV) measurements - use disposable sensors in which DNA strands, adsorbed onto the electrode surface, are the sensitive biological element. Indeed the DNA biosensor is sensitive to all the substances that cause modifications to double or single-stranded DNA.[13, 17] As a consequence of these modifications the height of the guanine oxidation peak decreases with respect to its height in the absence of toxic substances. It was found that cationic and anionic surfactants are moderately toxic, whereas non ionic surfactants are toxic.[16] In this chapter, in order to better understand the nature of DNA-surfactant interactions, we carried out zeta potential and FTIR measurements of buffer solutions containing DNA and different types of surfactants. In addition, by means of ATR-FTIR, we investigated the interactions of surfactants with screen printed electrode (SPE) adsorbed DNA.

5.2. **MATERIALS AND METHODS**

5.2.1 Chemicals

Calf thymus double-stranded DNA type XV was purchased from Sigma (Milan, Italy). Sodium acetate (98%), sodium dioctyl sulfosuccinate (AOT) 98%, cetylpyridinium chloride monohydrate (CPyCl), taurocholic acid (AcTC), poly(ethyleneglycol)-monooleate (PegMO), pluronic 127 (PF127)

and Triton X 100 were from Sigma-Aldrich (Milan, Italy). Hexadecyl-trymethylammonium chloride (CTAC) ≥ 98%, and didodecylmethylammonium bromide (DDAB) ≥ 98% were purchased from Fluka. Sodium dodecyl sulfate (SDS) ≥ 90% was from Merk and acetic acid ≥ 98% was from J.T. Backer. All samples were prepared by using purified water (conductivity ≤ 0.6 μS), prepared by means of a Millipore water purification system (Millipore, UK), as the solvent.

5.2.2 Interactions between DNA and surfactants in buffer solution through zeta potential and FTIR

Zeta potential and FTIR measurements were done preparing DNA, surfactants, and DNA-surfactant solutions with concentration 2 mg/mL in 0.25 M acetate buffer at pH 4.75 containing 10 mM KCl.
Zetasizer nano series (Malvern Instruments) was used for zeta potential measurement. The temperature of the scattering cell was fixed at 25°C and the data were analyzed with the Zetasizer software version 6.01.
FTIR spectra were obtained through a Bruker Tensor 27 spectrophotometer (120 scans; resolution 4 cm^{-1}) at 25 °C. The collected spectra were manipulated using OPUS (version 6.5) software. In particular, for FTIR measurements in solution a BIOATR accessory and a MCT (mercury-cadmium-telluride) detector regularly cooled with nitrogen were used.

5.2.3 Interactions between DNA adsorbed on SPE and surfactants trough ATR- FTIR spectroscopy

According to the procedure reported in paragraph 4.2.4 DNA was adsorbed on SPE (**DNA_{SPE}**) and then the biosensor was lyophilized. After the interaction between DNA_{SPE} and surfactants the oxidation was

performed as reported in paragraph 4.2.4. After the oxidation, the DNA_{SPE} was again lyophilized.
The interaction between DNA_{SPE} and surfactant are evaluated by ATR-FTIR spectroscopy. The AT-FTIR spectra of DNA_{SPE} before and after interaction with surfactants were collected through platinum ATR accessory with a diamond crystal and the DTGS (deuterated- tri-glycine- sulfate) detector.

5.3. RESULTS AND DISCUSSION

5.3.1 Zeta potential measurements

In order to better understand the nature of DNA-surfactant interactions showed in the preview chapter, firstly, interactions between DNA and surfactants were studied through zeta potential techniques. Table 5.1 shows the zeta potential measurement of DNA, surfactants (nine surfactants of which three are cationic, three anionic and three non ionic as shown in Table 4.1), and DNA-surfactant solutions in acetate buffer.

Table 5.1. Zeta potential results for surfactant and DNA-Surfactant solutions*

Surfactant name	***Z potential Surfactant (mV)***	***Z potential DNA- Surfactant (mV)***
CTAC	61.4 ± 1.9	17.1 ± 0.8
DDAB	96.6 ± 0.6	35.6 ± 0.7
CPyCl	58.4 ± 1.4	12.6 ± 0.7
SDS	-56.0 ± 2.0	-50.4 ± 0.8
AOT	-107.0 ± 5.6	-54.5 ±0.8
TCA	-73.2 ± 1.2	-52.6 ± 1.2
PEGMO	-7.7 ± 0.4	-49.9 ± 0.5
PF127	-3.7 ±0.1	-43.9 ± 1.3
Triton X 100	-8.4 ±0.4	-43.4 ±1.2

*Zeta potential of DNA is – 50 V (2mg/mL in acetate buffer 0.25 mM+ 10 mM in KCl)

Calf-thymus DNA has a highly negative zeta potential (-50 mV) due to the phosphate groups on its backbone. Cationic surfactants have a positive zeta potential, whereas anionic surfactants display a negative zeta potential according to the charge of surfactant head groups.

Table 5.1 reports also the data of zeta potential of the solutions obtained by mixing DNA and surfactants solutions. In the case of all cationic surfactants an increase of zeta potential (DNA-CTAC 17.1 mV, DNA-DDAB 35.6 mV and DNA-CPyCl 12.6 mV) is obtained. Zhao at al[18, 19] reported that zeta potential of DNA solution with increasing surfactant concentration increases up to reach a plateau corresponding to the DNA iso-electric point. In addition, they reported that the positive head group of surfactant molecules are adsorbed at the negatively charged DNA backbone, whereas their hydrophobic tails point outward. This favors hydrophobic attractions among surfactant molecules.[20]

The solutions containing DNA and anionic surfactants have zeta potential similar to those original DNA solution. Probably, surfactant molecules interact with DNA by partially screening its negative charges (DNA-SDS -50.4 mV, DNA-AOT -54.5 mV, DNA-TCA -52.6 mV)

The addition of a non ionic surfactant to DNA solution does not lead to a substantial variation of zeta potential (DNA-PEGMO -49.9 mV, DNA-PF127 -43.9 mV, DNA-triton X -43.4 mV).

The results obtained with cationic surfactants confirm that electrostatic forces are involved in the interactions, whereas for anionic and non ionic surfactants, also non polar groups are likely to be involved in the interaction with DNA, thus producing a more a complex interaction scheme.

5.3.2 FT IR measurements: study of interactions between DNA and surfactants in aqueous solution.

Figure 5.1 shows the FTIR spectrum of double stranded (ds) calf-thymus DNA in acetate buffer solution.

The main IR absorption bands fall in the region between 850 and 1800 cm^{-1}.[20] This spectral range has been subdivided into four regions. Each region contains bands belonging to specific parts of the nucleic acid structure, such as:

- nucleotide bases region (1800–1500 cm^{-1}): sensitive to effects of base pairing and base stacking ;
- base-sugar region (1500–1250 cm^{-1}): sensitive to glycosidic bond rotation, backbone conformation and sugar pucker;
- sugar-phosphate (1250–1000 cm^{-1}): sensitive to backbone conformation;
- sugar moiety region (1000–800 cm^{-1}): sensitive to sugar conformation.[21]

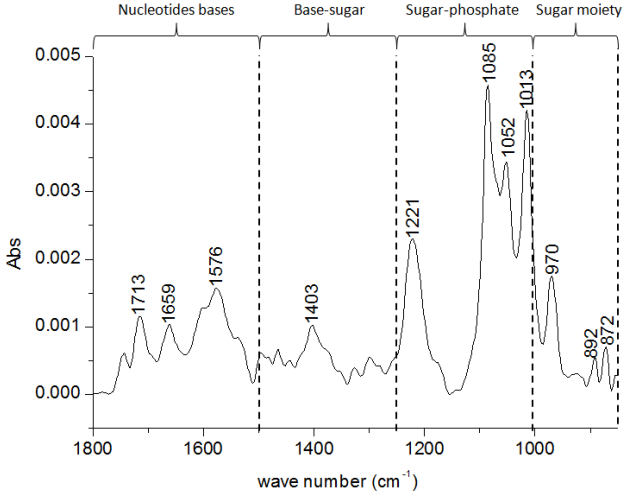

Figure 5.1. FTIR spectra of DNA in aqueous solution

Scheme 5.1 describes the relevant structures of DNA forming molecular species. Table 5.2 reports the assignments of the bands corresponding to the molecular groups shown in scheme 5.1 along with the corresponding literature references.

Table 5.2. Assignment of the main IR bands of DNA in aqueous solution

Wave -number (cm^{-1})	***Assignment***	***Reference***
1713-1715	C=O stretching of the base-paired residues	22
1671-1655	$C_{(4)}$=O stretching of thymine	23
1579-1576	Adenine in-plane ring vibration	21
1416-1403	Imidazole ring vibrations, and C-H/N-H bending	24
1225-1221	PO_2^- asymmetric stretching of sugar-phosphate backbone	21
1090-1085	PO_2^- symmetric stretching of sugar-phosphate backbone in-plane	22
1069-1044	O-$C_{(4)}$-C $_{(5)}$-O vibration of sugar-phosphate backbone	25
1020-1010	C-O vibration of deoxyribose	23
970-950	C-C vibration of sugar-phosphate backbone	21, 23
899-890	Deoxyribose ring vibration	21
882-877	N-sugar conformation	21

The band at 1713 and 1659 cm^{-1} are due to different C=O bonds present in the DNA molecule. The former is attributed to the C=O stretching of the base-paired residues, whereas the latter is assigned to the $C_{(4)}$=O vibration of thymine. The bands at 1221 and 1085 cm^{-1} are attributed to the PO_2^- asymmetric stretching and to the symmetric stretching (resulting from in plane vibration) respectively. The band at 1052 cm^{-1} is attributed to the vibration of O-C-$_{(4)}$-$C_{(5)}$-O Scheme 5.1) bonds of sugar-phosphate

backbone.[25] Other important bands are those at 1013 and 970 cm^{-1}, attributed to C-O (deoxyribose) and to C-C (backbone) vibrations respectively.

Hence, ds-DNA structure is characterized by the band at ≈1713 cm^{-1}. The disappearance of this band provides a spectral criterion for the denaturation of ds-DNA. In addition, also the bands occurring at 1085 cm^{-1} and 1052 cm^{-1}, due to sugar-phosphate vibrations, indicate the occurrence of the double stranded helical conformation.[22]

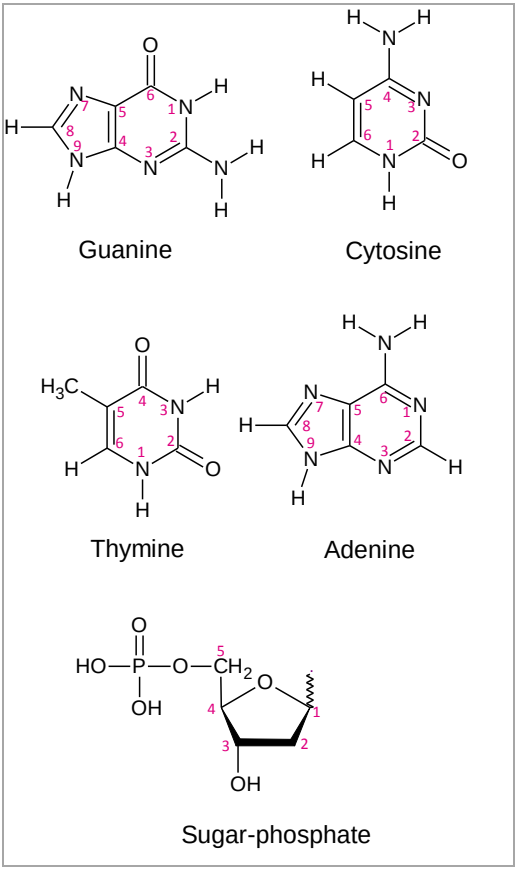

Scheme 5.1: **Structural elements of DNA indicating numbering of atoms**

Figure 5.2, 5.3 and 5.4 show the FT-IR spectra of aqueous solutions of surfactants in the absence and in the presence of DNA. The spectra of surfactants-DNA solutions show two strong bands, one of which, due to plane ring vibration mode of C-H and N-H of adenine and guanine rings[24], occurs at 1548-1550, while the second one, attributed to the imidazole ring vibration, occurs at 1411-1412 cm^{-1}, for all surfactants. Only in AOT case these bands are weak. This result suggests that DNA interacts with surfactants involving adenine and guanine rings mainly. The DNA band at ≈ 1710 cm^{-1} can still be identified in the presence of the surfactants except in the AOT case. The occurrence of this band can prove that DNA is not denatured by the surfactants. Indeed it remains in the double stranded helical configuration.[20]

In the spectrum of DNA-surfactants solution another characteristic band at 1276-1280 cm^{-1} occurs. This is due to the C-$N_{(3)}$-H bending of deoxyribose-thymine.[21] The band at 1225-1221 cm^{-1}, due to the asymmetric stretching vibrations of PO_2^-, is still observed in the spectra in the presence of the surfactants. The same situation occurs for bands at 1085,1052,1013 and 970 cm^{-1} that, in most cases, are shifted at higher wave numbers. In addition a change in the relative intensities of the various bands, compared to the spectrum of ds-DNA in solution, is often observed. In the case of DNA-AOT and DNA-non ionic surfactants spectra, these bands are likely to by hidden by the more intense bands of the surfactants.

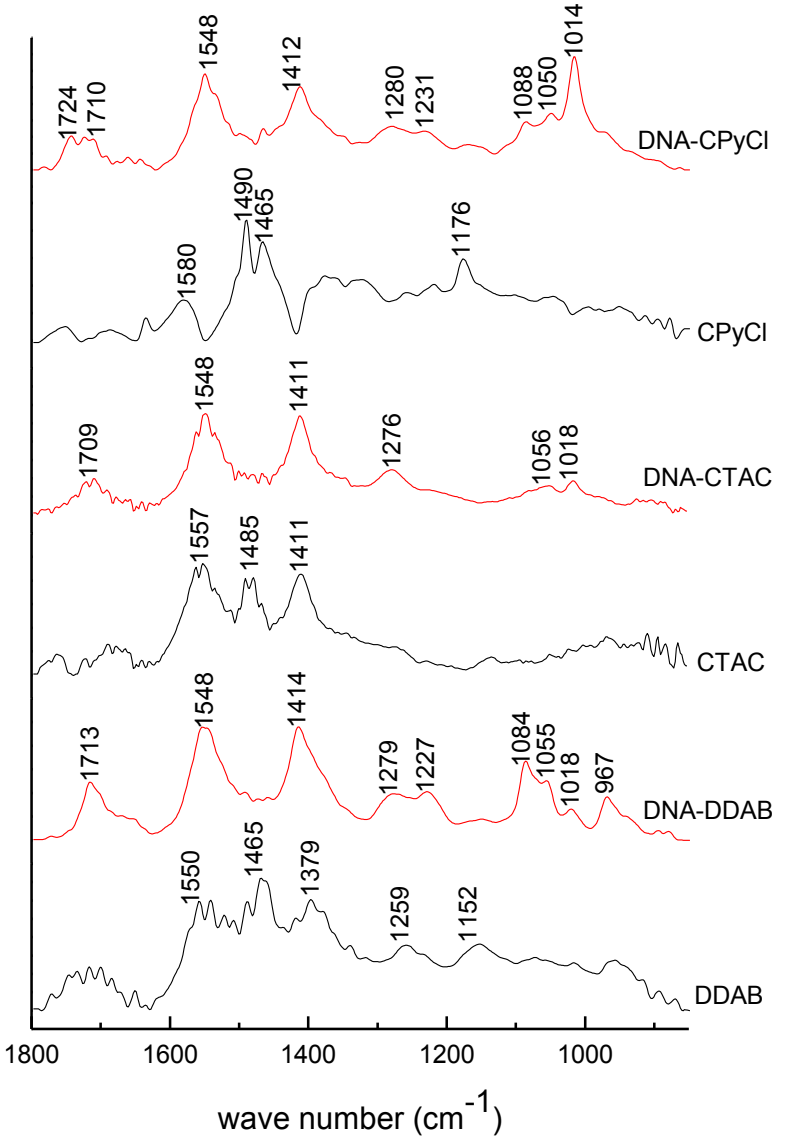

Figure 5.2: FTIR spectra in solution of cationic surfactants in the absence and in the presence of DNA.

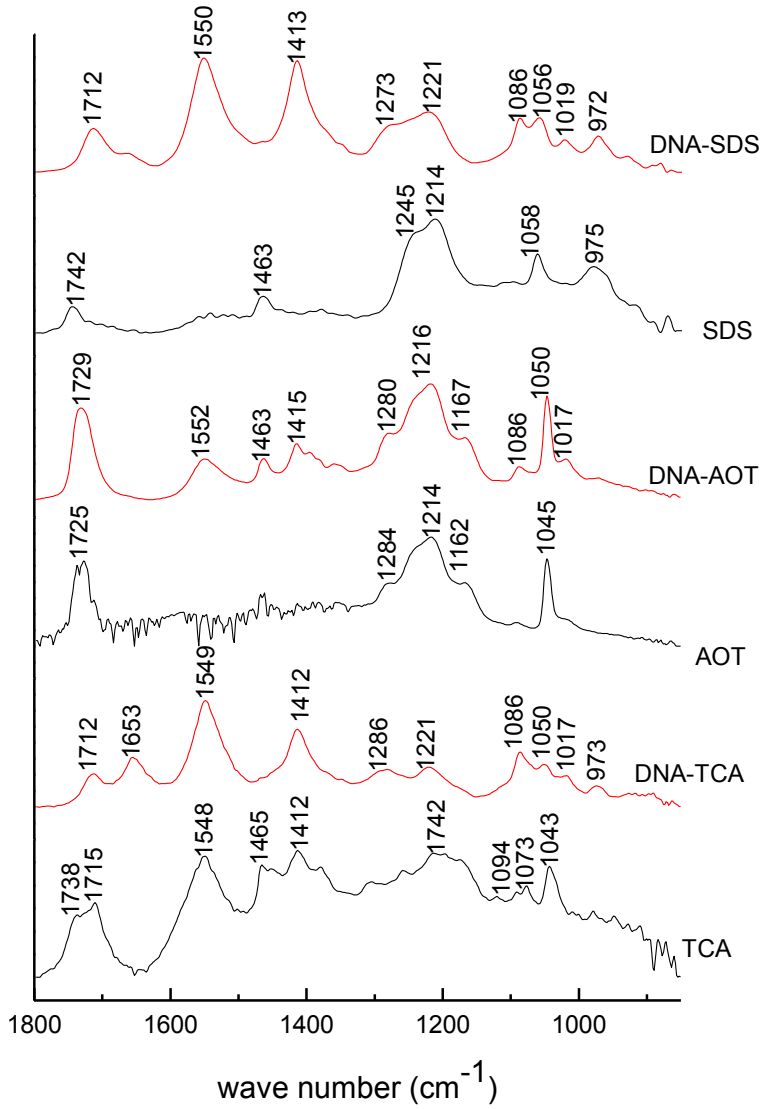

Figure 5.3: FTIR spectra in solution of anionic surfactants in the absence and in the presence of DNA.

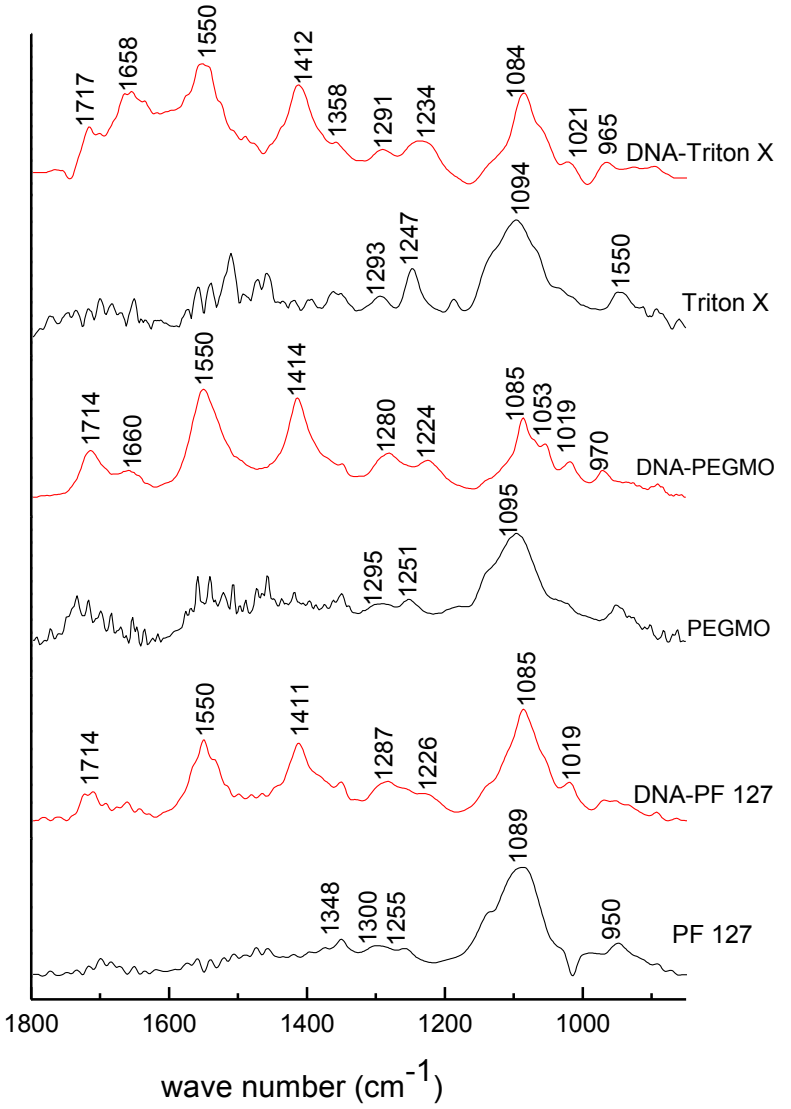

Figure 5.4. FTIR spectra in solution of nonionic surfactants in the absence and in the presence of DNA.

5.3.3 Characterization of DNA_{SPE} -surfactants interactions

Figure 5.5 shows the ATR-FTIR spectrum of lyophilized DNA. It is significantly different by that in solution, particularly the region between 1800 and 1300 cm^{-1} (Figure 5.1). Indeed, when the DNA is lyophilized a new band at ≈ 1694 cm^{-1}, attributed to the carbonyl group vibrations of unstacked bases, occurs.[22] A possible explanation could be that DNA presents different conformations depending on its physical state. This is the case of the bands at 1677–1653 cm^{-1} that are due to the stretching vibration of unpaired base ($C_{(6)}$=O of free guanine, $C_{(2)}$=O of free cytosine and $C_{(4)}$=O of free thymine).[21]

Other new bands, with respect to the spectrum of DNA in solution, occur at 1527, 1487 cm^{-1}. The first is assigned to in-plane vibration of cytosine in the single strand,[21] whereas the second one to the $C_{(8)}$-H group coupled with a ring vibration of guanine .

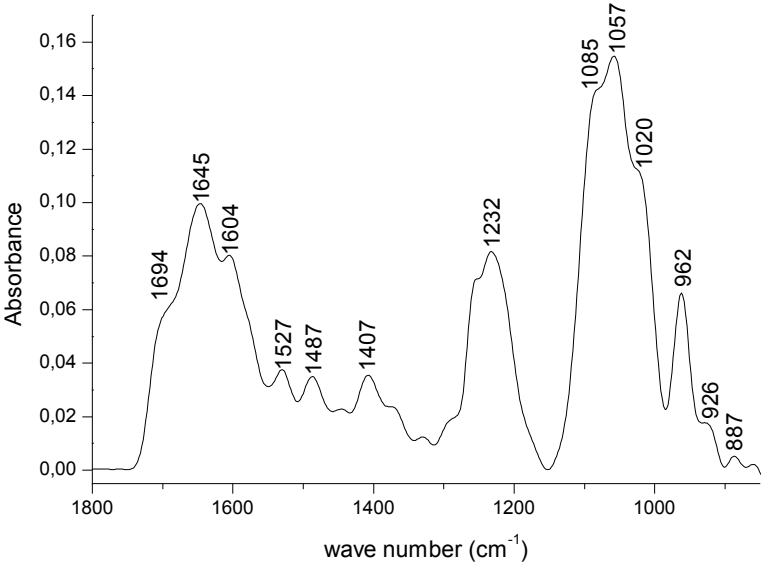

Figure 5.5. ATR-FTIR spectrum of lyophilized DNA

Figure 5.6 shows the ATR-FTIR spectrum of $DNA_{SPE,}$ i.e. after adsorption on the SPE surface. This spectrum is different by that of lyophilized DNA, probably because DNA structure is modified due to the interaction with SPE surface. In this spectrum seven bands can be clearly discerned: two strong bands at 1545 and at 1406 cm^{-1} and others five less intense bands at 1645, 1342, 1050, 1017 and 926 cm^{-1}. It is worth nothing that the bands at 1545 and 1406 cm^{-1} are very close to those observed in the spectra of DNA-surfactants in aqueous solution. Likely, in the adsorption process adenine and guanine rings interact with the graphite, as confirmed by the band at 1342 cm^{-1} that corresponds to the $N_{(7)}$-$C_{(8)}$-H vibrations adenine ring.[21] The bands at 1406 and 1017 cm^{-1} occur at higher wave numbers compared to DNA in aqueous solution. The absence of the bands at 1713,1223,1085 and 970 cm^{-1} suggests that the double helix is destroyed after adsorption on the electrode surface.[26]

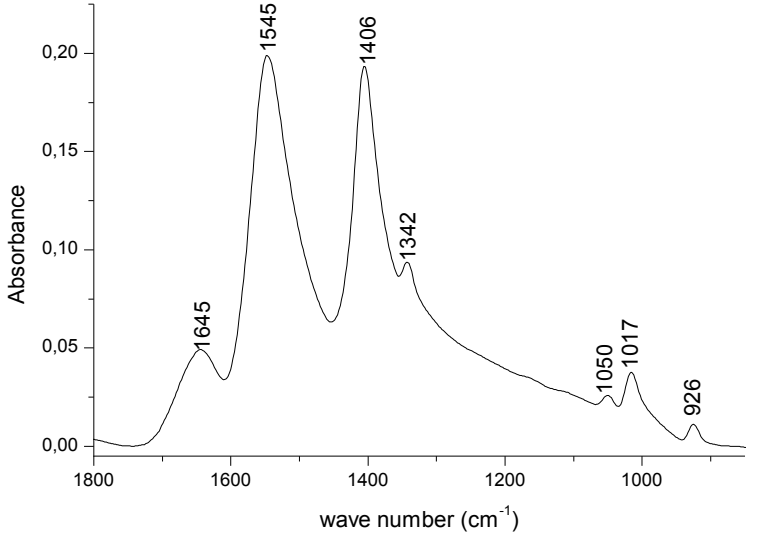

Figure 5.6. ATR-FTIR spectrum of DNA adsorbed on SPE

Also DNA_{SPE}-surfactant interactions were characterized by FTIR spectroscopy. Figure 5.7, 5.8 and 5.9 show the FTIR spectra of DNA adsorbed on SPE after treatment with surfactants, as described in paragraph 5.2.3. Generally the bands are less intense than in the spectrum before interaction with surfactants.

Figure 5.7 shows the FTIR spectra of DNA adsorbed on SPE after the treatment with cationic surfactants (DDAB,CTAC and CPyCl) . In general, there are the same bands occurring in the DNA_{SPE} spectrum although they are shifted to higher wave numbers (1-8 cm^{-1}).

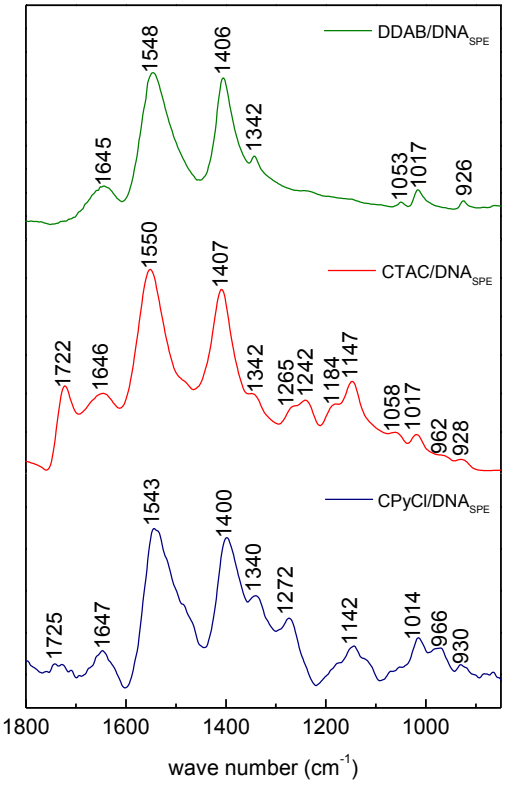

Figure 5.7. FTIR spectra of DNA biosensor after treatment with cationic surfactants.

The spectrum due to the interaction of DDAB with DNA_{SPE} is substantially the same as that of DNA_{SPE} shown in figure 5.6.

CTAC/DNA_{SPE} spectrum shows thirteen bands, among which six are new (1722, 1265, 1242, 1272, 1184, 1147 and 962 cm^{-1}.The band at 1722 cm^{-1} can be assigned to the in-plane stretching vibration mode of C=O of the bases. Upon considering that the FTIR spectrum of DNA in B-form shows a band at 1712-1715 cm^{-1} due to C=O stretching. The band at 1272 corresponds to the vibration of the pyrimidine ring.[27] In the spectrum of denatured DNA, the band shifts to higher wave numbers.[24] The band at 1184 cm^{-1} is assigned to the sugar-phosphate backbone vibration[21] and the band at 1147-1124 cm^{-1} is attributed to sugar vibration.[21] The band at 1242 cm^{-1} is assigned to the anti-symmetric PO_2^- stretching and the band at 1184 cm^{-1} is assigned to symmetric PO_2^- stretching of sugar-phosphate backbone.[21]

The CPyCl /DNA_{SPE} spectrum is very similar to that of CTAC/DNA_{SPE}. Only a couple of bands at 1242 and 1184 cm^{-1} disappeared.

Figure 5.8 shows the FTIR spectra of DNA adsorbed on SPE after the treatment with the anionic surfactants (SDS, TCA and AOT). SDS /DNA_{SPE} spectrum shows the same bands occurring in DNA_{SPE} spectrum, although with a lower intensity.

In the TCA /DNA_{SPE} spectrum new bands appear at 1271, 1121 and 978 cm^{-1}. These are the same bands occurring in the CTAC /DNA_{SPE} spectrum. DNA_{SPE} spectrum undergoes the same changes after interaction with AOT.

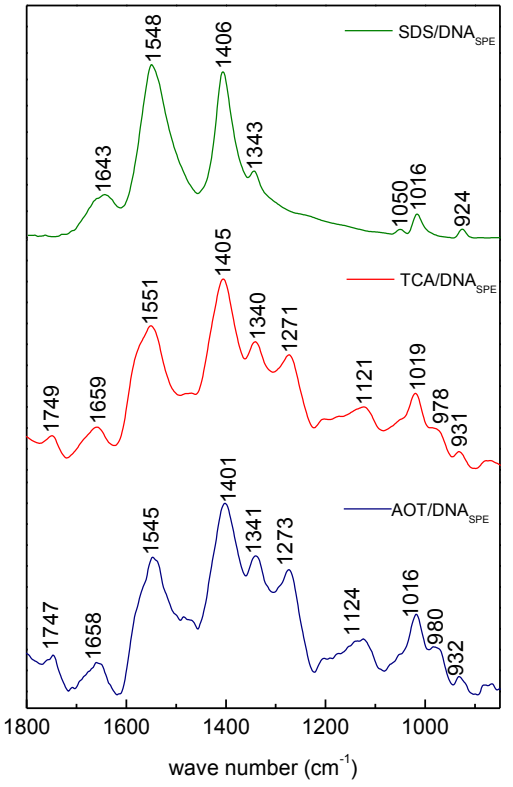

Figure 5.8 FTIR spectra of DNA biosensor after treatment with anionic surfactants

Figure 5.9 shows the FTIR spectrum of DNA_{SPE} after the treatment with the nonionic surfactants (PF 127, PegMO and Triton X 100).

In the case of PegMO /DNA_{SPE} new bands appear at 1225 and 1161 cm^{-1}.The interaction between DNA_{SPE} and Triton X 100 causes only a weak decrease of the initial bands.

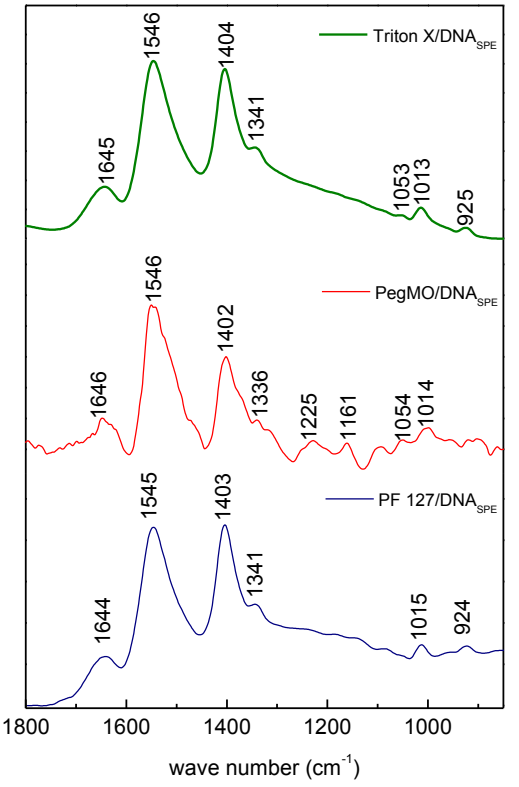

Figure 5.9. FTIR spectra of DNA biosensor after treatment with non ionic surfactants

5.3.4 FTIR-ATR spectra of oxidized DNA$_{SPE}$

According to the procedure reported in paragraph 4.2.4 the DNA adsorbed on SPE was oxidized in the presence of surfactants. Figure 5.10 and 5.11 show the spectra of oxidized DNA$_{SPE}$ after treatment with surfactants. All spectra show the same bands occurring in DNA adsorbed on SPE spectrum before treatment with surfactants (Figure 5.6). The oxidation involves only the DNA molecules (guanines and adenines) in direct contact with the electrode surface. indeed the bands of new

carbonyl groups (scheme 4.1) formed after the oxidation are not occurring in the spectra. Table 5.3 reports the absorbance of the bands at 1545 and 1406 cm^{-1} of DNA after treatment with the surfactants and successive oxidation. The data show that the oxidation causes an increase of the intensity of the bands, hence the surfactants do not favor DNA desorption from SPE. Moreover, after oxidation the surfactants molecules used in the experiments are probably been removed since in the spectra only the bands due to DNA_{SPE} are observed.

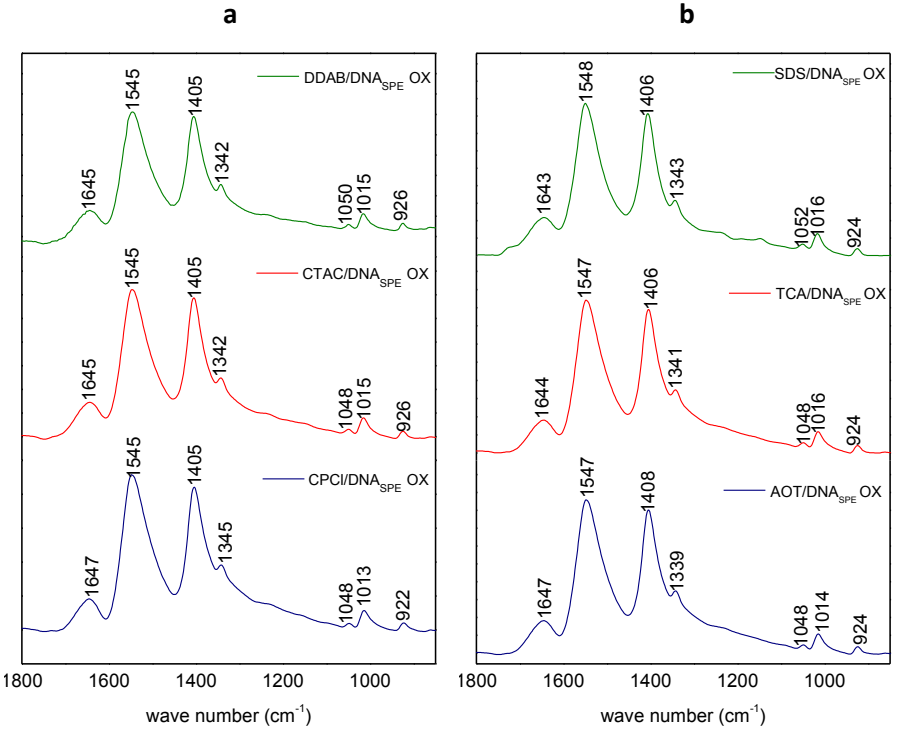

Figure 5.10: FTIR spectra of oxidized DNA_{SPE} after treatment with a) cationic surfactant ; b) anionic surfactants.

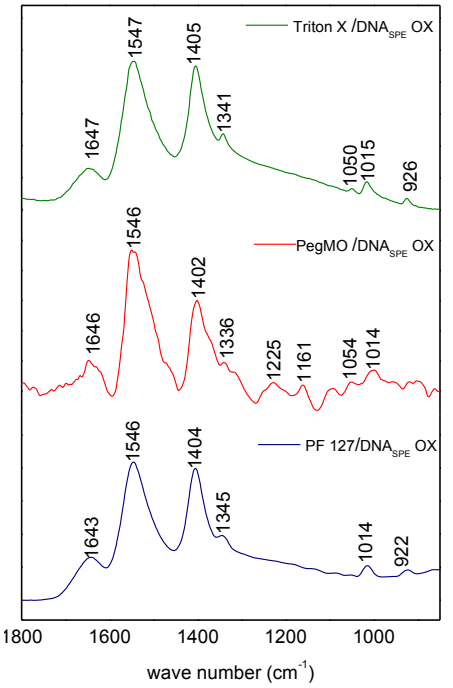

Figure 5.11: FTIR spectra of oxidized DNA_{SPE} after treatment with non ionic surfactant

Table 5.3: Absorbance values before and after oxidation of DNA_{SPE}-surfactant

Cationic surfactants- DNA_{SPE}			
Absorbance	***DDAB***	***CTAC***	***CPyCl***
A_{1546}	0.158	0.131	0.0086
A_{1406}	0.122	0.118	0.0086
$A_{1546\ OX}$	0.194	0.156	0.116
$A_{1406\ OX}$	0.181	0.147	0.110
Anionic surfactants- DNA_{SPE}			
Absorbance	***SDS***	***TCA***	***AOT***
A_{1546}	0.161	0.068	0.016
A_{1406}	0.158	0.091	0.022
$A_{1546\ OX}$	0.211	0.210	0.214
$A_{1406\ OX}$	0.20	0.197	0.20

Non ionic surfactants- DNA_{SPE}			
Absorbance	***Triton x***	***PegMo***	***PF 127***
A_{1546}	0.152	0.011	0.108
A_{1406}	0.147	0.008	0.108
$A_{1546\ OX}$	0.229	0.197	0.207
$A_{1406\ OX}$	0.226	0.199	0.199

5.4. CONCLUSIONS

In this chapter we investigated the interactions between surfactants and DNA, in solution, and adsorbed on screen printed electrodes by Zeta potential and FTIR spectroscopy.

Zeta potential measurements suggest an external interaction for cationic surfactants and also for anionic surfactants since DNA charge is lower in the DNA-surfactant solutions than in the DNA solution. For non ionic surfactants the zeta potential measurements suggest that surfactants molecules interact with internal groups of DNA.

In most cases, FTIR spectral studies in solution showed that the interaction involves purine (adenine and guanine) rings as confirmed by the two bands at 1548 and 1412 cm^{-1}. Moreover, in the DNA-surfactants spectra the bands at 1221 and 1085 cm^{-1}, due to PO^-_2 groups are observed. Therefore the groups involved in the interaction between DNA and surfactants, in agreement with the literature, are both external and internal groups of the double helices (imidazole ring of purines). Moreover, DNA maintains its double helical structure after the treatment with the surfactants.

When DNA is immobilized onto SPE the absence of the bands at 1712, 1088 and 1052 cm^{-1}, suggests that the double helix is destroyed. In most DNA biosensor-surfactant spectra (cationic and anionic) new bands at 1184, 1147-1124 and 1275-1264 cm^{-1} appear. The first is assigned to the sugar-phosphate backbone vibration and the second to sugar vibrations.

The last corresponds to the vibration of pyrimidine rings in nucleic acid. Therefore, also for the interaction between DNA adsorbed on SPE and surfactants both internal and external groups are involved, in agreement with zeta potential results.

REFERENCES

1. Hamaguchi, K.; Geiduschek, E. P., The Effect of Electrolytes on the Stability of the Deoxyribonucleate Helix. *Journal of the American Chemical Society* **1962,** 84, (8), 1329-1338.
2. Hamagucahndi, K.; Eiduscek, E., The Effect of Electrolytes on the Stability of the Deoxyribonucleate Helix. *Journal of the American Chemical Society* **1962,** 84, 1328-1338.
3. Osica, V. D.; Pyatigorskaya, T. L.; Polyvtsev, O. F.; Dembo, A. T.; Kiiya, M. O.; Vasilchenko, V. N.; Verkin, B. I.; Sukharevskv, B. Y., Preliminary morphological and X-ray diffraction studies of the crystals of the DNA cetyltrimethylammonium salt. *Nucl. Acids Res.* **1977,** 4, (4), 1083-1096.
4. Osica, V. D.; Pyatigorskaya, T. L.; Polyvtsev, O. F.; Dembo, A. T.; Kliya, M. O.; Vasilchenko, V. N.; Verkin, B. l.; Sukharevsky, B. Y., Preliminary morphological and X-ray diffraction studies of the crystals of the DNA cetyltrimethylammonium salt. *Nucleic Acids Research* **1977,** 4, 1083-1096.
5. Hayakawa, K.; Santerre, P.; Kwak, J. C. T., The binding of cationic-surfactants by DNA. *Biophysical Chemistry* **1983,** 17, 175-181.
6. Shirahama, K.; Takashima, K.; Takisawa, N., Interaction between Dodecyltrimethylammonium Chloride and DNA. *The Chemical Society of Japan* **1987,** 60, 43-47.
7. Pattarkine, M. V.; Ganesh, K. N., DNA-Surfactant Interactions: Coupled Cooperativity in Ligand Binding Leads to Duplex Stabilization. *Biochemical and Biophysical Research Communications* **1999,** 263, (1), 41-46.

8. Bhattacharya, S.; Mandal, S. S., Interaction of surfactants with DNA. Role of hydrophobicity and surface charge on intercalation and DNA melting. *Biochimica et Biophysica Acta* **1997,** 1323, 29-44.
9. Mel'nikov, S. M.; Sergeyev, V. G.; Yoshikawa, K., Discrete Coil-Globule Transition of Large DNA Induced by Cationic Surfactant. *Journal of the American Chemical Society* **1995,** 117, 2401-2408.
10. Mel'nikov, S. M.; Dias, R.; Mel'nikova, Y. S.; Marquesa, E. F.; Miguela, M. G.; Lindmana, B., DNA conformational dynamics in the presence of catanionic mixtures. *FEBS Letters* **1999,** 453, 113^118.
11. Kuhn, P. S.; Barbosa, M. C.; Levin, Y., Complexation of DNA with cationic surfactant. *Physica A: Statistical Mechanics and its Applications* **1999,** 269, (2-4), 278-284.
12. Kuhn, P. S.; Yan, L.; Barbosa, M. C., Charge inversion in DNA-amphiphile complexes: possible application to gene therapy. *Physica A* **1999,** 274, 8-18.
13. Lucarelli, F.; Palchetti, I.; Marrazza, G.; Mascini, M., Electrochemical DNA biosensor as a screening tool for the detection of toxicants in water and wastewater samples. *Talanta* **2002,** 56, (5), 949-957.
14. Chatterjee, A.; Moulik, S. P.; Majhi, P. R.; Sanyal, S. K., Studies on surfactant–biopolymer interaction. I. Microcalorimetric investigation on the interaction of cetyltrimethylammonium bromide (CTAB) and sodium dodecylsulfate (SDS) with gelatin (Gn), lysozyme (Lz) and deoxyribonucleic acid (DNA). *Biophysical Chemistry* **2002,** 98, 313-327.
15. Mel'nikov, S. M.; Yoshikawa, K., First-Order Phase Transition in Large Single Duplex DNA Induced by a Nonionic Surfactant. *Biochemical and Biophysical research communicarions* **1997,** 230, 514-517.
16. Cugia, F.; Salis, A.; Barse, A.; Monduzzi, M.; Mascini, M., Surfactants toxicity towards an electrochemical DNA biosensor. **Submitted**.
17. Chiti, G.; Marrazza, G.; Mascini, M., Electrochemical DNA biosensor for environmental monitoring. *Analytica Chimica Acta* **2001,** 427, (2), 155-164.

18. Zhao, X.; Shang, Y.; Liu, H.; Hu, Y., Complexation of DNA with cationic gemini surfactant in aqueous solution. *J. Colloid Interface Sci.* **2007,** 314, (2), 478-483.
19. Zhao, X.; Shang, Y.; Liu, H.; Hu, Y.; Jiang, J., Interaction of DNA with Cationic Gemini Surfactant Trimethylene-1,3-bis (dodecyldimethyl-ammonium bromide) and Anionic Surfactant SDS Mixed System. *Chinese Journal of Chemical Engineering* **2008,** 16, (6), 923-928.
20. Lee, H.; Mijovic, J., Bio-nano complexes: DNA/surfactant/single-walled carbon nanotube interactions in electric field. *Polymer* **2009,** 50, (3), 881-890.
21. Banyay, M.; Sarkar, M.; Gräslund, A., A library of IR bands of nucleic acids in solution. *Biophysical Chemistry* **2003,** 104, (2), 477-488.
22. Sukhorukov, G. B.; Montrel, M. M.; Petrov, A. I.; Shabarchina, L. I.; Sukhorukov, B. I., Multilayer films containing immobilized nucleic acids. Their structure and possibilities in biosensor applications. *Biosensors and Bioelectronics* **1996,** 11, (9), 913-922.
23. Dovbeshko, G. I.; Gridina, N. Y.; Kruglova, E. B.; Pashchuk, O. P., FTIR spectroscopy studies of nucleic acid damage. *Talanta* **2000,** 53, (1), 233-246.
24. Wang, Z.; Liu, D.; Dong, S., In-situ FTIR study on adsorption and oxidation of native and thermally denatured calf thymus DNA at glassy carbon electrodes. *Biophysical Chemistry* **2001,** 89, (1), 87-94.
25. Shabarchina, L. I.; Montrel, M. M.; Sukhorukov, G. B.; Sukhorukov, B. I., The structure of multilayer films of DNA-aliphatic amine is preparation technique dependent. *Thin Solid Films* **2003,** 440, (1-2), 217-222.
26. Braun, C. S.; Jas, G. S.; Choosakoonkriang, S.; Koe, G. S.; Smith, J. G.; Middaugh, C. R., The Structure of DNA within Cationic Lipid/DNA Complexes. *Biophysical Journal* **2003,** 84, (2), 1114-1123.
27. Wang, Z.; Liu, D.; Dong, S., In situ infrared spectroelectrochemical studies on adsorption and oxidation of nucleic acids at glassy carbon electrode. *Bioelectrochemistry* **2001,** 53, (2), 175-181.

Chapter VI

Hybridization assay coupled to magnetic beads for nucleic acid detection

6.1 INTRODUCTION

The DNA complementarity principle was discovered 50 years ago, along with the famous double-helical DNA structure.[1] This discovery soon led to several hybridization assays to detect specific nucleic acid sequences procedures in molecular biology and biotechnology.

A exciting area in analytical chemistry is the use of nucleic acids for biosensing: they act as biorecognition elements in the biosensors design.[2] Due to the use of nucleic acids hybridization, significant improvements has been made leading toward rapid and accurate detections of specific DNA or RNA sequences.[3, 4] The strong interaction between two complementary nucleic acid strands gives the basis for these nucleic acid hybridization devices. A single stranded DNA molecule (capture probe) is immobilized onto the surface of the sensor to form a hybrid with the complementary target strand in a sample. However, a problem with electrochemical DNA detection is the absorption of non-specific DNA sequences at the electrode surface. The phenomenon can reduce the sensitivity of the assay. Due to this problem many researchers exploited the possibility of realizing the hybridization assay on the surface of paramagnetic beads. Several magnetic bead based electrochemical genosensors have been reported in literature.[5-8]

In addition, to produce highly sensitive DNA sensors, it is essential to develop an oligonucleotide sequence having stronger hybridization with a complementary single-strand DNA. Many types of modifications have been introduced into native nucleic acids for developing nucleic acids with high affinity toward DNA, such as peptide nucleic acid (PNA), locked nucleic acid (LNA) as a reported in paragraph 1.4.1.4.

PNA and LNA show high affinity toward DNA and RNA single strands having a complementary base sequence to form the double-strand by hybridizing with Watson-Crick type hydrogen bonds.[9-11]

The melting temperatures for PNA-DNA and DNA-DNA double-strands with 15 base pairs into their single strands are 69 °C and 54 °C, respectively[9], indicating PNA-DNA is more stable than DNA-DNA.
LNA shows high affinity also towards RNA.[11] The melting temperatures of LNA-RNA and LNA-DNA double strands are 2-10 °C and 1-8 °C higher than those of DNA-RNA and DNA-DNA, respectively.[11] Therefore, it is expected that LNA single strand may accomplish stronger hybridization with DNA as well as with RNA. However, the origin of the stronger hybridization of LNA-DNA and LNA-RNA double strands has never been elucidated theoretically.
In this chapter the investigation of the properties of PNA and LNA capture probes in the development of an enzyme-amplified electrochemical hybridization assay is reported. The hybridization event as well as the labeling step was performed on paramagnetic microbeads.
The assay was applied to the analytical detection of DNA as well as RNA sequences. In particular, we have compared the analytical properties of PNA and LNA capture probes with classical DNA sequences. Hybridization with RNA target as well as with the corresponding DNA sequence was also performed.

6.2 Materials and methods

6.2.1 Chemicals

Streptavidin–alkaline phosphatase (1000Umg^{-1}), α-naphthylphosphate, bovine serum albumin (BSA), magnesium chloride, and diethanolamine were obtained from Sigma–Aldrich. Disodium hydrogenphosphate and potassium chloride were purchased from Merck. Streptavidin-coated paramagnetic beads (iron oxide microparticles with the diameter of approximately 1.0±0.5 μm) were purchased from Promega (USA). MilliQ water was used throughout this work.

When RNA target was analyzed, DEPC (diethilpyrocarbonate) was added to water. DEPC treatment of solutions is accomplished by adding 1 ml DEPC per liter of water, stirring overnight, autoclaving for 1 h to hydrolyze any remaining DEPC, and then passing the solution through a 0.2 µm filter RNAse free (Sarstedt, Germany). Synthetic DNA and RNA oligonucleotides were obtained from MWG Biotech AG (Germany). Synthetic LNA oligonucleotides were obtained from Eurogentec S.A. (Belgium). Synthetic PNA oligonucleotides were obtained from Panagene (Korea).
The sequences of synthetic oligonucleotides are reported below:

DNA capture probe	5' – TAT TTA CGT GCT GCT A – TEG-biotina - 3'
LNA capture probe	5' – TA**T** **T**TA **C**GT G**C**T G**C**T A – TEG-biotina - 3' (LNA nucleotides are in bold)
PNA capture probe	5' – TAT TTA CGT GCT GCT A – TEG-biotina - 3'
RNA target	5'-UAG CAG CAC GUA AAU A -3'
DNA target	5' TAG CAG CAC GTA AAT A–TEG–biotin-3'

LNA capture probe is a DNA–LNA sequence, but for brevity it will be called simply LNA capture probe[12], and its sequence was optimized in PNA stock solution was prepared in trifluoroacetic acid (TFA), following the instruction of the manufacturer.
The compositions of the used buffers are:

- **PB**: phosphate buffer 0.1 M, pH 7.4.
- **PB-T**: phosphate buffer 0.5 M, pH 7.4, added of 0.005% of tween 20.
- **PBS**: phosphate buffer 0.1 M, pH 7.4, added of 0.1 M NaCl.

- **PBS-T**: phosphate buffer 0.1 M, pH 7.4, added of 0.1 M NaCl and 0.005% of tween 20.
- **DEA**: diethanolamine buffer 0.1 M, pH 9.6
- **DEA-T**: diethanolamine buffer 0.1 M, pH 9.6, added of 0.005% of tween 20

Electrochemical measurements were performed through an μAutolab type II interfaced to a Compaq iPAQ Pocket PC with Software GPES 4.9 software (Metrohm) using screen-printed electrodes as a transducer.
All potentials were referred to the Ag/AgCl screen-printed pseudo-reference electrode. All electrochemical experiments were carried out at room temperature (25 °C). To perform electrochemical measurement using magnetic beads, SPE were kept horizontally and a magnet holding block was placed on the bottom part of the electrode, to better localize the beads onto the working surface. Then, a known volume of a solution containing the enzymatic substrate was added on the SPE surface to close the electrochemical cell.

6.2.2 Steptavidin- Biotin binding

In this study we used streptavidin-coated magnetic beads and biotinylated capture probes to bind covalently the probes on the beads surface.
Streptavidin is a tetrameric protein that has various biochemical applications. Each monomer of streptavidin binds one molecule of biotin (a water soluble vitamin) with remarkably affinity.[13, 14] This bond is one of the stronger non covalent interaction found in biological systems. The extremely tight and specific biotin binding ability of streptavidin has made this protein a very powerful biological tool for a variety of biological and biomedical analyses.[15] The dissociation constant of the streptavidin-biotin complex is approx 10^{-15} M. The complex is stable over wide pH and

temperature ranges and it is generally disrupted only by conditions which lead to irreversible denaturation of the protein[16, 17]

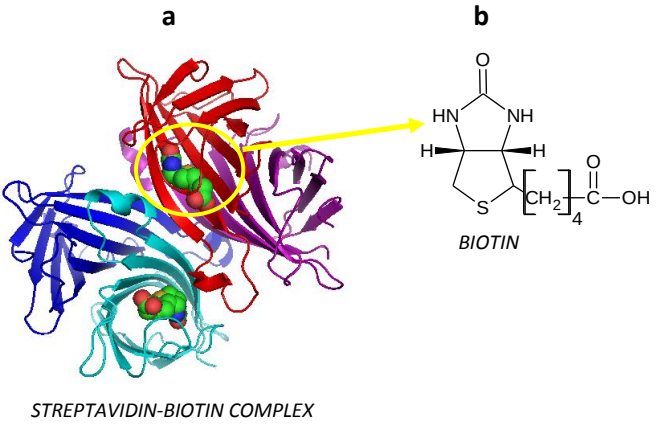

Figure 6.1: a) Tetrameric structure of streptavidin with two bound biotins; b) Biotin structure

6.2.3 Biomodification of streptavidin-coated magnetic beads

The functionalization with biotinylated capture probe was carried out on aliquots of 600µL, containing 1 mg/mL of beads. The beads were washed three times with 600 µL of phosphate buffer and re-suspended in 500 µl of 0.6 µM solution of capture probe. After an incubation of 30 min under continuous mixing, the beads were washed three times with PB-T. Finally, modified beads were incubated for 15 min with 500 µl of a 500 µM solution of biotin in PB-T, to block the remaining streptavidin active sites on the probe-functionalized surface, and hence to prevent the undesired binding of other biotinylated oligonucleotides. The probe-modified and biotin-blocked beads were then washed three times and re-suspended to

1 mg/ml in PB-T. Every aliquot, stored at 4 °C, can be used for several experiments.

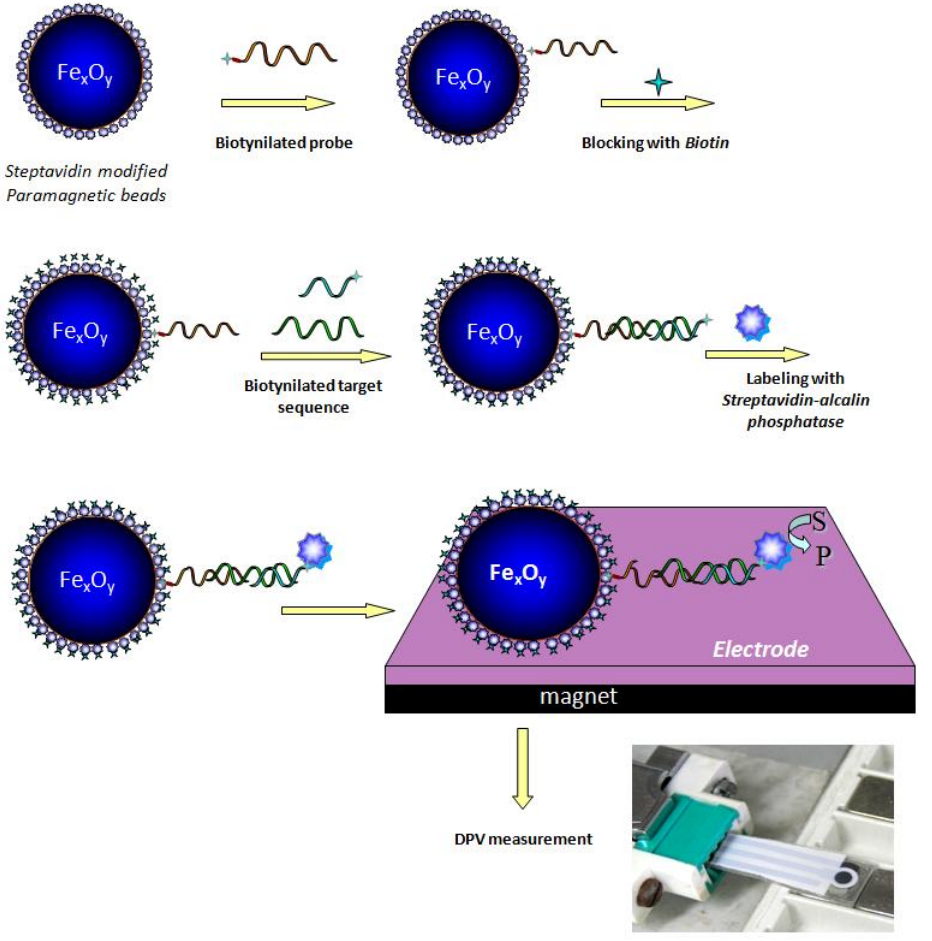

Scheme 6.1: Hybridization assay

6.2.4 Hybridization assay

Hybridization experiments were carried out as reported in Scheme 6.1. Biotinylated targets were diluted to the desired concentration in PB-T. Both the blank (without target) and the corresponding non-complementary strand were used as negative controls. For every assay 20 µl of probe-modified beads were employed. After magnetic separation of the beads, using a magnetic particle concentrator (MagneSphere Magnetic Separation Stand, Promega), the buffer was removed carefully and then the beads were incubated with 50 µl of the target solution for 15 min. After hybridization, the beads were washed three times with 100 µl of DEA-T, to remove non-specifically adsorbed sequences.

6.2.5 Labelling with alkaline phosphatase and electrochemical detection

The biotinylated hybrid obtained at the electrode surface was reacted with 10µL of a solution containing 0.8 U/mL of the streptavidin–alkaline phosphatase conjugate and 10 mg/mL of BSA (blocking agent) in DEA-T buffer. After 20 min, the sensors were washed twice with 15µL of DEA buffer. The planar electrochemical cell was then incubated with 400µL of a α-naphthyl phosphate solution (1mgmL^{-1} in DEA buffer). After 15 min, the electrochemical signal of the enzymatically produced α-naphthol (scheme 6.2) was measured by differential pulse voltammetry (DPV) (modulation time,0.05 s; interval time, 0.15 s; step potential, 5mV; modulation amplitude, 70mV; potential scan, from 0 to 600 mV).

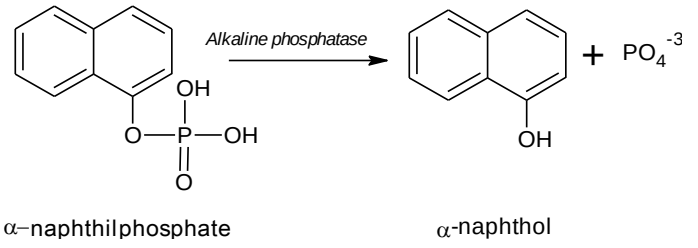

Scheme 6.2 : Oxidation of α-naphitlphosphate on SPE

Figure 6.2 shows the oxidation peaks obtained for the detection of DNA using different concentrations of DNA target. The height of each peaks was taken as the analytical signal. The corresponding current value is directly proportional to the target concentration.

All the results shown in this chapter are the mean of at least three measurements and the error bars correspond to the standard deviations.

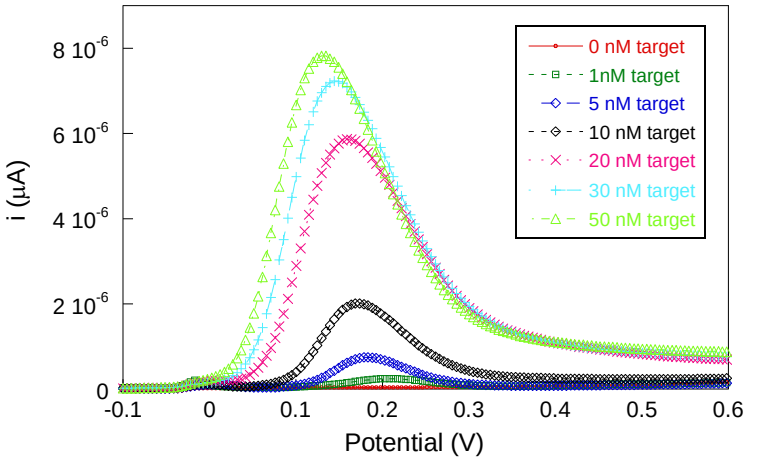

Figure 6.2 : DPV signals recorded after 6 min of substrate incubation for the detection of DNA target using DNA probe.

6.3 RESULTS AND DISCUSSION

In the next paragraphs are reported the results obtained for the detection of DNA and RNA targets through a hybridization assay using DNA,LNA and PNA probes. In particular, LNA and PNA are synthetic molecules where the sugar phosphate backbone has been replaced with some units of locked ribose in the 3'-*endo* conformation or by N-(2-amino-ethyl)-glycine respectively (as a reported paragraphs 1.4.14 and 1.4.1.5). The aim of this work was to determine if the use of a particular probe was able to increase the sensitivity of the hybridization assay.

6.3.1 Assay for detection of DNA target using DNA, LNA and PNA probes

In order to test the analytical performance of the assay, a calibration experiment was realized using DNA target. Figure 6.3 shows the calibration curves obtained using different probes (DNA, LNA and PNA) through DPV measurements.

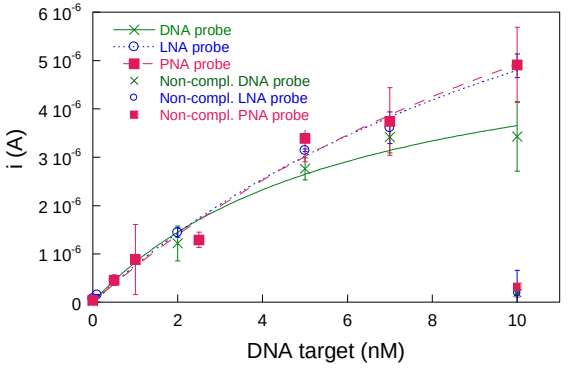

Figure 6.3: Calibration curves of target DNA. DPV measurements were performed at −0.2 V vs. Ag/AgCl.

The voltammetric response increased with the target concentration up to 10 nM, that is the highest concentration used for the different probes. In the linear part of the curves (range 0-2 nM) all probes show similar current values. Above the concentration 2 nM of the target, LNA and PNA probes display higher current values than DNA probe.
The tree probes have similar behavior when used with DNA target. The use of LNA and PNA probe increases the sensitivity of the assay for concentration higher than 2 nM with respect to DNA. The selectivity of the assay was ascertained using a fully non-complementary sequence, as also reported in Figure 6.3. The low values obtained show that absorption of non-specific DNA sequence at the beads surface is almost negligible.

6.3.2 Assay for detection of RNA target using DNA, LNA and PNA probes

Figure 6.4 shows the calibration curves of RNA target obtained using the different probes. Also in this case, the voltammetric response increased with the target concentration up to 10 nM, for all probes.

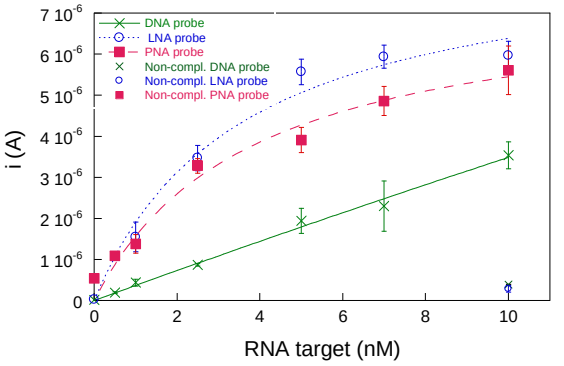

Figure 6.4: Calibration curves of target RNA. DPV measurements were performed at -0.2 V vs. Ag/AgCl.

The DNA calibration curve shows a linear trend in the whole investigated range, and the sensitivity of the assay is lower than LNA and PNA. The affinity of probes toward the RNA sequence increases in the order: DNA< PNA <LNA.
Again, the selectivity of the assay was checked using a fully non-complementary sequence, as reported in Figure 6.4. The low values obtained show that absorption of non-specific RNA sequence at the beads surface is again negligible.

6.4 CONCLUSIONS

In this chapter we reported preliminary results concerning the comparison of three different capture probes (DNA, LNA and PNA) toward two different target sequences (DNA and RNA) for the development of a hybridization assay. The analytical detection of DNA and RNA sequences was performed on paramagnetic microbeads.
For all probes the hybridization reaction allows for the determination of DNA and RNA targets with a detection limit of 0.5 nM, that is the lowest examined concentration.
In the case of the analysis of a DNA target, the results show that the use of LNA and PNA as a capture probe does not increase the sensitivity of the assay. The opposite occurs in the case of a RNA sequence. LNA and PNA probes increase the sensitivity assay, particularly for concentrations of target above 2 nM. The affinity of probes towards the RNA target increases in the order: DNA< PNA <LNA.
It should be remarked that, the immobilization on paramagnetic beads is a method suitable to monitor affinity reactions between DNA or RNA complementary sequences.
In conclusion, a prototype of electrochemical DNA biosensor to determine specific oligonucleotide sequences has been obtained. Next step of this work will be the application of this method to real samples.

REFERENCES

1. Watson, J. D.; Crick, F. H. C., Molecular Structure of Nucleic Acids: A Structure for Deoxyribose Nucleic Acid. *Nature* **1953,** 171, (4356), 737-738.
2. Palchetti, I.; Mascini, M., Nucleic acid biosensors for environmental pollution monitoring. *Analyst* **2008,** 133, (7), 846-854.
3. Sassolas, A.; Leca-Bouvier, B. D.; Blum, L. J., DNA Biosensors and Microarrays. *Chemical Reviews* **2007,** 108, (1), 109-139.
4. Hahn, S.; Mergenthaler, S.; Zimmermann, B.; Holzgreve, W., Nucleic acid based biosensors: The desires of the user. *Bioelectrochemistry* **2005,** 67, (2), 151-154.
5. Wang, J.; Xu, D.; Erdem, A.; Polsky, R.; Salazar, M. A., Genomagnetic electrochemical assays of DNA hybridization. *Talanta* **2002,** 56, (5), 931-938.
6. Palecek, E.; Billová, S.; Havran, L.; Kizek, R.; Miculková, A.; Jelen, F., DNA hybridization at microbeads with cathodic stripping voltammetric detection. *Talanta* **2002,** 56, (5), 919-930.
7. Palecek, E.; Fojta, M., Magnetic beads as versatile tools for electrochemical DNA and protein biosensing. *Talanta* **2007,** 74, (3), 276-290.
8. Berti, F.; Laschi, S.; Palchetti, I.; Rossier, J. S.; Reymond, F.; Mascini, M.; Marrazza, G., Microfluidic-based electrochemical genosensor coupled to magnetic beads for hybridization detection. *Talanta* **2009,** 77, (3), 971-978.
9. Egholm, M.; Buchardt, O.; Christensen, L.; Behrens, C.; Freier, S. M.; Driver, D. A.; Berg, R. H.; Kim, S. K.; Norden, B.; Nielsen, P. E., *Nature* **1993,** 365, 556–568.
10. Eriksson, M.; Nielsen, P. E., Solution structure of a peptide nucleic acid DNA duplex. *Nature Structural Biology* **1996,** 3, (5), 410-413.
11. Petersen, M.; Wengel, J., LNA: a versatile tool for therapeutics and genomics. *Trends in Biotechnology* **2003,** 21, (2), 74-81.
12. Laschi, S.; Palchetti, I.; Marrazza, G.; Mascini, M., Enzyme-amplified electrochemical hybridization assay based on PNA, LNA and DNA probe-modified micro-magnetic beads. *Bioelectrochemistry* **2009,** 76, (1-2), 214-220.

13. Chaiet, L.; Wolf, F. J., The properties of streptavidin, a biotin-binding protein produced by Streptomycetes. *Archives of Biochemistry and Biophysics* **1964,** 106, 1-5.
14. Green, N., Avidin and streptavidin. *Methods Enzymol* **1990,** 184, 51-67.
15. Sano, T.; Smith, C. L.; Cantor, C. R., Expression and Purification of Recombinant Streptavidin-Containing Chimeric Proteins. In 1997; Vol. 63, pp 119-128.
16. Bayer, E. A.; Ben-Hur, H.; Gitlin, G.; Wilchek, M., An improved method for the single-step purification of streptavidin. *Journal of Biochemical and Biophysical Methods* **1986,** 13, (2), 103-112.
17. Hofmann, K.; Wood, S. W.; Brinton, C. C.; Montibeller, J. A.; Finn, F. M., Iminobiotin affinity columns and their application to retrieval of streptavidin. *Proc. Natl. Acad. Sci USA* **1980,** 77, (8), 4666-4668.

CONCLUDING REMARKS

The aim of this work was the development of two different DNA based biosensors for environmental and medical applications.

The first was an electrochemical DNA biosensor for the detection of toxicity substances. In particular the toxicity of nine surfactants (three cationic, anionic and non ionic) was investigated. All surfactants caused a decrease of the guanine peak. In particular, the nonionic surfactants were highly toxic, followed by the moderately toxic anionic and cationic surfactants. In several cases it was observed that toxicity decreases with increasing concentration as a consequence of surfactant self-assembly. Indeed, the self-assembly process competes with the interaction with DNA.

Some selected surfactants were investigated both in sea water and tap water, and data were compared to those obtained in acetate buffer. The matrix in which the surfactant is dissolved is able to modulate the interaction with DNA. In particular sea water seems to promote the interaction between surfactants and DNA.

The interaction between surfactants and Calf Thymus DNA in solution and adsorbed on the sensor surface was investigated by FTIR spectroscopy. In most cases, FTIR studies in solution showed that the interaction involves purine (adenine and guanine) rings and the backbone PO^-_2 groups. Therefore the groups involved in the interaction between DNA and surfactants, are both external and internal groups of the double helices.

Significant specific modification of DNA bands appear after the immobilization process on the graphite solid surface and after the interaction with the surfactant. When DNA is immobilized onto SPE the double helix is almost lost. In most DNA biosensor-surfactant spectra and also in the spectra of DNA adsorbed on SPE and treated with the surfactants, both internal and external groups are involved.

Zeta potential measurements suggest an external interaction for cationic and anionic surfactants, whereas internal interactions seem to occur in the case of non ionic surfactants in agreement also with FTIR results.

The second kind of biosensor studied was a Genosensor for the analytical detection of DNA and RNA sequences. Preliminary studies concerning the comparison of three different probes (DNA, LNA and PNA) toward two different target sequences (DNA and RNA) for the development of a hybridization assay, were carried out. The results obtained for the analysis of a DNA target, show that the use of LNA and PNA as capture probes does not increase the sensitivity of the assay. The opposite occurs in the case of a RNA sequence. LNA and PNA probes increase the sensitivity assay.

In conclusion, a prototype of electrochemical DNA biosensor to determine specific oligonucleotide sequences has been obtained.

PUBLICATIONS

1. Cugia, F.; Salis, A.; Barse, A.; Monduzzi, M.; Mascini, M., Surfactants toxicity towards an electrochemical DNA biosensor. *Chemical Sensors* **2010**.